Downloaded from orbit.dtu.dk on: May 05, 2023

DTU Library

Notes for DTU course 46100: Introduction to micro meteorology for wind energy

Berg, Jacob; Mann, Jakob; Nielsen, Morten

Publication date:
2013

Document Version
Publisher's PDF, also known as Version of record

Link back to DTU Orbit

Citation (APA):
Berg, J., Mann, J., & Nielsen, M. (2013). *Notes for DTU course 46100: Introduction to micro meteorology for wind energy*. DTU Wind Energy. DTU Wind Energy E No. 0009(EN) rev. ed.

General rights
Copyright and moral rights for the publications made accessible in the public portal are retained by the authors and/or other copyright owners and it is a condition of accessing publications that users recognise and abide by the legal requirements associated with these rights.

- Users may download and print one copy of any publication from the public portal for the purpose of private study or research.
- You may not further distribute the material or use it for any profit-making activity or commercial gain
- You may freely distribute the URL identifying the publication in the public portal

If you believe that this document breaches copyright please contact us providing details, and we will remove access to the work immediately and investigate your claim.

DTU Wind Energy

Notes for DTU course 46100:

Introduction to micro meteorology for wind energy

Department of Wind Energy Report 2013

Jacob Berg, Jakob Mann and Morten Nielsen

DTU Wind Energy E-0009 (EN)

ISBN 978-87-92898-15-5

February 2013

DTU Vindenergi
Institut for Vindenergi

Author (s): Jacob Berg, Jakob Mann and Morten Nielsen
Department: Department of Wind Energy
Corresponding author: Jacob Berg (jbej@dtu.dk)

DTU Wind Energy E-0009 (EN)
February 2013

Technical University of Denmark
Department of Wind Energy
Frederiksborgvej 399
Building 125
4000 Roskilde
Denmark

www.vindenergi.dtu.dk

CONTENTS

CHAPTER 1

COURSE INTRODUCTION

Micro meteorology is a broad subject with roots in both geophysics and engineering. Both branches will be covered in this course, although the main focus will be on practical engineering applications - mainly through programming exercises. Programming and the use of software packages are therefore at the core of the course through mandatory assignments. If programs such as Mathematica, Matlab or Octave (Matlab-look-alike - a freely redistributable software under the terms of the GNU General Public License) etc.) are new to you, this is not only the chance to learn, but also a requirement.

Probability concept and statistics play a crucial role in course. One could reasonably argue that micro meteorology, the main focus of this course, is *the statistical description of the state of the atmospheric boundary layer*. Some students might actually find themselves as part of math class the first month or so, but don't despair. During the course the meteorological content will hopefully become clear and the somehow tough mathematical introduction will prove itself worthy.

As a motivation I would like to mention the Bolund workshop (Berg et al., 2011; Bechmann et al., 2011). More than 60 model simulations made by people in industry and academia were compared with each other and with measurements. Besides telling us a lot about how different numerical models behave in complex terrain we learned that different models give different results. However, we also learned that the same models ALSO gives different results. Based on experience and background of the user of the models different results were obtained with similar models. Why am I telling you this? The reason is off course that in order to perform well in micro meteorology and the associated branch within wind energy called site assessment where numerical models are standard tools, it is far from enough to know which button to press in your favorite wind simulation software package. You really need to know the basics, the assumptions and hence the applicability of the different theories which the numerical models are based on. This course will guide you through the most important of these.

Students who wants to know more about micro meteorology and/or turbulence in general than presented in this course (there is a lot more to know!) can consult textbooks such as: *Atmo-*

spheric Boundary Layer Flows by Kaimal and Finnigan (1994), *Turbulence in the Atmosphere* by Wyngaard (2010), *A First Course in Turbulence* by Tennekes and Lumley (1972), *Turbulent Flows* by Pope (2000).

I (JB) would like to thank fellow colleague Søren E. Larsen, who guided me through the course *Boundary-layer meteorology* at the University of Copenhagen too many years ago. He has been of valuable assistance during the writing of these notes.

1.1 Course and learning objectives:

The course objective is to give a general understanding of atmospheric turbulence and wind resources.

The learning objectives are given by:
A student who has met the objectives of the course will be able to:

- Apply simple statistical concepts in the description of time series of the wind, e.g. the mean, moments and probability density functions.
- Analyze meteorological time series using more advanced statistical tools such as the correlation function, spectra and cross-spectra.
- Explain the basic mechanisms responsible for winds in the atmosphere.
- Explain the concept of the atmospheric boundary layer and how it is affected by atmospheric stability and the Coriolis force.
- Use micro-meteorological concepts such as roughness length, momentum flux and the geostrophic drag law.
- Qualitatively explain how various types of terrain and the topography affect the atmospheric flow.
- Apply the above-mentioned concepts to estimate the wind energy resource in a simple terrain.
- Describe atmospheric turbulence by means of variances, spectra and coherence, and explain the connection to dynamic loads on structures.
- Characterize a few in situ and remote sensors of wind.
- Explain wind-related aspects of the IEC 61400-1 standard for wind turbine safety.

The following learning objectives can be obtained by going through these lecture notes. Sections and exercises labeled with an asterix are necessary to read and do in order to meet the learning objectives.

1.2 Guidelines to assignments

Five larger exercises, *the assignments*, can be found in the notes. Following the list of guidelines most issues leading to negative feedback of the handed-in report can be ruled out.

Guidelines of practical character

- Write name and student number on front page.
- Hand in electronically through CampusNet in pdf format and only one file! Use the Assignments menu and the correct folder.
- Do not write long essays outside the context of the questions. A report do not have to be that many pages long...
- Use spelling control
- Append your code in the back of the report.
- Do not use Excel!!!

Guidelines for report content

- Write and explain what you have done in simple terms. Use rather formulas than long meaningless sentences...
- Explain the functionality of any built-in functions you use, like for example `weibullfit` in Matlab.
- Put labels on all figure axes. For spectra - is it the normal frequency, f or the angular frequency, $\omega = 2\pi f$, which is plotted on the x-axis. And what about the y-axis. Is it $S(f)$, $S(\omega)$, $fS(f)$ or maybe $\omega S(\omega)$?
- Use log scale in figures if it makes sense.
- Make figures in readable resolution and zoom in on the relevant features. For example. Do not plot correlation functions for very large time lags, τ, if the correlation drops to zero within a few units of τ.
- Check your results if possible. For example, do the pdf normalized to one? and do the spectrum integrate to the variance?
- When writing code; try to reuse as much as possible. Use loops if possible to avoid errors.

After feedback is given: make sure that you understand the what was correct and what was not. And follow up on the wrong parts.

CHAPTER 2

A SHORT INTRODUCTION TO GENERAL METEOROLOGY

Within wind energy we are mainly concerned with the atmospheric flow closest to the ground, perhaps only the first few hundred meters, often denoted the surface layer. In the surface layer the wind is largely influenced by the presence of the ground: vegetation, buildings, orography (changes in elevation), land-sea interfaces etc. all contribute to the character of the wind. It is, however, the large scale pressure fields which are ultimately responsible for the wind patterns. If no pressure differences exist - no wind.

Wind observed at different locations are associated with different meteorological patterns: frontal systems in Denmark where heavy cold polar air meets light warm tropical air, tropical cyclones in the Caribbean where the warm sea surface generate deep convection in the lower atmosphere in late summer, monsoon in India due to a large scale sea breeze effect, just to mention some.

In this chapter we will look closer at some general concepts in meteorology giving rise to different weather patterns and ultimately wind - the main focus not only of this course but of the whole enterprise of wind energy as such.

The following sections are all meant as light introductions to the subject and hence readers with extensive background in meteorology might find some of the description too crude. For a more consistent picture consult for example *An Introduction to Dynamic Meteorology* by Holton (1992) or *Global Atmospheric Circulations* by Grotjahn (1993).

2.1 The global atmospheric circulation

The imbalance in solar radiation reaching the Earth surface causes a poleward transport of heat in the atmosphere and in the oceans. The atmosphere is more or less transparent to solar radiation (short wave), so the atmosphere is heated from below. At the equator air therefore rises from the surface because warm air is lighter than cold air[2.1.1].) - and moves poleward at higher altitudes.

[2.1.1] We will assume the validity of the ideal gas law, $p = \rho RT$, where p is pressure, ρ is density, $R = 287\,\mathrm{J\,Kg^{-1}\,K^{-1}}$ is the gas constant for dry air, and T is temperature.

At the poles air is consequently sinking and moves toward the equator at low altitudes. On its way towards the pole and the equator, the two air masses are hence cooled and heated, respectively. Somewhere in between the pole and the equator, in the mid latitudes, the two air masses meet and creates frontal systems, most recognisable through the alternating movement of low and high pressure systems due to baroclinic instability.

The region above the first kilometer or so, the atmospheric boundary layer (ABL) (see Chapter 4), is called the troposphere (in principle the ABL is also part of the troposphere). It extends up to the tropopause in 8-12 kilometers height, depending on latitude - highest in the tropics (due to convection) and lowest at the poles. In the troposphere, like in the boundary layer, the temperature is decreasing with height (see Exercise 4.2.4) and most of the weather is located here. Above, the stratosphere, mesophere and ionsphere are located but they have no influence on wind energy and we can hence forget about them in this course.

In order to go a little deeper we introduce two important forces in the atmosphere: the pressure gradient force and the Coriolis force.

2.1.1 Pressure gradient force

Lets first take a look at the pressure gradient force. Consider an air parcel, a cube with sides δx, δy and δz centered at (x_0, y_0, z_0) with pressure p_0 - see Figure 2.1.1. To first order the pressures at wall A and B are:

$$A: \qquad p = p_0 + \frac{1}{2}\frac{\partial p}{\partial x}\delta x \tag{2.1.1}$$

$$B: \qquad p = p_0 - \frac{1}{2}\frac{\partial p}{\partial x}\delta x. \tag{2.1.2}$$

Since, force = pressure $\times$ area, we can express the forces, $F_{a,x}$ and $F_{b,x}$ as (x is positive towards the right)

$$F_{a,x} = -\left(p_0 + \frac{1}{2}\frac{\partial p}{\partial x}\delta x\right)\delta y \delta z \tag{2.1.3}$$

$$F_{b,x} = \left(p_0 - \frac{1}{2}\frac{\partial p}{\partial x}\delta x\right)\delta y \delta z. \tag{2.1.4}$$

The total force in the x direction, $F_p = F_{a,x} + F_{b,x}$ per unit mass, $m = \rho \delta x \delta y \delta z$ (ρ being the density of air $\sim 1.2\text{kg m}^{-3}$) can hence be written

$$F = -\frac{1}{\rho}\frac{\partial p}{\partial x}. \tag{2.1.5}$$

We can repeat the same exercise in the y and z direction, and finally write the pressure gradient force, $\boldsymbol{F}_p$

$$\boldsymbol{F}_p = -\frac{1}{\rho}\nabla p, \tag{2.1.6}$$

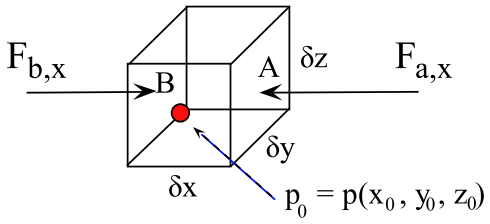

Figure 2.1.1: Air parcel with forces, $F_{a,x}$ and $F_{b,x}$ acting upon its sides, A and B, with area, $\delta y \delta z$. x is positive in the direction from left to right.

with $\boldsymbol{F}_p$ now expressed as a vector. The sign indicates that the force is in the opposite direction of the pressure gradient (as expected, I guess...), i.e. the wind is blowing from high pressure towards low pressure.

In the vertical direction and in absence of vertical motion the pressure gradient force is balances by the gravity force, expressed through the acceleration of gravity, $g = 9.8\ \mathrm{m\,s^{-2}}$. This is the hydrostatic balance:

$$\boxed{\frac{\partial p}{\partial z} = -\rho g.} \tag{2.1.7}$$

Except in the proximity of very intense weather phenomena, such as tornadoes, the hydrostatic balance is a very good approximation to the vertical structure of the atmosphere.

Exercise 2.1.1 *Solve eq. 2.1.7 for an atmosphere with constant temperature. Use the ideal gas law. What can you say about its depth?*

2.1.2 The Corolis force

The Coriolis force is a fictitious force arising because the coordinate system in which we describe the movement of air rotates with the Earth. On the northern hemisphere it causes all movement to deflect towards the right while it causes deflection to the left on the southern hemisphere.

In mathematical terms the Coriolis force is given by (per unit mass)

$$F_{co} = -2\Omega \times \boldsymbol{U}, \tag{2.1.8}$$

where $\Omega = \omega(0, \cos(\phi), \sin(\phi))$. ϕ is the latitude and $\omega = 7.2921 \cdot 10^{-5}\ \mathrm{s^{-1}}$. If we disregard vertical motion (which is by all means much smaller than the horizontal), we find that the horizontal force only depends on $\sin(\phi)$ and the magnitude of $\boldsymbol{U}$. We therefore introduce the Coriolis parameter, $f = 2\omega\sin(\phi)$. On mid latitudes, $\phi \sim 45^\circ$ and $f \sim 10^{-4}\ \mathrm{s^{-1}}$. The Coriolis force in the horizontal direction is thus given by

$$F_{co} = -f\boldsymbol{k} \times \boldsymbol{U}, \tag{2.1.9}$$

where $\boldsymbol{k}$ is the unit vector pointing upwards in the z direction. Since $\sin(0^\circ) = 0$ and $\sin(90^\circ) = 1$ the Coriolis force is zero at the equator and maximum at the poles. At the southern hemisphere $f < 0$.

If we look back at the large scale circulation, we said that air rises at the equator. Due to conservation of mass this air is replaced by a horizontal flow of air towards the equator. The pressure gradient force then dictates that there must be a low pressure at the equator. Due to the Coriolis force the horizontal flow will have a component towards the west. This is the famous trade winds bringing ships fast across the big oceans in the old days (hence the name). When air rises above a low pressure it is gradually cooled in its upward motion. When it reached the dew temperature condensation happens. This is why rain showers are mostly associated with low pressure.

At the poles the picture is reversed, i.e. high pressure reside at the poles with wind towards the poles with an westerly component. See Figure 2.1.2 for an illustration.

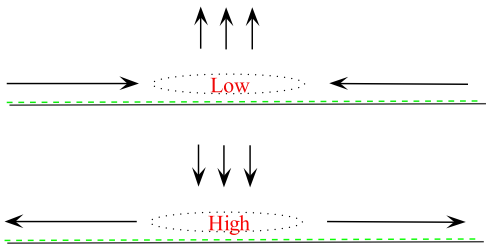

Figure 2.1.2: Low (top panel) and high (bottom panel) pressure system close to the surface of the Earth with associated winds dictated by the pressure gradient force.

Due to the Coriolis force the air moving polewards from the equator at high altitudes only extend to around 30°, where the deflection westward becomes to powerful. Since the air is very dry here, this is also the approximately the latitude where most deserts are found. The latitude is often called the horse latitude: due to low wind speeds encountered at the surface, sailors (again in the old days!) would say, that it would take a horse to cross it...

We have now crudely sketched some of the key features of the large scale circulation of the atmosphere. The closed circulation, roughly described, is named the Hadley cell. A similar cell extend just equatorwards of the poles and terminates around the polar front, separating cold heavy air from the north and warmer lighter air to the south (on the northern hemisphere). This cell is named the Polar cell. The mid latitudes between the Hadley cell and the Polar cell are dominated by strong climatic westerly wind (we will explain the reason for this wind in the next section). The wind in Denmark is therefore primarily from the west. A sketch is given in Figure 2.1.3. In between the Hadley and Polar cell an indirect Ferrel cell resides - but this is another story, much too complicated for this light introduction.

2.2 The geostrophic and gradient winds

We have mentioned the two most important forces determining atmospheric motion away from the surface, namely the pressure gradient force, F_p, and the Coriolis force, F_{co}. If these two forces

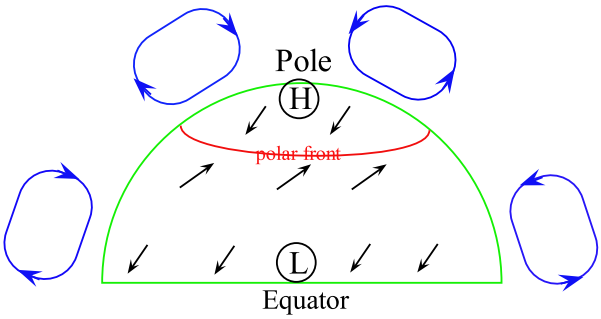

Figure 2.1.3: Hemispheric plot of the general circulation. The Hadley and Polar cells are drawn by the blue rectangles, while surface winds are shown with arrows. The polar front is shown by the red curve.

are in balance we have geostrophic conditions and wind is named the geostrophic wind, $\boldsymbol{G}$. It is

$$\boxed{\boldsymbol{k}\times\boldsymbol{G} = -\frac{1}{\rho f}\nabla p.} \tag{2.2.1}$$

The geostrophic wind is hence parallel to the isobars (lines of constant pressure):

$$\begin{aligned} U_g &= -\frac{1}{f\rho}\frac{\partial p}{\partial y} \\ V_g &= \frac{1}{f\rho}\frac{\partial p}{\partial x}, \end{aligned} \tag{2.2.2}$$

where we have split the geostrophic wind, $\boldsymbol{G} = (U_g, V_g)$, in its two components along the mean wind, x-direction and perpendicular, y-direction, respectively. The geostrophic balance is present in the troposphere, where the radius of curvature of isobars is small. If the curvature is significant an air parcel will also be affected by the centrifugal force. This force, like the Coriolis force, is a fictitious force appearing in rotating coordinate systems. The centrifugal force (opposite to the centripetal force) is given by

$$F_{ce} = \frac{U^2}{R_c}, \tag{2.2.3}$$

where R_c is the radius of curvature. The centrifugal force is well known from everyday lives: when riding a carousel or turning at high speed in a car we experience a force in opposite direction that our movement. Notice, that R_c can be both positive and negative depending on the direction. By convention, $R_c > 0$ when the motion is counterclockwise and $R_c < 0$ when the motion is clockwise.

For simplicity we look in the direction normal to the flow, and hence use eq. 2.2.11 to express the pressure gradient force by the geostrophic wind U_g. With all three forces present the balance is given by

$$\frac{U^2}{R_c} + fU - fU_g = 0. \tag{2.2.4}$$

This is a simple second order polynomial which can be solved for the wind speed U:

$$U = -\frac{fR_c}{2} \pm \sqrt{\left(\frac{fR_c}{2}\right)^2 + U_g fR_c}. \tag{2.2.5}$$

Since fR_c can be both positive and negative there are many solutions. We will only consider the two most common, namely the regular low and high pressure. In these, the pressure gradient force and the Coriolis force are in opposite directions so that the geostrophic balance is obtained for $R_c \to \infty$. From eq. 4.3.8 we have by performing a series expansion for $R_c \to \infty$:

$$U \sim -\frac{fR_c}{2} \pm \sqrt{\left(\frac{fR_c}{2}\right)^2}\left(1 + 2\frac{U_g}{fR_c}\right). \tag{2.2.6}$$

When $fR_c > 0$ (the regular low) it can be seen that the positive root gives rise to U_g, while for $fR_c < 0$ (the regular high) the negative root gives U_g. These solutions are sketched in Figure 2.2.1. On the northern hemisphere we thus recover the counterclockwise cyclonic motion around low pressure and clockwise anti-cyclonic motion around high pressure. On the southern hemisphere the direction of cyclonic and anti-cyclonic motion is reversed. For the regular high,

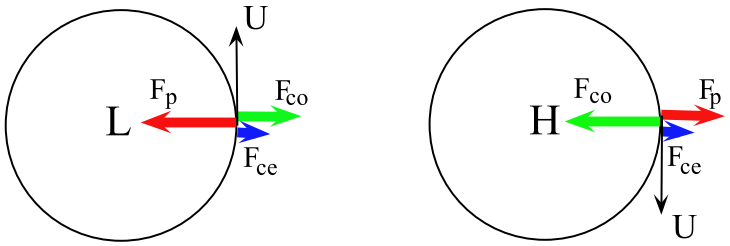

Figure 2.2.1: Gradient wind on the northern hemisphere ($f > 0$) with forces, F_p, F_{co} and F_{ce} at pressure systems with radius of curvature, R_c. *Left*: Regular low pressure ($fR_c > 0$). *Right*: Regular high pressure ($fR_c < 0$).

in which $R_c < 0$ we have a maximum wind speed equal to $U = -f_c R_c/2$. There is no upper limit for the regular low, since the expression inside the square root is always positive. This means that high wind speeds will primarily be associated with winds around a low pressure.

If we divide eq. 2.2.4 by fU we have

$$\frac{U_g}{U} = 1 + \frac{U}{fR_c}. \tag{2.2.7}$$

The last term on the right hand side thus determines the fractional deviation from pure geostrophic balance. Its norm is called the Rossby number, $Ro = |U/fR_c|$. For $U_g > U$ the flow is cyclonic and for $U_g < U$ the flow is anti-cyclonic.

On mid latitudes, $Ro \ll 1$, and the geostrophic balance is often a very good approximation to the flow. In subtropical regions $Ro > 1$ and hence the gradient wind must be used. A tropical cyclone (hurricane) is a good example of the latter. It is formed in late summer when the ocean

is warmest. The warm ocean enhances atmospheric convection, which in turn creates a strong low pressure. This low pressure will continue to grow as long as there is moisture to feed it. It therefore dies out rather quickly once it hits land. Since it is a low pressure system the motion will always be cyclonic.

For very large *Ro* the Coriolis force becomes unimportant, and the flow may either be cyclonic or anti-cyclonic. This situation is called cyclostrophic flow. Tornados and the the vortex in a bathtub are examples of such flows.

2.2.1 The thermal wind and the westerlies

An important consequence of the geostrophic balance is the presence of westerly winds on mid latitudes. First lets introduce the hypsometric relationship, which relates the thickness of a layer, δz, with a pressure interval, δp. We combine the hydrostatic equation, eq. 2.1.7, and the ideal gas law and arrive at

$$RT\,\delta \log p = -g\delta z = -\delta\Phi, \tag{2.2.8}$$

where we have introduced the geopotential, $\Phi(z)$, which is the the work required to raise a unit mass of air from sea level at $z = 0$ to some height z:

$$\Phi(z) = \int_0^z g dz. \tag{2.2.9}$$

We can now express the the geostrophic balance through the geopotential:

$$\begin{aligned} U_g &= -\frac{1}{f}\frac{\partial\Phi}{\partial y} \\ V_g &= \frac{1}{f}\frac{\partial\Phi}{\partial x}, \end{aligned} \tag{2.2.10}$$

where the partial derivatives is taken while keeping pressure constant. i.e. on isobars. We now differentiate with respect to pressure, p, utilize eq. 2.2.9 and obtain *the thermal wind* equations:

$$\begin{aligned} \frac{\partial U_g}{\partial \log p} &= \frac{R}{f}\frac{\partial T}{\partial y} \\ \frac{\partial V_g}{\partial \log p} &= -\frac{R}{f}\frac{\partial T}{\partial x}, \end{aligned} \tag{2.2.11}$$

again evaluated on isobar lines. The thermal wind is illustrated in Figure 2.2.2. Due to cooling at the north pole the isobar lines are sloping and hence the thickness of a layer between two isobar lines increases towards the equator ($\delta z_1 > \delta z_2$). This gives rise to a westerly geosptrophic wind which increases with height. Its upper maximum is often denoted the jet stream.

In general we say that the atmosphere is *baroclinic* if the geostrophic wind changes with height and *barotropic* if it is constant. Other situations where baroclinicity is important could in coastal areas where the land-sea interface sets up a horizontal temperature gradient.

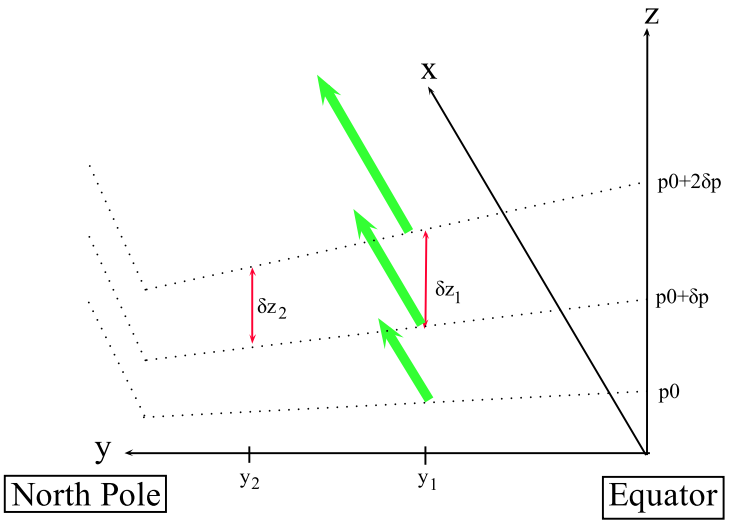

Figure 2.2.2: The thermal wind situation: westerly geostrophic winds, U_g, are presented by the green arrows. The surfaces spanned by the dotted lines are isobars with pressure, $p_0 + j\delta p$ and $\delta p < 0$.

Exercise 2.2.1 (Land-sea interface) *Sketch the flow around a land-sea interface during day (seabreeze) and night (landbreeze).*
Hint*: Land has a lower heat capacity than water and thus warm up faster.*

The monsoon in India giving rise to very large wind speeds is a large scale seabreeze. The Indian plateau heats up much faster than the ocean and hence a strong surface wind is set up, blowing relatively cold and humid air from Indian ocean in over the Indian plateau.

CHAPTER 3

WORKING WITH REAL DATA IN WIND ENERGY

Before moving on with the physics of the atmospheric boundary layer we will start with some (perhaps known) important and for this course necessary concepts in probability theory and time series analysis. The concepts in this chapter might seem a little abstract to the more application driven wind engineer. The concepts are nevertheless quite important and at the core of wind energy and especially, wind power meteorology with the underlying tasks of siting and load estimation. The random nature of the wind makes it impossible to say anything meaningful about individual air parcels (and if we could its usage would be almost non-existing). Averages and departures from the wind speed (variance) over time, for example, are, on the other hand, extremely useful concepts in wind energy.

3.1 Random variables and distributions

In the following section we will consider a continuous random variable, X. By random we understand a variable, X, that varies irregular in time and space and as such cannot be predicted. A straightforward example is the wind speed measured by a cup anemometer mounted on a meteorological mast (See Section 5).

3.1.1 Probability density functions and cumulative distribution functions

The probability, P, that X takes a value between, x and $x+dx$, where dx is considered very small is given by

$$P\{x < X \leq x+dx\} = f_X(x)dx, \tag{3.1.1}$$

where $f_X(x)$[3.1.1] is denoted the probability density function (pdf) and has the following well known properties

$$\int_{-\infty}^{\infty} f_X(x)dx = 1 \qquad \text{and} \tag{3.1.2}$$

$$f_X(x) \geq 0. \tag{3.1.3}$$

The probability, P, that $x_1 \leq X \leq x_2$ (again, for example a wind speed between $4\,\mathrm{m\,s^{-1}}$ and $25\,\mathrm{m\,s^{-1}}$, a typical operational range of a wind turbine) is given by

$$P\{x_1 < X \leq x_2\} = \int_{x_1}^{x_2} f_X(x)dx. \tag{3.1.4}$$

The probability, $P\{X \leq x\}$, that $X \leq x$ is denoted, $F_X(x)$ and is named the cumulative distribution function (cdf). In terms of the pdf, $f_X(x)$, the cdf $F_X(x)$ of X is given by

$$F_X(x) = \int_{-\infty}^{x} f_X(x')dx', \tag{3.1.5}$$

so that

$$f_X(x) = \frac{d}{dx}F_X(x). \tag{3.1.6}$$

Eq. 3.1.4 can therefore be expressed as

$$P\{x_1 < X \leq x_2\} = F_X(x_2) - F_X(x_1). \tag{3.1.7}$$

3.1.2 Moments and expectation value

The expectation value is a quite useful concept. The expectation value of the pdf, $f_X(x)$, is denoted $E[\cdot]$.

If $g(x)$ is some arbitrary function of the random variable, X the expectation value is defined as

$$E[g(X)] = \int_{-\infty}^{\infty} g(x)f_X(x)dx. \tag{3.1.8}$$

When $g(x)$ equals a polynomial, X^n, we encounter the n'th non-central moments of X,

$$E[X^n] \equiv \mu_n = \int_{-\infty}^{\infty} x^n f_X(x)dx). \tag{3.1.9}$$

For $n = 1$ we encounter the well known mean, μ (most often we don't explicitly write the subscript 1 or sometimes we write μ_X - especially if we have more than one random variable like in Section 3.3), of the distribution:

$$\boxed{E[X] \equiv \mu = \int_{-\infty}^{\infty} x f_X(x)dx.} \tag{3.1.10}$$

[3.1.1] The subscript, X is often omitted. Later on, when dealing with joint and conditional probabilities it, however, becomes handy in order to identify the different distributions involved.

We can now define the central moments of the distribution

$$E[(X-\mu)^n] \equiv v_n = \int_{-\infty}^{\infty} (x-\mu)^n f_X(x)dx). \tag{3.1.11}$$

This means that $v_1 = 0$. For $n = 2$ we encounter the variance,

$$\boxed{E[(X-\mu)^2] \equiv \sigma^2 = \int_{-\infty}^{\infty} (x-\mu)^2 f_X(x)dx,} \tag{3.1.12}$$

with square root, σ, named the standard deviation and quantifying the spread around the mean, μ. It can easily be verified that the variance can be written as

$$\sigma^2 = \mu_2 - \mu^2. \tag{3.1.13}$$

Other *famous* moments often encountered are the skewness

$$Sk \equiv \frac{v_3}{\sigma^3}, \tag{3.1.14}$$

and the kurtosis

$$Ku \equiv v_4/\sigma^4. \tag{3.1.15}$$

Sometimes, although rare, the integrand in eq. 3.1.9 does not converge for some values of $n \leq n_{crit}$ and the distribution does not have corresponding well defined moments.

Exercise 3.1.1 (Cauchy distribution) *Show that the Cauchy distribution*

$$f_X(x) = 1/(\pi(1+x^2)) \tag{3.1.16}$$

does not have finite mean and variance.

Besides moments one is often interested in the mode and percentiles of a distribution. The mode correspond to the maximum value of $f_X(x)$, which can be found by solving the equation

$$\frac{df_X(x)}{dx} = 0. \tag{3.1.17}$$

The n'th percentile, P_n, is defined as the value where $F_X(P_n) = n/100$. Of these the most well known is the median, M, for which $F_X(M) = 0.5$ and the lower and upper quartiles, Q_l and Q_u, for which $F_X(Q_l) = 0.25$ and $F_X(Q_u) = 0.75$, respectively.

3.2 Some distribution functions in wind energy

In wind energy a few different distributions are used. The fast fluctuations in time of the wind velocity[3.2.1] known as turbulence is often characterised by Gaussian distributions. On the other hand, the mean wind speed, like for example a 10 minutes average of the horizontal wind speed, follows a Weibull distribution. In Chapter 7 we will also meet the Poisson distribution and the Gumbel distribution. Both are distributions involved in characterising extreme events, such as for example the largest wind which on average will occur within 50 years.

[3.2.1] Velocity refers to the three dimensional vector of wind while, speed is the magnitude.

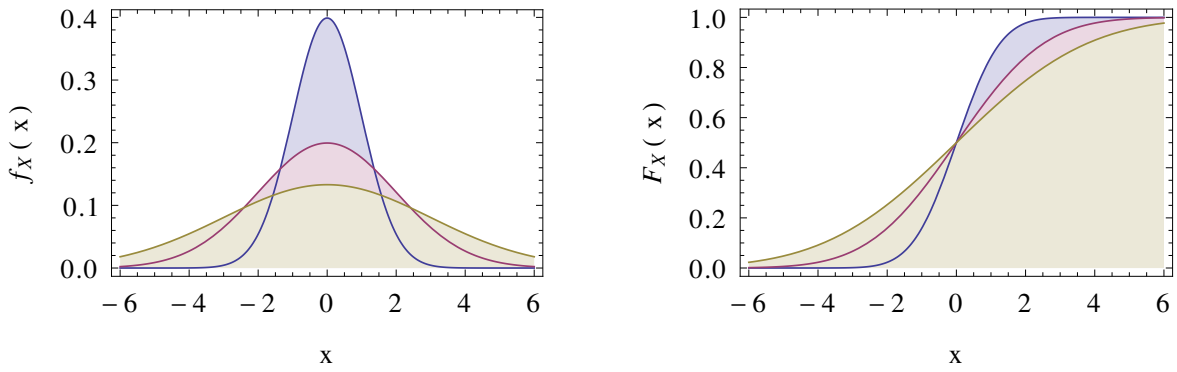

Figure 3.2.1: Gaussian distributions with zero mean and variance equal to 1 (blue), 2 (red) and 3 (yellow): pdf (*left*) and cdf (*right*)

3.2.1 The Gaussian distribution

The Gaussian (also denoted the Normal distribution) pdf is given by

$$\boxed{f_X(x) = \frac{1}{\sqrt{2\pi}\sigma} \exp\left(-\frac{1}{2}\left(\frac{(x-\mu)}{\sigma}\right)^2\right).} \tag{3.2.1}$$

The cdf cannot be evaluated analytically. Instead tabulated values of the normalized variable, $Z = (X - \mu_X)/\sigma_X$, are often utilized. Some important probabilities are: $P\{-1 < Z \leq 1\} = 68.3\%$, $P\{-2 < Z \leq 2\} = 95.4\%$ and $P\{-3 < Z \leq 3\} = 99.7\%$. I.e. the probability that any x is within one, two or three standard deviations, σ, from the mean, μ, respectively.

The pdf and the cdf are shown in Figure 3.2.1. As observed, the Gaussian distribution is symmetric around the mean, μ, indicating that the skewness, *Sk*, is zero. As we will later learn, the Gaussian distribution plays a special role in probability theory through the *central limit theorem*.

Exercise 3.2.1 (*Moments of the Gaussian distribution) *Consider the integral*

$$\int_{-\infty}^{\infty} \frac{d}{dz}\left(\frac{z^n}{\sqrt{2\pi}} \exp(-z^2/2)\right) dz$$

and use it to obtain a recurrence relation for the moments of a normalized Gaussian variable, Z. Show then that all odd moments are zero and that the fourth and sixth even moments are $\mu_4 = 3$ *and* $\mu_6 = 15$*, respectively.*
Hint*: Show that the integral is zero by using the identity*

$$\int_A^B \frac{d}{dz}[f(z)]dz = f(B) - f(A). \tag{3.2.2}$$

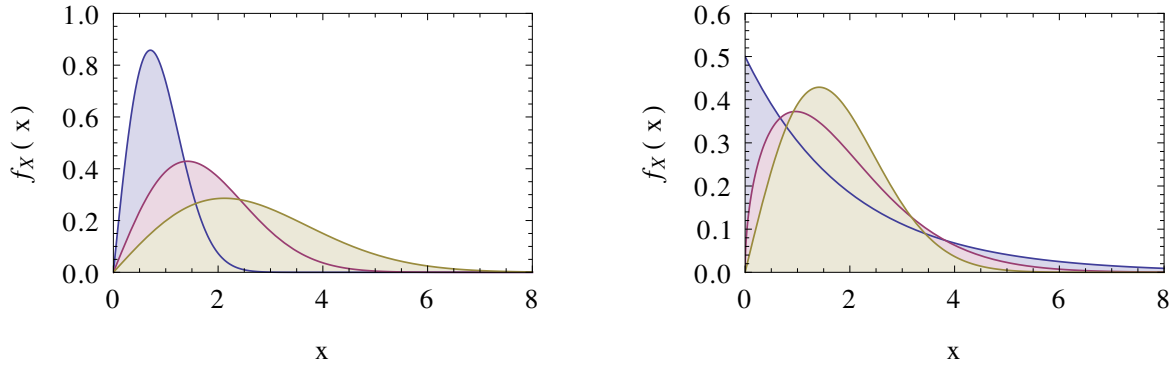

Figure 3.2.2: Weibull distributions. *Left:* Constant $k = 2$ and A equal to 1 (blue), 2 (red) and 3 (yellow). *Right:* Constant $A = 2$ and k equal to 1 (blue), 1.5 (red) and 2 (yellow).

3.2.2 The Weibull distribution

The Weibull distribution pdf is given by

$$\boxed{f_X(x) = k\frac{x^{k-1}}{A^k}\exp\left(-\left(\frac{x}{A}\right)^k\right).} \tag{3.2.3}$$

Both the scale parameter, A, and the shape parameter, k are positive. The pdf for various combinations of k and A is shown in Figure 3.2.2. As can be seen in the figures, x can only take positive values.

In wind resource assessment, where accurate estimation of the mean annual energy production is the main goal, the Weibull distribution plays a key role. A good example is the much established European Wind Atlas which contains a collection of the Weibull parameters, k and A, obtained from different wind directions with a given frequency of occurrence at different sites all over Europe (Troen and Petersen, 1989).

Exercise 3.2.2 (Weibull distribution) *Find the cumulative distribution function (cdf) of the Weibull distribution in eq. 3.2.3. Then calculate the non-central moments, μ_n, and use that result to show that the mean, μ, and variance, σ^2, of the Weibull distribution are given by*

$$\mu_X = A\Gamma\left(1+\frac{1}{k}\right) \tag{3.2.4}$$

$$\sigma_X^2 = A^2\left(\Gamma\left(1+\frac{2}{k}\right)-\Gamma^2\left(1+\frac{1}{k}\right)\right), \tag{3.2.5}$$

where the gamma function, $\Gamma(x)$, is defined through

$$\Gamma(x) = \int_0^\infty t^{x-1}e^{-t}dt. \tag{3.2.6}$$

$\Gamma(x)$ *has some useful properties:*

$$\begin{aligned} \Gamma(x+1) &= x\Gamma(x) && (3.2.7)\\ \Gamma(n+1) &= n\Gamma(n) = n! \quad \textit{for } n = 0,1,2,... && (3.2.8)\\ \Gamma(1/2) &= \sqrt{\pi}. && (3.2.9) \end{aligned}$$

Exercise 3.2.3 (*Exponential distribution) *A Weibull distribution with $k = 1$ corresponds to the exponential distribution.*

Verify that the exponential *distribution:*

$$f_X(x) = \begin{cases} \lambda e^{-\lambda x} & x \geq 0 \\ 0 & x < 0 \end{cases}$$

is a probability density function (pdf) for $\lambda > 0$ and find the mean and variance.

3.2.3 The law of transformation of probabilities

Another useful concept in probability theory is the law of transformation of probabilities. If X and Y are two random variables with pdfs, $f_X(x)$ and $g_Y(y)$, respectively, and functional relation, $Y = h(X)$, then

$$|f_X(x)dx| = |g_Y(y)dy|. \tag{3.2.10}$$

If $f_X(x)$ is known we have

$$\begin{aligned} g_Y(y) &= f_X(x)\left|\frac{dx}{dy}\right| && (3.2.11)\\ &= f_X(x)\frac{1}{|h'(x)|}. \end{aligned}$$

Strictly speaking this result only holds if $y = h(x)$ is single valued. The extension is straightforward but will not be considered here. The Following exercise illustrates the power of the transformation.

Exercise 3.2.4 (Rayleigh distribution) *The Rayleigh distribution is the special case of the Weibull distribution when $k = 2$. Find the distribution of the stochastic variable $Y = X^2$ where X has a Rayleigh distribution. The resulting pdf is called the χ^2 distribution with two degrees of freedom. The Rayleigh distribution is simply the pdf of two Gaussian variables, W and Z for which $X = \sqrt{W^2 + Z^2}$. In terms of wind speed, it means that if the two individual horizontal components are Gaussian distributed the wind speed is Rayleigh distributed.*

3.3 Two (and possible more) random variables

The picture from the previous section can easily be expanded to two random variables,X and Y.

3.3.1 Joint and conditional distributions

We define the two-variable joint probability density function, $f_{XY}(x,y)$, in a way similar to $f_X(x)$ in the one-variable case:

$$P\{x_1 \leq X \leq x_2, y_1 \leq Y \leq y_2\} = \int_{x_1}^{x_2}\int_{y_1}^{y_2} f_{XY}(x,y)dxdy, \tag{3.3.1}$$

with normalization

$$\int_{-\infty}^{\infty}\int_{-\infty}^{\infty} f_{XY}(x,y)dxdy = 1. \tag{3.3.2}$$

Also like in the one random variable case, we can define joint cumulative distributions given by the probability, $P\{X \leq x, Y \leq y\}$:

$$F_{XY}(x,y) = \int_{-\infty}^{x}\int_{-\infty}^{y} f_{XY}(x',y')dx'dy'. \tag{3.3.3}$$

This means that eq. 3.3.1 can be expressed as

$$P\{x_1 \leq X \leq x_2, y_1 \leq Y \leq y_2\} = F(x_1,y_1) - F(x_1,y_2) - F(x_2,y_1) + F(x_2,y_2). \tag{3.3.4}$$

If only the random variable, X is considered, we have

$$f_X(x) = \int_{-\infty}^{\infty} f_{XY}(x,y)dy, \tag{3.3.5}$$

which is called the marginal distribution of X. Two random variables, X and Y are said to be statistically independent if and only if their joint pdf, $f_{XY}(x,y)$ is given by

$$f_{XY}(x,y) = f_X(x)f_Y(y). \tag{3.3.6}$$

With two random variables we can furthermore define conditional probabilities, i.e. *Given the occurrence of some event B, the probability of some other event A is... expressed by* $P\{A|B\}$[3.3.1]. In terms of distributions we define the probability function, $f_{X|Y}(x|Y=y_0) = P\{X|Y=y_0\}$, of X given that $Y = y_0$:

$$f_{XY}(x,y_0) = f_{X|Y}(x|Y=y_0)f_Y(y_0). \tag{3.3.7}$$

A typical example is the measurement of wind speed: lets assume that we are only interested in situations where the thermal properties of the atmosphere can be neglected, i.e. we only want to look at measurements in, what is called, strictly neutral stratification (see Section 4.2). In this case we let X be the wind speed and Y some measure of thermal stability (for example the Obukhov length, L) with y_0 corresponding to neutral stratification (in which case $L = \pm\infty$).

[3.3.1] From the definition $P\{A|B\} = P\{A,B\}/P\{B\}$, Bayes' theorem relates the conditional probability to its inverse: $P\{A|B\}P\{B\} = P\{B|A\}P\{A\}$

3.3.2 Moments and correlation

Just like we can calculate the variance, σ_X^2, for a random variable, X we can calculate the covariance

$$E[(X-\mu_X)(Y-\mu_Y)] \equiv \sigma_{XY}^2 = \int_{-\infty}^{\infty}\int_{-\infty}^{\infty}(x-\mu_X)(y-\mu_Y)f_{XY}(x,y)dxdy. \tag{3.3.8}$$

If $X = Y$ we obtain $\sigma_{XX}^2 \equiv \sigma_X^2$, i.e. the variance of the single random variable, X. From the covariance we can construct the correlation coefficient, ρ_{XY}:

$$\rho_{XY} = \frac{\sigma_{XY}^2}{\sigma_X \sigma_Y}. \tag{3.3.9}$$

Exercise 3.3.1 (Correlation) *Given two correlated stochastic variables X and Y prove that the correlation coefficient obeys*

$$1 \geq \rho_{XY} \geq -1$$

Hint: Calculate the mean of $\left(\frac{X-\mu_X}{\sigma_X} \pm \frac{Y-\mu_Y}{\sigma_Y}\right)^2$.

Exercise 3.3.2 (The sample mean) *This exercise is about the variance of the sample mean. Suppose you have a series of independent, identically distributed random variables* $X_1, X_2, ...X_N$ *with mean* $\langle X \rangle = \mu$ *and variance* $\sigma^2(X) = \sigma^2$. *The most obvious estimate of the mean, in case it is not known in advance, is the sample mean*

$$M = \frac{1}{N}\sum_{i=1}^{N} X_i$$

Now M is a new stochastic variable and its mean is indeed μ *(verify that). Prove that the standard deviation of M is* $\sigma/\sqrt{N}$. *This means that if you have four times as many data you can decrease the uncertainty on the mean estimate by a factor of two.*

What is the uncertainty of the mean estimation if X_i *is a Cauchy distribution? Does it help to have more data in this case?*

3.3.3 *Central Limit theorem

The *central limit theorem* considers a series of independent, identically distributed random variables $X_1, X_2, ...$ with mean μ and variance σ^2, which is required to exist (the Cauchy distributions therefore does not apply!). The sample mean M defined in Exercise 3.3.2 can be standardized as

$$\hat{M} \equiv \frac{(M-\mu)N^{1/2}}{\sigma}$$

such that $\langle \hat{M} \rangle = 0$ and $Var(\hat{M}) = 1$. The central limit theorem states that the pdf of $\hat{M}$ tends to a normalized gaussian as $N \to \infty$, no matter the pdf of the X's. We shall not prove the theorem. The theorem together with many other things show that Gaussian variables play a crucial role in

probability theory. The following exercises are therefore on Gaussian random variables. First we will, however, define the Gaussian distribution in two dimensions.

For two random variables, X and Y the gaussian joint pdf is given by:

$$f_{XY}(x,y) = \frac{1}{2\pi\sigma_X\sigma_Y\sqrt{1-\rho_{XY}}}\exp\left(-g_{XY}(x,y)\right), \tag{3.3.10}$$

with

$$g_{XY}(x,y) = \frac{1}{2(1-\rho_{XY}^2)}\left[\left(\frac{x-\mu_X}{\sigma_X}\right)^2 + \left(\frac{y-\mu_Y}{\sigma_Y}\right)^2 - 2\rho_{XY}\frac{(x-\mu_X)(y-\mu_Y)}{\sigma_X\sigma_Y}\right]. \tag{3.3.11}$$

A nice property is that if X and Y has a joint Gaussian pdf given by above, both X and Y are individually Gaussian distributed. In the case $\rho_{XY} = 0$, the joint pdf reduces to the product of the single variable Gaussian pdfs and X and Y can be said to be statistically independent. This is a special case of Gaussian distributed variables. In general two uncorrelated random variables can not be said to be statistically independent. The opposite does however always holds: two statistical independent random variables are always uncorrelated.

Exercise 3.3.3 (*Polar coordinates and Gaussian variables) *Let the stochastic, independent variables X and Y be Gaussian with zero mean and variance σ^2:*

$$\begin{aligned} f_{XY}(x,y) &= \frac{1}{\sqrt{2\pi}\sigma}\exp\left(-\frac{x^2}{2\sigma^2}\right)\frac{1}{\sqrt{2\pi}\sigma}\exp\left(-\frac{y^2}{2\sigma^2}\right) \\ &= \frac{1}{2\pi\sigma^2}\exp\left(-\frac{x^2+y^2}{2\sigma^2}\right) \end{aligned}$$

Calculate the pdf of the stochastic variable $Z = X^2 + Y^2$.
Hint*: Use polar coordinates:*

$$\int_{-\infty}^{\infty}\int_{-\infty}^{\infty} f(x,y)dxdy = \int_0^{2\pi}\int_{-\infty}^{\infty} rf(r,\theta)drd\theta. \tag{3.3.12}$$

Exercise 3.3.4 (*Sum of Gaussian variables) *Suppose X and Y are two random variables with joint pdf, $f_{XY}(x,y)$. Show that the cumulative distribution function $F_Z(z)$ of the sum $Z = X + Y$ can be written as*

$$F_Z(z) = \int_{-\infty}^{\infty}\int_{-\infty}^{z-x} f_{XY}(x,y)dydx$$

Now make the variable substitution $y = v - x \Leftrightarrow v = x + y$ and prove that

$$F_Z(z) = \int_{-\infty}^{z}\int_{-\infty}^{\infty} f_{XY}(x,v-x)dxdv$$

Finally, conclude that the pdf of Z is

$$f_Z(z) = \int_{-\infty}^{\infty} f_{XY}(x,z-x)dx$$

and that it is the convolution

$$f_Z(z) = \int_{-\infty}^{\infty} f_X(x) f_Y(z-x) dx$$

if X and Y were independent.

What is the pdf of $Z = X + Y$ if X and Y are independent gaussian variables with means μ_X and μ_Y and variances σ_X^2 and σ_Y^2?

3.4 Time series analysis

Ultimately we are interested in physical processes and hence realizations of some physical event. We let $\langle X \rangle$ denote the ensemble mean, i.e. the average over an ensemble of realization of some random variable, X. If X is given by the pdf, f_X, the framework from the previous sections apply.

If $x(t_1), x(t_2), ...$ is a series of random distributed numbers we say that $X(t)$ is a stochastic process (again the measured wind speed in time, $u(t)$, is a prime example of a such). A process is stationary if the pdfs does not change over time, i.e. the moments are constant. Mathematically the mean of X can be expressed as

$$\mu(t_1) = \lim_{T \to \infty} \frac{1}{T} \int_{t_1}^{t_1+T} X(t) dt, \tag{3.4.1}$$

where the integration (sum) should be performed over some reasonable time interval. If μ is independent of the specific choice of t_1 we say that $X(t)$ is independent of time and hence stationary. Just like the mean, shown here, we can calculate all the different moments of $X(t)$.

Ergodicity is the assumption that we can substitute ensemble averaging with time averaging and hence construct the mean value from any measured time series

$$\langle X(t) \rangle = \lim_{T \to \infty} \frac{1}{T} \int_{t_1}^{t_1+T} X(t) dt. \tag{3.4.2}$$

In wind energy we are often interested in the 10-min average of wind speed. A typical cup anemometer samples at 10 Hz, i.e. 6000 samples comprise a 10-min average. For second order moments, such as the variance, we often need at least 30 minutes or longer in order to reach convergence of the integrand (Lenschow et al., 1994), which means that stationarity can sometimes be questioned, for example around the time of sunrise and sunset. To overcome this problem of stationarity different methods of detrending the data exist. These are, however, not part of the current course.

3.4.1 Covariances, autocorrelation and integral time scale

In this subsection we will define some different important concepts which all have names quite similar for the inexperienced. In general the word *covariance* refers to the second order moment of any two time series separated by a time lag, τ. *auto* is the prefix to covariances where the two

time series are the same, and finally *cross* is the prefix to covariances where the to time series are different.

The autocovariance of $X(t)$ as function of the time lag, τ, is defined

$$\boxed{R_X(\tau) = \langle (X(t)-\mu_X)(X(t+\tau)-\mu_X)\rangle = \langle X(t)X(t+\tau)\rangle - \mu_X^2,} \tag{3.4.3}$$

where we have removed the dependence of t by assuming stationarity. One can easily verify

$$\begin{aligned} R_X(\tau) &= R_X(-\tau) && (3.4.4)\\ R_X(0) &= \sigma^2 && (3.4.5)\\ -R_X(0) \le R_X(\tau) &\le R_X(0) && (3.4.6) \end{aligned}$$

From the autocovariance function, the autocorrelation function is defined as

$$\boxed{\rho_X(\tau) = \frac{R_X(\tau)}{\sigma^2}.} \tag{3.4.7}$$

From the previous inequality it follows that $-1 \le \rho_X(\tau) \le 1$ (see also Exercise 3.3.1). The autocorrelation is a measure of memory in the process: for increasing time lags, τ, $\rho_X(\tau)$ decreases and hence looses correlation. The time scale of the *memory* is the integral time scale (or simply *the time scale*) defined by

$$\boxed{T = \int_0^\infty \rho_X(\tau)d\tau.} \tag{3.4.8}$$

In figure 3.4.1 we show the autocorrelation function (middle lower panel) of a 30-min time series (presented in the top panel) of wind speed measured in Roskilde Fjord, 5 m above sea level. The measurements are part of the Bolund Hill project (Berg et al., 2011). The data are sampled at 20 Hz by a sonic anemometer (See section 5.2).

For two stochastic processes, X and Y we can in a similar way construct the crosscovariance function

$$R_{XY}(\tau) = \langle (X(t)-\mu_X)(Y(t+\tau)-\mu_Y)\rangle = \langle X(t)Y(t+\tau)\rangle - \mu_X\mu_Y, \tag{3.4.9}$$

where we have again assumed stationarity. It can easily be shown that $R_{XY}(\tau) = R_{YX}(-\tau)$. The crosscorrelation function is defined by

$$\rho_{XY}(\tau) = \frac{R_{XY}(\tau)}{\sigma_X\sigma_Y}. \tag{3.4.10}$$

Exercise 3.4.1 (Covariance and time differentiation) *Consider a stationary stochastic process, $X(t)$. Show that if $X(t)$ is one-time differentiable, then*

$$R_{X\dot{X}}(0) = 0 \tag{3.4.11}$$

where $\dot{X}$ denotes differentiation with respect to time. This means that a time series and its time derivative (for example velocity and acceleration) are uncorrelated at zero time lags. Show furthermore that

$$\frac{d^2R_X(\tau)}{d\tau^2} = -R_{\dot{X}}(\tau). \tag{3.4.12}$$

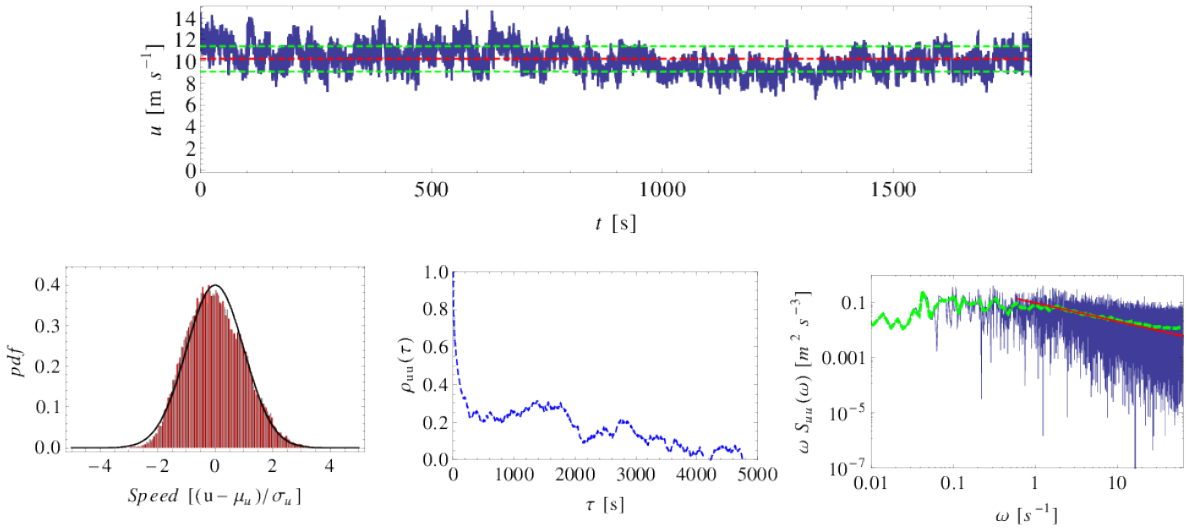

Figure 3.4.1: 30-min time series of wind speed, u, from the Bolund Hill campaign. *Top panel*: The mean, μ_u and standard deviation, σ_u, are shown with red and green lines respectively. *Lower left:* Pdf of u. The argument is normalized with the standard deviation, σ_u. The Gaussian pdf is shown on top. *Lower middle:* Autocorrelation, $\rho_{uu}(\tau)$ of time lag, τ. *Lower right*: Autospectrum, $\omega S_{uu}(\omega)$ A log-log smoothing filter is applied and shown by the green curve. The red curve represents the K41 prediction (see Section 6).

Hint: Use the fact that $\mu_{\dot{X}} = 0$.

Assignment 1 (Mean wind speed and the Weibull distribution) *Data from a 70 m mast at the island of Sprog in the Great Belt separating Fyn and Zealand are uploaded to CampusNet in the "Data" directory in a zip file. The data columns are a time mark, the wind speed at 70 m, and the direction in degrees at 67.5 m and 70 m. Invalid speed data are indicated by 99.99 and direction data by 999.9. All data are 10-min averages.*

Inspect the time series and calculate the following:

- *The mean wind speed and its standard deviation.*
- *The pdf of wind speed (you might want to use the histogram function, but beware of normalization).*
- *The cdf of wind speed.*
- *The A and k parameters of the weibull distribution. This can be done by calculating the first and second (non-central) moments, μ and m_2, and solving the theoretical expressions.*

  You may also consider other ways to estimate A and k - for example the WAsP Wind Atlas method, where the third order moment, m_3, and percentile of the mean, $F(\mu)$, is used. Since the power of a wind turbine is a function of the wind speed to the third power, this method is directly related to wind energy: the upper half of the Weibull distribution is matched the best, i.e. the high wind speed regime.
- *Plot the Weibull pdf based on the estimated A and k values together with the data pdf.*
- *Do the same for data limited to twelve directional sectors 30° wide and centered on 0°, 30°, ... , 330° (be careful around 0°). A note about wind directions: in meteorology the convention is that winds from the north have a direction of 0°, and increasing clockwise to winds from the east, south and west, respectively. This is in contrast to the mathematical definitions of angles, which increases anticlockwise from the first quadrant.*

What do you conclude from all this?

3.5 Generation of random numbers

The generation of random numbers are maybe not at the core of wind energy. It, however, comes in through applications such as for example wind load simulations. On the other hand, its role in more pedagogical founded tasks make it interesting to introduce at this early stage.

Mathematica and Matlab can both generate random numbers from all kinds of different dis-

tributions. So in principle this section could be dropped. Again, however, the purpose of this section is more to give a deeper understanding of time series analysis and hence wind data in general. Therefore, forget that you can do all sort of things in software like Mathematica and Matlab and assume that we can only generate random numbers which are uniformly distributed. I.e. where the pdf is constant. The most famous example probably being a fair dice, where the probability of getting a specific number (between one and six) is $1/6$.

The uniform distribution is the most simple and normally outputs a number, u, lets say of type Real, uniformly distributed on the interval $]0;1[$. In Mathematica the command for this is `RandomReal[]` while the command is `rand()` in Matlab.

To change the desired interval, for example $x \in [-1;1[$ one simply calculate $x = 2(u-0.5)$. From the law of transformation of probabilities given in eq. 3.2.10 it follows that if a stochastic variable X has some continuous distribution with cdf, F_X, then another stochastic variable Y given by $Y = F_X(X)$, has a uniform distribution. By applying the inverse, $X = F_X^{-1}(Y)$ we can thus generate all kinds of distributions from the uniform distributions. An example is the exponential distribution for which $F_X(x) = 1 - \exp(-x)$ leading to $X = -\log(1-Y)$.

Exercise 3.5.1 (Box-Muller transform) *Let X_1 and X_2 be uniformly distributed on the circle disk with radius one. Let $S = X_1^2 + X_2^2$ and let $F = \sqrt{-2\log(S)/S}$. It is given without proof that the X_1F and X_2F are independent, Gaussian variables with zero mean and standard deviation one. The algoritm is known as the Box-Muller transform (Press et al., 2002). Make a computer code that generates gaussian random variables. Compare the outcome with the outcome of a possible built-in Gaussian random number function like* `RandomReal[NormalDistribution[`μ`, `σ`]]` *in Mathematica or* `randn()` *in Matlab.*
Hint: Select numbers, $x_1 \in X_1$ and $x_2 \in X_2$ obeying $Y_1^2 + Y_2^2 \leq 1$ where Y_1 and Y_2 are both uniformly distributed on the interval $]-1;1[$.

Exercise 3.5.2 (Sum of two random variables) *In general, if $Z = X + Y$ is the sum of two random variables with joint pdf, $f_{XY}(x,y)$, then the pdf of Z is given by*

$$f_Z(z) = \int_{-\infty}^{\infty} f_{XY}(x, z-x)dx.$$

As an example let X and Y be uniformly distributed on the interval $[0,1]$. Calculate the pdf of $Z = X + Y$.

Assignment 2 (Autoregressive process) *Consider a simple autoregressive process, X_1, X_2, X_3, ... In such a series of numbers the $n+1$'th number is given from the n'th by*

$$X_{n+1} = \alpha X_n + \xi_n, \tag{3.5.1}$$

where $\xi_1, \xi_2, \xi_3, ...$ are independent Gaussian random variables with zero mean and unit variance, and $0 < \alpha < 1$.

Now, consider a number of realizations of the process given by eq. 3.5.1. The initial random number is supposed to have zero mean.

- *Prove mathematically that every X_n then also have zero mean.*
- *Prove mathematically that if n is large, then the variance of X_n is $1/(1-\alpha^2)$.*

Make a computer program that simulates such a process, with the initial value X_1 Gaussian distributed with zero mean and variance $1/(1-\alpha^2)$. Simulate some long (at least several thousand points) time series and calculate the following:

- *The mean and variance of the time series*
- *The autocorrelation function for different values of α*

From eq. 3.5.1, show that the autocorrelation function is given by $\rho(n) = \alpha^n$ and compare with the simulated. Finally you should comment on the following questioned

- *What is the relation of the simulated time series to measured wind speeds? and, What is the role of α?*

3.6 Spectral theory and time series

Let us look at the surface measurements of wind speed in a spectral way. In Figure 3.6.1 the spectrum of such quantity is presented. On the abscissa we have the frequency. i.e. high frequencies (to the right) refer to fast fluctuations (small time scales) while low frequencies (to the left) refer to slow fluctuations (large time scales). Later, we will see that the fast fluctuations are associated with small spatial scales while the slow fluctuations are associated with the large spatial scales. On the ordinate the kinetic energy associated with a given frequency is plotted.

In the Figure, two local maximum are identified: the small one to the right at frequencies around $10^{-2} - 10^{-1}$ Hz, corresponds to motion with time scales around minutes. This part of the spectrum is associated with what we term turbulence. To the left in the spectrum a maxima at frequencies around $10^{-6} - 10^{-5}$ Hz, corresponding to a a couple of days, is located. This part is associated with the local weather, which in this particular case is the Danish weather.

Not coincidentally the time scale here, a couple of days, is the predictable range of most good weather forecasts. The gap between the two *bumps* is called the spectral gap. It is located around 10 minutes to one hour. The existence and location of the gap is one of the reasons why we often use 10-30 minutes averages when characterizing the mean wind and its standard deviation.

In the context of wind energy the spectrum is a very important way of looking at the wind fluctuations. Fluctuations on high frequencies are directly associated to turbulence and hence loads and fatigue on wind turbines. The low part of the spectrum, on the other hand, is associated with fluctuations of the mean wind. Considering grid integration and power output from nearby turbines, knowledge of the precise form of the low pass spectrum is important.

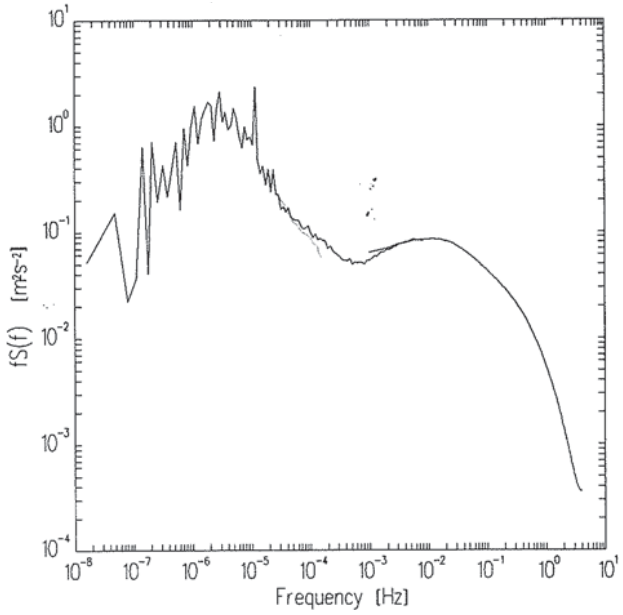

Figure 3.6.1: Spectrum of wind speed fluctuations at 30 m height from data measured at Lammefjord, Denmark from June 1988 to June 1989. With permissions from M.S. Courtney (Courtney and Troen, 1990)

.

3.6.1 Mathematical definition

The basis for spectral theory is the covariance function (at the moment we do not distinguish between the autocovariance and the crosscovariance), $R_{XY}(\tau)$, and its Fourier transform, the spectrum, $S_{XY}(\omega)$. Here, $\omega = 2\pi f$ is the angular frequency while f is the cyclic frequency. The two functions form the very useful Fourier transform pair

$$S_{XY}(\omega) = \frac{1}{2\pi}\int_{-\infty}^{\infty} R_{XY}(\tau)e^{-i\omega\tau}d\tau \tag{3.6.1}$$

$$R_{XY}(\tau) = \int_{-\infty}^{\infty} S_{XY}(\omega)e^{i\omega\tau}d\omega, \tag{3.6.2}$$

with the imaginary unit $i^2 = -1$. The spectrum describes how the covariance is distributed on different frequencies. As we will learn later in the course this is quite important in turbulence studies. For example, in a turbulent flow the most variance is located on slowly evolving eddies corresponding to large spatial scales compared to the faster and smaller scales.

Setting $\tau = 0$ we obtain the covariance

$$\sigma_{XY}^2 = \int_{-\infty}^{\infty} S_{XY}(\omega) d\omega. \tag{3.6.3}$$

We can expand the complex exponential in eq. (3.6.1) as

$$\begin{aligned} S_{XY}(\omega) &= \frac{1}{2\pi}\int_{-\infty}^{\infty} R_{XY}(\tau)(\cos(\omega\tau) - \mathrm{i}\sin(\omega\tau))d\tau & (3.6.4)\\ &= \frac{1}{2\pi}\int_{-\infty}^{\infty} R_{XY}(\tau)\cos(\omega\tau)d\tau - \frac{\mathrm{i}}{2\pi}\int_{-\infty}^{\infty} R_{XY}(\tau)\sin(\omega\tau)d\tau & (3.6.5)\\ &= Co_{XY}(\omega) - \mathrm{i}Q_{XY}(\omega). & (3.6.6) \end{aligned}$$

$Co_{XY}(\omega)$ and $Q_{XY}(\omega)$ are named the cospectrum and quadspectrum respectively. Since $\sin(\tau)$ is an odd function of τ, the quadspectrum must be zero if $R_{XY}(\tau)$ is an even function in τ. This happens if $X = Y$. This means that the autospectrum, $S_X(\omega)$, is real-valued. In the more general case where $X \neq Y$, the crosscovariance $R_{XY}(\tau)$, is not necessarily an even function, and hence the crossspectrum, $S_{XY}(\omega)$, is complex

3.6.2 Spectra from measured time series

In practical terms, the definition given by eq. 3.6.1 turns out to be a little clumsy and quite time consuming. In this section we will therefore sketch a much nicer road, one which is easyly adapted to real measurements of for example wind speed.

For a single stochastic process, $X(t)$, described by an ensemble of infinitely long time series $\{x_1(t), x_2(t), ..., x_k(t), ...\}$, the autospectrum

$$S_X(\omega) = \frac{1}{2\pi}\int_{-\infty}^{\infty} R_X(\tau)\mathrm{e}^{-\mathrm{i}\omega\tau}\mathrm{d}\tau \tag{3.6.7}$$

is equivalent to

$$\boxed{S_X(\omega) = \lim_{T\to\infty}\left\langle S_{X,k}(\omega, T)\right\rangle,} \tag{3.6.8}$$

where

$$X_k(\omega, T) = \frac{1}{2\pi}\int_0^T x_k(t)\mathrm{e}^{-\mathrm{i}\omega t}\mathrm{d}t, \tag{3.6.9}$$

and $S_{X,k}(\omega, T)$ is defined as

$$S_{X,k}(\omega, T) = \frac{2\pi}{T}\left|X_k(\omega, T)\right|^2. \tag{3.6.10}$$

The proof goes as follows. From the definitions above

$$S_{X,k}(\omega, T) = \frac{1}{2\pi T}\int_0^T\int_0^T x_k(t)x_k(t')\mathrm{e}^{-\mathrm{i}\omega(t'-t)}\mathrm{d}t'\mathrm{d}t \tag{3.6.11}$$

Taking the average on both sides we get

$$\begin{aligned}\left\langle S_{X,k}(\omega,T)\right\rangle &= \frac{1}{2\pi T}\int_0^T\int_0^T R_X(t-t')\mathrm{e}^{-\mathrm{i}\omega(t'-t)}\mathrm{d}t'\mathrm{d}t \\ &= \frac{1}{2\pi}\int_{-T}^{T} R_X(\tau)\mathrm{e}^{-\mathrm{i}\omega\tau}\left(1-\frac{|\tau|}{T}\right)\mathrm{d}\tau \\ &\to S_X(\omega) \quad \text{as } T\to\infty. \end{aligned} \tag{3.6.12}$$

The main result expressed in eq. 3.6.8 means that we can obtain the spectrum, $S_X(\omega)$, by Fourier transforming the individual time series, $x_k(t)$, and then average the absolute squares. This is indeed much simpler than calculating the autocorrelation function, R_X, and then Fourier transforming.

Real measurements are, however, not given as a continuous function of time but as discrete values separated in time by a fixed value Δt,

$$x(n\Delta t), \quad \text{for } n = 0,1,2,....$$

This means that we have to work out a discrete form of eqn. 3.6.8. It goes something like this...

The *sampling frequency* is defined as $f_s = 1/\Delta t$. Also we do not in practice have infinite time series ($T\to\infty$) or infinitely many realizations. Rather we are left with a single time series of finite duration.

Nevertheless, we can use eq. 3.6.8 in the following way. Split the time series into K parts each of length N:

$$\begin{gathered} x_1(t) = x(\Delta t), x(2\Delta t), ..., x(N\Delta t) \\ \vdots \\ x_K(t) = x([(K-1)N+1]\Delta t), x([(K-1)N+2]\Delta t), ..., x(KN\Delta t). \end{gathered}$$

For a time series sampled at f_s the highest frequency, at which one can hope to estimate the spectrum is the *Nyquist frequency* $f_N = f_s/2$. The spectrum is hence estimated at the frequencies

$$f_l = \frac{\omega_l}{2\pi} = f_s\frac{l}{N} = \frac{l}{\Delta t N} \text{for } l = 1,...N/2. \tag{3.6.13}$$

Now approximate eq. 3.6.9 with (taking the first time series $x_1(t)$, defining $x_n = x(n\Delta t)$, and dropping the subscript k)

$$X(\omega_l,T) = X(l,T) = \frac{1}{2\pi}\sum_{n=0}^{N-1} x_n \exp\left(-\mathrm{i}\frac{2\pi l n}{N}\right)\Delta t. \tag{3.6.14}$$

Finally, eq. 3.6.10 is approximated by

$$\boxed{S_{X,k}(\omega,T) = \frac{1}{2\pi N f_s}\left|\sum_{n=0}^{N-1} x_n \exp\left(-\mathrm{i}\frac{2\pi l n}{N}\right)\right|^2,} \tag{3.6.15}$$

which then has to be averaged over the K time series as expressed through eq. 3.6.8. The higher the value of K chosen, the smaller the time series and the more you miss out on the lowest frequencies, whereas the highest frequencies are more averaged, and hence appear less noisier in the plot of the spectra. The discrete Fourier transform of eq. 3.6.15 is easily performed in Mathematica or Matlab by the routines, `Fourier[X, FourierParameters -> {1, 1}]` and `fft(X)` respectively.

When you calculate spectra from time series, keep in mind, whether you use the angular frequency, ω, which have been extensively used in these notes or the cyclic frequency, f. It can easily be verified that,

$$\boxed{\omega S_{XY}(\omega) = f S_{XY}(f).} \tag{3.6.16}$$

The covariance is given by eq. 3.6.3. Graphically this means that plotting the spectra with linear abscissa, the covariance equals two-times the area under the curve (if integrated from minus to plus infinity). Since atmospheric motion possesses many orders of magnitude, from seconds to years it is often convenient to plot spectra with logarithmic abscissa. Since $d\log f = df/f \Rightarrow df = f d\log f$, the covariance can also be written as

$$\sigma_{XY}^2 = \int_{-\infty}^{\infty} \omega S_{XY}(\omega) d\log\omega. \tag{3.6.17}$$

This means that plotting with logarithmic abscissa and with $\omega S_{XY}(\omega)$ on the ordinate, the area under the curve (if integrated from minus to plus infinity) still equals half the covariance.

Exercise 3.6.1 (Derivation of ensemble spectra) *Go through the step from the first to the second line in eq. 3.6.12.*
Hint: Make a change of variables with $u = t - t'$ and $v = t + t'$ and recall that for any function, $f(t,t')$ we have

$$f(t,t')dtdt' = f(u(t,t'),v(t,t'))|J|dudv, \tag{3.6.18}$$

where $|J|$ is the determinant of the Jacobian, $J = \partial(t,t')/\partial(u,v)$. Express v as $v(u)$ to get rid of one of the integrals.

Exercise 3.6.2 (Spectrum and time differentiation) *Show, that if the spectrum of X is $S_X(\omega)$, then the spectrum of $\dot{X} = dX/dt$ is*

$$S_{\dot{X}}(\omega) = \omega^2 S_X(\omega). \tag{3.6.19}$$

Assignment 3 (Turbulence and spectra) *You are provided via CampusNet with a time series of horizontal (u) wind speeds measured 10 times per second in two hours, that is 72000 samples. The file name is* `sonic1u10Hz.dat` *and it is stored in the data directory. The data are measured at the top of 70 m mast on the island of Sprogø.*

- *Calculate the average wind speed.*
- *Calculate the variance and standard deviation.*
- *When plotting the spectrum in a log-log coordinate system with frequency, ω, on the abscissa and $\omega S_{XY}(\omega)$ on the ordinate, the high frequency end of the spectrum may appear quite noisy or crowded.*

  Make a computer program (algorithm) that average neighboring frequency bins, so that at most n spectral estimates appear in each decade. n should typically be between 10 and 20.
- *Calculate and plot in a log-log plot the spectrum. The sum appearing in eq. 3.6.15 is called the discrete Fourier transform. Read carefully the definition of discrete Fourier transform in your programming language. Try different values of K. Apply the log-log smoothing filter from the previous question.*
- *Calculate the spectrum of the 21 year time series Sprogø time series of 10-min averages provided in assignment 1. Can you see a diurnal peak or an annual peak?*
- *Calculate the spectrum for the Autoregressive process you simulated in Assignment 2. Here we assume that the sampling time is $\Delta t = 1$ and that $\alpha = \exp(-\Delta t/T)$. Then the theoretical autocovariance function of that process is known to be $R_X(\tau) = \alpha^\tau/(1-\alpha^2)$. Using eq. 3.6.7, calculate the theoretical spectrum and compare with the simulated.*

3.6.3 Coherence

As a last thing in this section we define the coherence (or spectral coherence)

$$\mathrm{coh}_{XY}(\omega) = \frac{|S_{XY}(\omega)|^2}{S_X(\omega)S_Y(\omega)}. \tag{3.6.20}$$

The definition implies $0 \leq \mathrm{coh}_{XY}(\omega) \leq 1$, where the upper limit corresponds to X=Y. The coherence is a measure of the spectral correlation. Its definition and usage will become much more clear when we will look at dynamical loads on turbines and buildings in general.

3.7 Fourier simulation

The previous section on generation of random numbers is vital for this section on Fourier simulations. The application lies primarily within load calculations. Coming from the section on spectra, we will in this section reverse the order of Fourier transforming, so to speak: Instead of calculating the spectrum from a given time series, we want to simulate a time series from a given spectrum.

A natural starting point is therefore the last section...

Multiply eq. 3.6.14 by $\exp(\mathrm{i}2\pi lm/N)$, sum over all $l = 0, 1, ..., N-1$, and divide by N (which is the definition of the *inverse discrete Fourier transform*),

$$\begin{aligned} \frac{1}{N}\sum_{l=0}^{N-1} X(l,T)\exp\left(\mathrm{i}\frac{2\pi lm}{N}\right) &= \frac{\Delta t}{2\pi N}\sum_{l=0}^{N-1}\sum_{n=0}^{N-1} x_n \exp\left(\mathrm{i}\frac{2\pi l(m-n)}{N}\right) \\ &= \frac{\Delta t}{2\pi N}\sum_{n=0}^{N-1} x_n \sum_{l=0}^{N-1} \exp\left(\mathrm{i}\frac{2\pi l(m-n)}{N}\right) \end{aligned} \tag{3.7.1}$$

Now we use a property of the geometric series

$$\sum_{l=0}^{N-1} a^l = \frac{1-a^N}{1-a}$$

where a is any complex number different from 1. We now set $a = \exp(\mathrm{i}2\pi(m-n)/N)$ and look at the two cases:

$$\frac{1-a^N}{1-a} = \begin{cases} 0, & n \neq m \\ N, & n = m. \end{cases} \tag{3.7.2}$$

The result of $m \neq n$ is a consequence of the 2π periodicity of $\exp(\mathrm{i}2\pi n)$, where n is an integer, while L'Hôpital's rule was used to obtain the result for $n = m$. Finally eq. 3.7.2 becomes

$$\frac{1}{N}\sum_{l=0}^{N-1} X(l,T)\exp\left(\mathrm{i}\frac{2\pi lm}{N}\right) = \frac{\Delta t}{2\pi} x_m. \tag{3.7.3}$$

So, if we know all the Fourier modes, $X(l,T)$ we can generate the time series x_m in physical space. It is easy to verify the inverse discrete Fourier transformation in the above equation by taking a look at the forward discrete Fourier transformation given in eq. 3.6.14.

It is easily seen that the mean of $X(l,T)$ is zero, except for $l = 0$. For large T, the mean square of $X(l,T)$ is

$$\sigma^2_{X,l} = \frac{T}{2\pi} S_X(\omega). \tag{3.7.4}$$

It can also be shown that if $l \neq l'$ then $X(l,T)$ and $X(l',T)$ are uncorrelated. If x_n is Gaussian, then $X(l,T)$ is complex Gaussian and $X(l,T)$ and $X(l',T)$ are independent.

The inverse Fourier transform on the left hand side of eq. 3.7.3 can be calculated in Mathematica and Matlab with the functions `Fourier[X, FourierParameters -> {-1, 1}]` and `ifft(X)` respectively.

IMPORTANT: The vector of Fourier components is complex, but it should have a special complex conjugated symmetry in order to produce a real-valued time series. With Matlab and Mathematica (and most other program packages) index rules we write this vector as

$$\overline{X} = \left\{ \begin{array}{c} \boxed{1} \quad \boxed{2} \quad \boxed{3} \quad \boxed{4} \quad \boxed{\text{N/2+1}} \quad \boxed{\text{N-1}} \quad \boxed{\text{N}} \\ a_0, a_1 + \imath b_1, a_2 + \imath b_2, a_3 + \imath b_3, \ldots, a_{N/2} + 0, \ldots, a_2 - \imath b_2, a_1 - \imath b_1 \end{array} \right\} \tag{3.7.5}$$

There is no systematic phase lag in the random Fourier components, so the variance is distributed equally among real and imaginary parts

$$\sigma_{a_l}^2 = \sigma_{b_l}^2 = \frac{1}{2}\sigma_{X,l}^2 \tag{3.7.6}$$

The highest frequency in the power spectrum is half the sample frequency $f_{N/2} = 0.5 f_s$ and the lowest frequency is $f_1 = f_s/N$. They respectively correspond to positions $N/2+1$ and 2 in the Fourier component vector. The sample frequency is $f_s = 1/\Delta t$ and the duration of the time series is $T = N\Delta t$. Notice that for $l = 1$ and $l = N/2+1$, $X(l)$ is real. There is two ways you can determine the first value (a_0 in eqn 3.7.5). X_1 should be set to $X_1 = T/(2\pi)U$ or alternatively set $X_1 = 0$ and add U to the result of the transformation as a last step.

Exercise 3.7.1 (Finite geometric series) *Proof eq. 3.7 by expanding the l.h.s*

$$S = \sum_{l=0}^{N-1} a^l. \tag{3.7.7}$$

Assignment 4 (Fourier simulation) *The Kaimal spectrum is defined by*

$$S_u(f) = u_*^2 \frac{52.5z/U}{(1+33n)^{5/3}} \tag{3.7.8}$$

where $n = fz/U$. We will come back to the physical reasoning behind the Kaimal spectrum in Section 6. Make a program that generates time series with this spectrum at $z = 70\,m$, $U = 20\,m\,s^{-1}$ and $u_* = 1\,m\,s^{-1}$. Calculate the spectrum from the generated time series to check that you get the Kaimal spectrum back. **Notice** *that the Kaimal spectrum as defined above is given as a function of f and not ω!*

A recipe *for generating a time series, x_n, with a given spectrum, in this case the Kaimal spectrum, could look something like this:*

1. *Choose a record length, N.*
2. *Make a list, $X(l)$, of random complex numbers of length $N/2$. Use a zero mean unit variance Gaussian distribution. Make a random number for both the real part and the imaginary part. This means that you should generate $2*N/2$ random numbers. We use the letter l to index the members of X.*
3. *Multiply each member, l in X with the correct standard deviation $\sigma(X,l)$, which you get from the Kaimal spectrum.*
4. *Expand X with the index rules given by to eq. 3.7.5. Use the build-in function of complex conjugation,* `Conjugate[X]` *and* `conj(x)`*, in Mathematica or Matlab respectively.*
5. *Inverse Fourier transform X and make the correct normalization. If the resulting time series, x is not real valued but instead complex, you did not do step 4 correct.*

CHAPTER 4

TURBULENCE AND MICROMETEOROLOGY

The atmospheric boundary layer (ABL) is the part of the atmosphere closest to the ground. It is also the part of the atmosphere mostly dominated by turbulent motion: on a warm sunny day with deep convection the height of the layer might reach a kilometer or two while it on clear nights might only be of the order a hundred meters. The layer is capped by a strong temperature inversion, with $d\theta/dz > 0$ aloft - θ being the potential temperature (see Exercise 4.2.4).

Turbulence in the ABL is generated by in principle two different mechanisms: wind shear (mechanical forcing) and heat convection (thermal forcing). The first mechanism is due to the fact that the wind speed has to approach zero as the surface is approached. The second mechanism is due to thermal effects: in situations of strong convection (unstable conditions) the warm surface releases heat to the relatively colder atmosphere and hence enhancing the turbulence level by converting potential energy to kinetic energy (remember that the atmosphere is heated from below!). The picture is reversed during night time with strong cooling (stable conditions), where the strong stratification of the ABL prohibits the development of turbulence. The best way to get a idea of the stability at a given day is to look at the smoke from a chimney: whereas almost laminar horizontal plumes are signatures of stable stratification, erratic and irregular growing plumes correspond to unstable stratification.

At the top of the ABL in the free atmosphere the wind is close to geostrophic (at mid latitudes at least) as given by eq. 2.2.11. In the ABL the Coriolis force also gives rise to the so called Ekman spiral which causes the wind direction to change with height (to the right on the northern hemisphere and to the left on the southern) - see Exercise 4.3.2.

Until now, there has been a tendency in the wind energy community to ignore the effects of both stratification and wind veer, since both effects has the largest impact at high altitudes above the hub height of most wind turbines. The modern development of large wind turbines, however, forces us to change our view and introduce these two effects in both modeling of the wind resources and of the turbulence used for load calculations.

4.1 Introducing turbulence

Some initial remarks about turbulence might seem relevant. A lot can be said, instead of being systematic I will present a few different pictures of turbulence, which I believe, might help to understand some of the basic features and challenges. One definition could be:

> *Turbulence is the physical manifestation of the solutions to the Navier-Stokes equation when the Reynolds number is large...*

So, what is the Navier-Stokes equations and what is the Reynolds number then? The Navier-Stokes equation describes the motion of fluids, that is, liquids and gases. For some large non-dimensional number, the Reynolds number, the motion becomes turbulent. The Reynolds number is defined as

$$Re = \frac{\widetilde{U}\widetilde{L}}{\nu}, \tag{4.1.1}$$

where $\widetilde{U}$, $\widetilde{L}$ are the characteristic velocity and length of the flow, respectively, and ν is the kinematic viscosity of the fluid. In the atmospheric surface layer (approximately the lowest 100 m of the atmosphere we have

$$Re \sim \frac{10\,\mathrm{m\,s^{-1}} \times 100\,\mathrm{m}}{15 \cdot 10^{-6}\,\mathrm{m^2\,s^{-1}}} \sim 10^8. \tag{4.1.2}$$

This is indeed a large number, and the surface layer can be characterized as being in a turbulent state.

Exercise 4.1.1 (Navier-Stokes equation) *The Navier-Stokes equation for a Newtonian fluid (basically non-elastic!) with velocity, $\boldsymbol{U}(\boldsymbol{x},t)$, density, ρ and kinematic viscosity, ν, is given by*

$$\frac{\partial \boldsymbol{U}(\boldsymbol{x},t)}{\partial t} + \boldsymbol{U}(\boldsymbol{x},\boldsymbol{t})\nabla \boldsymbol{U}(\boldsymbol{x},\boldsymbol{t}) = -\frac{1}{\rho}\nabla p(\boldsymbol{x},t) + \nu\nabla^2 \boldsymbol{U}(\boldsymbol{x},\boldsymbol{t}), \tag{4.1.3}$$

where $p(\boldsymbol{x},t)$ is pressure and ∂ refers to partial differentiation. In the ABL the air is close to incompressible. This is expressed through the continuity equation

$$\nabla \cdot \boldsymbol{U}(\boldsymbol{x},\boldsymbol{t}) = 0. \tag{4.1.4}$$

Show that for high Reynolds numbers the influence of the viscous term vanish (the last term on the r.h.s.). Hint*: Choose a characteristic length scale, $\widetilde{L}$ and velocity, $\widetilde{U}$ and non-dimensionalize eq. 4.1.3.*

The mathematical intractability of the Navier-Stokes equation in high Reynolds number flow is obvious: even the slightest perturbation to the initial of boundary conditions will result in chaotic behavior. This is considered the *problem of turbulence*. Solving the Navier-Stokes equation is on the other hand not the most important task in a wind energy context. We really don't care about how each individual air parcel governed by the Navier-Stokes equation behave: a wind

turbine is a large structure which only react on larger scales in the flow or you could say averaged properties of the wind. At the core of this is the Reynolds Average Navier-Stokes equation (RANS). We will, however, not introduce it before later in this section. Instead we will introduce another way - and perhaps the best way! - of defining turbulence. This is due to Tennekes and Lumley (1972). They summarize the physical properties of turbulence by the following seven items:

1. *Irregularity*: It is irregular and random. We must therefore use statistical methods when dealing with turbulence. Section 3 is therefore essential learning.

2. *Diffusivity*: Rapid mixing and transport of momentum and heat.

3. *Large Reynolds number*: The turbulent state is reached trough a transition from a laminar state when some critical Reynolds number has been exited. The critical Reynolds number varies largely from case to case.

4. *Three-dimensional*: Turbulent motion is three dimensional and dominated by fluctuating vorticity (the curl of velocity). It is therefore natural to consider turbulence as eddies of different size breaking up and forming new eddies.

5. *Dissipative*: Viscous forces converts kinetic energy into heat. This means that if the force generating the turbulence stops, the turbulence will die out.

6. *Continuum*: We don't consider individual molecules. The fluid is a continuum and is described through fields.

7. *Turbulence is a property of flows*: Turbulence is not a feature of fluids but of fluid flows.

4.1.1 The turbulent cascade

Lastly we will introduce the perhaps most widespread picture of turbulence: namely the one due to Richardson (Frisch, 1995). He came up with a simple phenomenological model of turbulent cascade shown in Figure 4.1.1: turbulence is created at large scales, L, in terms of rotating eddies by the application of some external force - think of the stirring in a cup of coffee with a tea spoon (in the atmosphere this could be a large scale vertical shear in the wind speed or convective overturning). The added energy injected into the fluid, the atmosphere in our case, is then transferred by the breaking up of larger eddies into smaller eddies, until at some small scale molecular forces become important and convert kinetic energy into heat. The scale, η, at which viscous forces become important is known as the Kolmogorov scale while the kinetic energy cascading from large scales to small scales is equal to the kinetic energy dissipation, ε.

Even though the Richardson picture is somehow naive it still provides us with valuable insight into the phenomenology of turbulence. Deviations from this simple picture is way beyond the scope of this course (see Frisch (1995) for a detailed account).

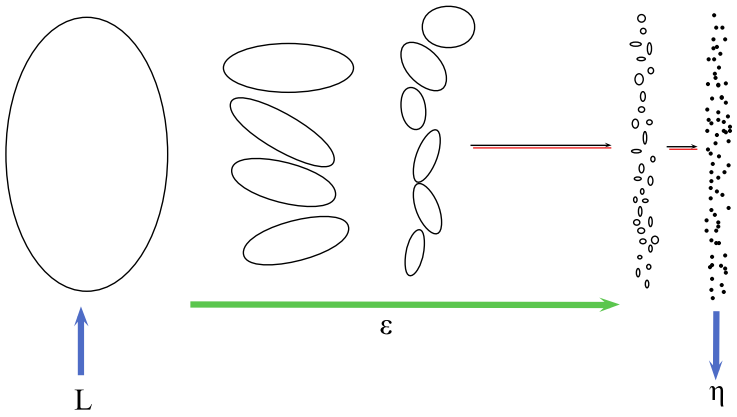

Figure 4.1.1: The Richardson phenomenological model of turbulence. Energy is injected into the fluid at a scale, L and converted into heat at a smaller scale, η. By the breaking up of larger eddies into smaller eddies, the dissipative kinetic energy, ε, is cascading from large scales to small scales.

4.1.2 Buckingham Π theorem

Because of our inability to solve the Navier-Stokes equation directly, we often use dimensional analysis. This kind of analysis is wide spread in fluid mechanics and in the atmospheric sciences. The drawback of the technique is that we are always left with some unknown constants, which have to be determined experimentally. At the core of the discipline is the Buckingham Π theorem which states that the optimal number of dimensionless groups, $\pi_1, \pi_2, ...$ which can be formed for a physical system equals $m-n$, where m is the number of physical relevant quantities describing the system and n is the number of independent physical dimensions of the system (like meter, seconds, Kelvin etc.). Furthermore the dimensionless groups are related in a way, such that $\pi_1 = f(\pi_2, ..., \pi_{m-n})$.

The perhaps most well known use of the theorem is due to Kolmogorov back in 1941 (Frisch, 1995). The theory therefore also bear the name K41. Kolmogorov hypothesized that there exist a range of scales, $L \ll \ell \ll \eta$, called the inertial range which are unaffected by both forcing at scale, L and viscous forces at scale, η. Furthermore the velocity, $u(\ell)$, at scale ℓ is a function of the kinetic energy dissipation, ε and ℓ only. From the Buckingham Π theorem we thus have $m = 3$ and $n = 2$ (meters and seconds), and therefore one dimensionless group, i.e. a constant (here taken to be one):

$$u(\ell) \sim \varepsilon^{1/3} \ell^{1/3}. \tag{4.1.5}$$

As we will see again when dealing with the spectral properties of turbulence in Section 6, the inertial range plays a significant role in turbulence and hence in the atmospheric boundary layer.

Exercise 4.1.2 (*K41) *Besides the existence of an inertial range, Kolmogorov furthermore postulated that the scales at which viscous effects become important, the Kolmogorov length scale, η, and Kolmogorov time scale, τ_η, respectively, are functions of the kinetic energy dissipation, ε and the kinematic viscosity of the fluid, ν, only. Find the expressions for η and τ_η.*

The kinematic viscosity for air is $\sim 1.5 \cdot 10^{-5} m^2\, s^{-1}$. *What is typical values for* η *and* τ_η *in the ABL?*

4.2 The surface layer

The surface layer of the atmosphere is defined as a region inside the ABL, above the ground, where the vertical momentum and heat fluxes are almost constant. Usually 'almost constant' means a variation of less than 10% implying that the surface layer is at most a few hundred meters for most situations relevant for wind engineering. In this layer the wind structure is determined primarily by surface friction and the vertical gradient of temperature.

When the effects of temperature differences, i.e. thermally driven turbulence, are negligible compared to the wind shear, the boundary layer flow is called *neutral*. Since this is the case for high wind speeds, the neutral state is the most relevant for wind energy.

We use the following coordinate system convention: a position in space is described in a right-handed coordinate system usually with the origin at the surface. 'x is in the direction of the mean wind, U, y is the horizontal direction perpendicular to the mean wind, and z is pointing vertically upwards. The mean wind speed at a height z is denoted by $U(z)$, while fluctuations along the x-, y-, and z-directions are called u, v and w, respectively. The average of a fluctuating quantities equals zero. The average of the product of fluctuating quantities are, however, not necessarily zero. The procedure sketched briefly here is called a Reynolds decomposition (see Exercise 4.3.1). To sum up: we have

$$\begin{aligned} U_m(x,y,z,t) &= U(z) + u(x,y,z,t) \\ V_m(x,y,z,t) &= v(x,y,z,t) \\ W_m(x,y,z,t) &= w(x,y,z,t), \end{aligned} \tag{4.2.1}$$

where we for clarity have added a subscript, m, to the total velocity in order to highlight that this could very well be a measured velocity.

4.2.1 The neutral wind profile

To determine the wind profile over horizontally homogeneous terrain we use dimensional analysis as presented through the Buckingham Π theorem.

In stationary neutral flow over flat terrain (homogeneous terrain, i.e. no variation of the flow in the streamwise or transverse direction) there is, because of the 'no-slip' condition, a continuous transmission of momentum from the flow to the surface, in other words drag. This drag is clearly in the true opposite direction of the mean flow and in order to get downward momentum transport it is necessary to have a velocity gradient. Conversely; What would the necessary gradient in the mean velocity be in order to sustain some frictional force per unit area of the terrain denoted by τ (not to be confused with a time lag), which is also the rate of momentum transmitted from the layers of air higher in the atmosphere to those nearer the ground? Since the viscosity, ν, is unimportant for the transportation of momentum (because of the usually very high Reynolds

numbers in the atmosphere), the only other independent parameter, except for τ and z, available for the description of dU/dz is the density of air, ρ. The only, since $m-n=4-3=1$ (the three dimensions being meter, seconds and kilogram), combination of these four quantities which has the dimension of velocity gradient is

$$\frac{dU}{dz} = \text{const}\sqrt{\frac{\tau}{\rho z^2}} = \frac{u_\star}{\kappa z}, \tag{4.2.2}$$

where the *friction velocity* u_* is defined by

$$\tau = \rho u_*^2. \tag{4.2.3}$$

Here $\kappa \approx 0.4$ is the dimensionless *von Kármán constant* which has to be determined experimentally. Since the viscosity is of no importance in the atmospheric boundary layer the frictional force may be written as $\tau = -\rho\langle uw\rangle$ (recall ensemble averaging from Section 3), i.e. the downward flux of horizontal specific momentum. The friction velocity can therefore be written as

$$u_*^2 = -\langle uw\rangle. \tag{4.2.4}$$

The solution to eq. 4.2.2 is the logarithmic velocity profile (log-law):

$$\boxed{U(z) = \frac{u_\star}{\kappa}\log\left(\frac{z}{z_0}\right),} \tag{4.2.5}$$

where the roughness length, z_0, is an integration constant. In Figure 4.2.1, the logarithmic wind profile is shown for various values of $u_\star$ and z_0. The roughness length cannot directly be interpreted as a typical length of the surface inhomogeneities, but rather as a measure of their ability to 'catch' momentum from the wind. Typical values are given in Table 4.2.1.

In Figure 4.2.2 we have sketched the full ABL with the inner layer, the surface layer in neutral stratification is assumed.

4.2.2 Turbulence intensity

The turbulence in flow over flat terrain with uniform roughness length, z_0, often stated as homogeneous conditions, is also often easy to characterize. Some rule of thumbs exist based on a large number of field measurements relating the standard deviations of the wind fluctuations, σ_u, σ_v and σ_w, to the surface friction, $u_\star$:

$$\sigma_u = Au_\star, \quad \sigma_v \sim 0.75\sigma_u \text{ and } \quad \sigma_w \sim 0.5\sigma_u, \tag{4.2.6}$$

where A depends on the roughness length, z_0. Some typical numbers are $z_0 = 0.05\,\text{m}$, $A = 2.5$ while for $z_0 = 0.3\,\text{m}$, $A = 1.8$. Since the turbulent fluctuations, σ_u, σ_u and σ_w are approximately independent of height in the surface layer, we have removed the height dependence. It is also worth noting that, $\sigma_u \gg \sigma_v \gg \sigma_w$.

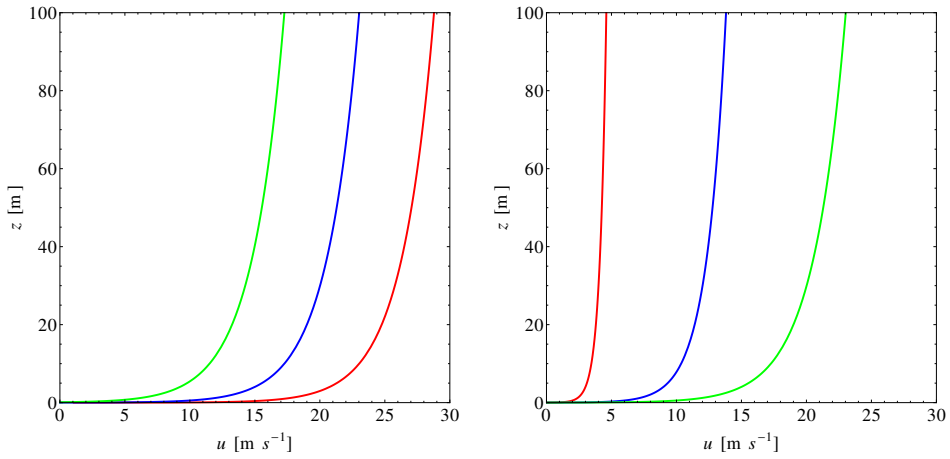

Figure 4.2.1: The log-law for different values of z_0 and $u_\star$. *Left panel*: Constant u_{star} and $z_0 = 0.001\,\mathrm{m}$ (red), $z_0 = 0.01\,\mathrm{m}$ (blue) and $z_0 = 0.1\,\mathrm{m}$ (green). *Right panel*: Constant z_0 and $u_\star = 0.2\,\mathrm{m\,s^{-1}}$ (red), $u_\star = 0.6\,\mathrm{m\,s^{-1}}$ (blue) and $u_\star = 1.0\,\mathrm{m\,s^{-1}}$ (green).

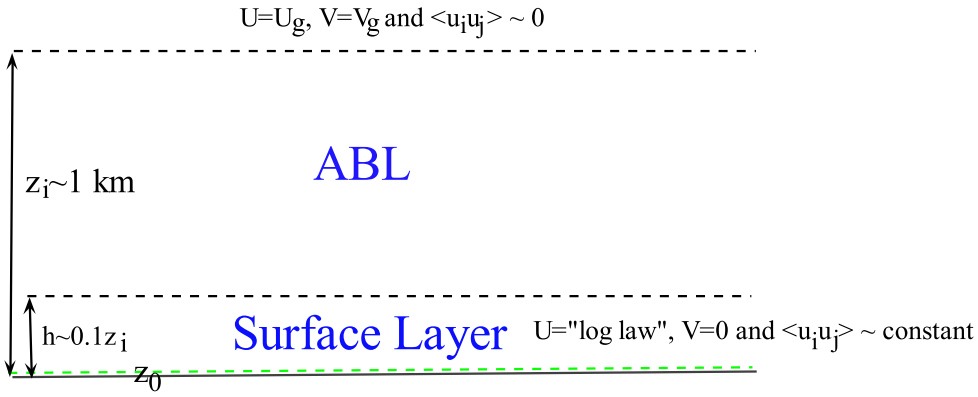

Figure 4.2.2: The atmospheric boundary layer (ABL) in neutral stratification with characteristic properties given inside the surface layer and above the ABL. The Reynolds stresses $\langle u_i u_j \rangle$ is presented in tensor notation with i and j running from 1 to 3.

Another often used quantity is the turbulence intensity, $I_u(z)$, defined as

$$I_u(z) = \frac{\sigma_u}{U(z)}. \tag{4.2.7}$$

For most applications it is between 0.05 an 0.2. Following the IEC standard (International Electrotechnical Commission, 2005) turbines are chosen according to (among others) the site specific I_u (See Chapter 9.

Exercise 4.2.1 (turbulence intensity) *Show that for $A = 2.5$, the turbulence intensity is given by*

$$I_u(z) = \frac{1}{\log(z/z_0)}. \tag{4.2.8}$$

z_0 m	Terrain
1.00	city
0.80*	forest
0.50	suburbs
0.30	shelter belts
0.20	many trees and/or bushes
0.10	farmland with closed appearance
0.05	farmland with open appearance
0.03	farmland with very few buildings / tress
0.02	airport areas with buildings and trees
0.01	airport runway areas
0.008	mown grass
0.005	bare soil (smooth)
0.001	snow surfaces
0.0003	sand surfaces (smooth)
0.0001	water areas (lakes, fjords, open sea)

Table 4.2.1: Roughness lengths for different terrain types (Troen and Petersen, 1989). *The roughness length for forests is not at all well established. Often z_0 as large as 2 m or 10% the height of the canopy gives the most promising results.

4.2.3 Water roughness length

Contrary to a land surface, which is fairly undisturbed by the wind, a water surface responds readily to wind. Stronger wind means a more irregular and wavy surface implying larger roughness. Charnock (1955) argued that the roughness, z_0, of a water surface is determined by the momentum transport through the surface, the acceleration due to gravity, $g = 9.8\ \mathrm{m\,s^{-2}}$, which enters the wave equation, and the density of air. The only dimensionally correct relation (again good old Buckingham...) between those quantities is

$$z_0 = A_c \frac{u_\star^2}{g}, \tag{4.2.9}$$

where A_c, the dimensionless Charnock constant, must be determined experimentally. Together with the log-law this relation gives an equation relating mean wind speed at some height and roughness showing, as expected, the stronger the wind the rougher the sea. On the basis on an extensive literature study of ocean data, Garratt (1977) found by fitting somewhat scattered data $A_c = 0.0144$ while ESDU International (1982) recommends $A_c = 0.0162$. Among the various reasons for this variability are atmospheric stability, surface currents, 'wave age', length of the fetch over water, and water depth (Geernaert, 1987).

4.2.4 Power-law wind profile

In many wind engineering applications and in the IEC Standard a power-law wind profile is often used instead of eq. (4.2.5). In situations where wind speed is only measured at one height, the reference height, for example close to the hub height of a wind turbine, and only a narrow range around that reference height is studied, for example the rotor area, the power law is often a good approximation:

$$U(z) = U_{ref}\left(\frac{z}{z_{ref}}\right)^{\alpha}. \tag{4.2.10}$$

The shear exponent α is normally between 0.1 and 0.2.

Exercise 4.2.2 (Shear exponent and log-law) *Find the shear exponent, α, for the logarithmic wind profile given by eq. 4.2.5.*

4.2.5 Buoyancy driven wind profiles

Eq. 4.2.5 is only valid for neutral stratification. If we include temperature effects we can repeat the analysis adding two new variables; the surface heat flux, $Q_0 = \langle \theta w \rangle$ and buoyancy, g/T_0. Q_0 denotes the vertical advection of potential temperature. In an unstable atmosphere, Q_0 is positive, since the heat is released from the earth. In a stable atmosphere Q_0 is negative. In the buoyancy term T_0 is surface air temperature. With these two new variables the number of physical relevant quantities is $m = 5$. Similar we have $n = 3$ since temperature (in units of Kelvin) is now also a physical dimension of the system.

Now, $m - n = 2$ and we can therefore form two dimensionless groups. We take these to be $\pi_1 = \frac{z}{u_\star^3}\frac{du}{dz}$ (as in the neutral case) and $\pi_2 = \frac{z}{u_\star^3}\frac{g}{T_0}Q_0$. If we now define a length scale

$$\boxed{L = -\frac{T_0}{\kappa g}\frac{u_\star^3}{Q_0},} \tag{4.2.11}$$

we can write $\pi_2 = z/L$. L is known as the the Obukhov length scale. The factor $-1/\kappa$ has been included for practical reasons. From the Buckingham Π theorem we know that π_1 is a function of π_2. if we denote this function, ϕ_m we end up with an expression for the general wind profile including thermal stratification

$$\boxed{\frac{du}{dz} = \frac{u_\star}{\kappa z}\phi_m\left(\frac{z}{L}\right).} \tag{4.2.12}$$

If we compare eq. 4.2.5 and eq. 4.2.12, we see that for the neutral case $\phi_m = 1$. The neutral case is defined though the neglecting of temperature effects, i.e. Q_0 approaching zero. In this case we therefore have that $L = \pm\infty$. Similar we see that $L > 0$ in the stable case and $L < 0$ in the unstable case. The smaller the value of L the more important is the stratification. Roughly speaking we can use L as an indication of the height above the surface at which stability effects become important.

From measurements we can find the functional forms of $\phi_m(z/L)$ for stable and unstable conditions. Högström (1988) proposed the following forms: $\phi_m(z/L) = 1.0 + 4.8z/L$ for stable conditions and $\phi_m(z/L) = (1.0 - 19.3z/L)^{-1/4}$ for unstable conditions.

Exercise 4.2.3 (ϕ functions) *Plot the $\phi_m(z/L)$ functions for various values of z/L. Inspect and comment on the different profiles for unstable and stable flow.*

Another good parameter for quantifying stability is the *Richardson number* defined as

$$\boxed{Ri = \frac{g}{T}\frac{dT/dz - \Gamma_d}{(dU/dz)^2}.} \tag{4.2.13}$$

Here the dry adiabatic lapse rate, $\Gamma_d = -0.0098\,\mathrm{K\,m^{-1}}$, is valid for a neutrally stratified flow. This is a good number to remember: the temperature decreases (in the dry air surface layer) one degree per 100 m. T is the absolute mean temperature.

If two flows have the same Richardson number, then the relative deviations from the logarithmic velocity profiles are the same. A convective unstable flow has $Ri < 0$, a stable flow has $Ri > 0$, and neutral stratification corresponds to $Ri = 0$. See Figure 4.2.3 for a graphical explanation. From the definition of the Richardson number the *competition* between mechanical produced turbulence (in the denominator) and the thermally generated (the nominator) is evident. For very stable flows at which $Ri > 0.25$ turbulence is fully suppressed.

Exercise 4.2.4 (potential temperature) *The potential temperature is the temperature of an air parcel if you move it adiabatically to the surface. By adiabatically we understand that no heat exchange with the surroundings take place, in other words, the movement is very fast. The definition of the potential temperature, θ, is*

$$\theta = T(z)\left(\frac{p_0}{p(z)}\right)^{R/c_p}, \tag{4.2.14}$$

where $R = 287\,J kg^{-1} K^{-1}$ is the gas constant for dry air and $c_p = 1004\,J kg^{-1} K^{-1}$ is the specific heat at constant pressure. p_0 are the surface pressure and $p(z)$ and $T(z)$ is pressure and temperature at a given height, z, respectively. Derive the dry adiabatic lapse rate (temperature profile), $\Gamma_d = -0.0098\,K\,m^{-1}$. Hint: Use the hydrostatic balance, eq. 2.1.7, which is valid for neutral stratification, and the ideal gas law $p = \rho RT$.

The details in the above relations between Ri and z/L are at present not important. The key point is that both Ri and z/L are measures of the efficiency by which the buoyancy forces enhances or suppresses the mechanically produced turbulence. For most structural engineering applications effects of buoyancy can be neglected. However, there are important exceptions. Sometimes in stable flows, far above the surface, turbulence is almost completely suppressed. In these situations vortex shedding[4.2.1] (Simiu and Scanlan, 1996; Dyrbye and Hansen, 1997) is greatly

[4.2.1] Vortex shedding happens when air passes a blunt object as for example a round chimney. The passing air causes alternating low pressure vortices on the object, which in turn makes the object oscillate.

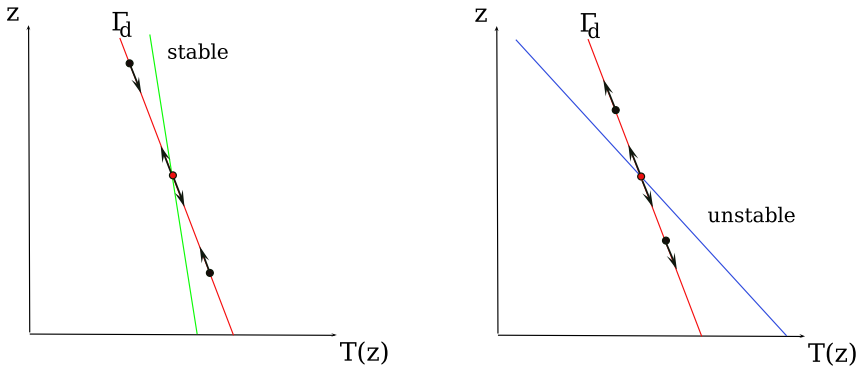

Figure 4.2.3: Temperature profiles: *Left:* Stable conditions (green profile): an air parcel which is pushed upwards (downwards) from its initial position (red dot) following the adiabatic lapse rate (red profile), will find itself colder (warmer) than the surroundings and will return to its original position. *Right:* Unstable conditions (blue profile): an air parcel which is pushed upwards (downwards) from its initial position (red dot) following the adiabatic lapse rate (red profile), will find itself warmer (colder) than the surroundings and hence continue its upward (downward) motion.

enhanced because it is not disturbed by turbulence. Some chimneys may experience their extreme loads in light stable winds. Also the Great Belt East Bridge has experienced (for the traffic) unacceptably large excitations of vertical motions, probably in situations where warm air moved out over a cold Great Belt, creating stable flow with absence of turbulence. This led to the last minute decision to mount guide vanes on the lower side of the bridge deck. The vanes were in place just before the official opening June 1998 and has apparently stopped the unwanted oscillations.

Another area where stability might be of importance is within the new generation of large wind turbines. Here the wind turbines' hub heights are above 100 m and therefore often above the surface layer.

Although being important in some situations we shall not discuss non-neutral atmospheric turbulence in the rest of these notes, but rather concentrate on neutral stability which prevails in the case of high wind speeds and hence relevant in most wind engineering applications.

4.3 Geostrophic drag law and siting

Siting and estimation of wind resources should ideally be based on long records of measurements of wind speed and turbulence. Often, however, no measurements exist and models of varied complexity are utilized in order to predict the quality of a given site. Meso-scale models are numerical weather prediction models covering an area approximately the the size of Denmark ($\sim 400\,$km), with a resolution of several kilometers (Hahmann et al., 2010). These can hence be used to generate large maps of geostrophic winds, which can then in some sense be extrapolated to surface winds important for wind energy. The Wind Atlas Method by Troen and Petersen (1989) uses exactly such a method (see later in this section). The extrapolation refers to the

application of the geostrophic drag law (GDL).

4.3.1 Turbulence eddy viscosity

An alternatively derivation of the log-law is based on the assumption of the existence of a turbulent eddy viscosity, ν_T. First, however, we will look at the following exercise, an exercise at the core of numerical modeling of micro meteorological flows (See Section 8.3).

Exercise 4.3.1 (RANS equation) *In this exercise we will derive the Reynolds averaged Navier-Stokes (RANS) equations. The Navier-Stokes equation are given in eq. 4.1.3. Since we are in the atmosphere (a rotating coordinate system) we will include the Coriolis force, $f\boldsymbol{U}(\boldsymbol{x},t)$. Since centrifugal and gravity forces are both body forces they can be absorbed into the pressure term. We assume neutral stratification and hence neglect buoyancy.*

For simplicity we will introduce Einstein notation, i.e. the three different components of a vector are denoted by a subscript, $i = 1,2$ or 3. Summation over repeated indices is understood. We can thus describe the velocity vector by u_i. We now decompose the velocity into its mean value, U_i, and its fluctuating part, u_i (notice the change in notation. u_i is no longer the total velocity but the fluctuation!) , i.e. performing a Reynolds decomposition. Take the ensemble average $\langle\cdot\rangle$ of the Navier-Stokes equation in eq. 4.1.3 and verify that the result, the RANS equations, for the mean wind, U_i are given by:

$$\boxed{\frac{\partial}{\partial t}U_i + U_j\frac{\partial}{\partial x_j}U_i = -\frac{1}{\rho}\frac{\partial}{\partial x_i}P - \frac{\partial}{\partial x_j}\langle u_i u_j\rangle - 2\varepsilon_{ijk}\Omega_j U_k,} \tag{4.3.1}$$

where we have neglected the viscous terms due to the high Reynolds number encountered in the ABL. Remember that average of any fluctuating quantity like u_i is zero, i.e. $\langle u\rangle = 0$. $\langle u_i u_j\rangle$ is named the Reynolds stresses. The last term is the Coriolis force, eq. 2.1.8, with the Levi-Civita symbol, ε_{ijk}.

The incompressibility condition reduces to

$$\frac{\partial}{\partial x_i}U_i = 0. \tag{4.3.2}$$

For stationary ($\partial/\partial t$) and homogeneous ($\partial/\partial x = \partial/\partial y = 0$, except from pressure) flow the equations reduce to eq. 4.3.5.

If we compare the RANS equation, eq. 4.3.1, and the Navier-Stokes equation, eq. 4.1.3, the only difference (besides of course the fact that $\boldsymbol{U}$ is now the mean flow!) seems to be that the flux term, $(\partial/\partial x_j)\langle u_i u_j\rangle$ has replaced the viscosity term in the Navier-Stokes equation. Can we assume that the turbulent fluxes behaves in way similar to molecular motion, as described through kinematic viscosity? Perhaps not, but this is, however, exactly what is assumed in the eddy viscosity hypothesis. For a flow in homogeneous conditions it takes the form:

$$\langle uw\rangle = -\nu_T\frac{\partial U}{\partial z}, \tag{4.3.3}$$

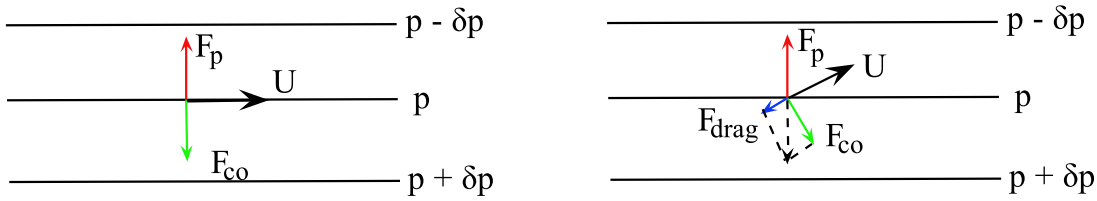

Figure 4.3.1: *Left:* Forces and wind at the top of the ABL. *Right:* Forces and wind inside the ABL. F_p is the pressure gradient force, F_{co} is the Coriolis force, and F_{drag} is the drag force due to turbulence.

where the eddy viscosity, ν_T, is assumed much larger than the kinematic viscosity, ν, in agreement with the Continuum item by Tennekes and Lumley (1972). Inspired by kinetic gas theory we postulate that ν_T is the product of a characteristic velocity and length scale (molecular speed and mean free path in gas theory). In the surface layer we take these to be, $u_\star$ and z (only relevant parameters). Introducing (again) the *von Kármán constant* constant, κ we have

$$\nu_T = \kappa u_\star z. \tag{4.3.4}$$

Equating eq. 4.3.3 and eq. 4.3.4 we arrive at the log-law.

The appearing of Reynolds stresses, $\langle u_i u_j \rangle$, upon averaging the Navier-Stokes equation leads directly to what is known as the *closure problem*. This means that the equations are not closed. We can write down an equation for $\langle u_i u_j \rangle$ using the same methodology as in exercise 4.3.1. This will, however, induce an even higher order term. And so on... In this context, the eddy viscosity hypothesis is a neat way to *close* the equations. Pope (2000) has an in depth review of the different closure strategies for the RANS equation in turbulent flow.

4.3.2 Geostrophic drag law and Ekman layers

We will now derive the geostrophic drag law (GDL) and show how it can be applied to wind resource estimation. Besides the Coriolis force, forces due to turbulent drag are the major players in the ABL. The forces are sketched in Figure 4.3.1 (we have implicitly assumed that the isobars are not too curved, in which case the gradient wind is a better candidate for the wind in the free atmosphere above the ABL). At the top of the ABL, the wind is parallel to the isobars, while the wind inside the ABL crosses the isobars due to the presence of turbulent drag associated with the Reynolds stresses, $\langle u_i u_j \rangle$.

In the ABL, in principle from $z = z_0$ to $z = z_i$ (the ABL top), see also Figure 4.2.2, the equations of motion (see exercise 4.3.1) are given by:

$$\begin{aligned} f(U - U_g) &= -\frac{\partial}{\partial z}\langle vw \rangle \\ f(V - V_g) &= \frac{\partial}{\partial z}\langle uw \rangle, \end{aligned} \tag{4.3.5}$$

where we have used the definitions of the geostrophic wind in eq. 2.2.11. By the convention of the orientation of the coordinate system we have $V = 0$ and $\langle vw \rangle = 0$ close to the surface. The

above equations are the ones giving rise to the Ekman spiral (see Exercise 4.3.2), where the wind direction is increasing to the right (on the Northern hemisphere) as z increases from the surface to the height of the ABL. The change in wind direction between the surface and the top of the ABL is also in seen in Figure 4.3.1: In the left panel (at the top of the ABL) the wind is to the right of the wind in the right panel (inside the ABL).

We now introduce a non-dimensional number $\xi = z/z_i$, with $z_i = u_\star/f$ being the ABL height. The actual height of the ABL, z_i, is a hot topic of research (Peña, 2009) and the simple functional form assumed here, might be too naive (probably around a factor of five to large). After some rearrangements, eq. 4.3.5 can be written

$$\begin{aligned}
\frac{U-U_g}{u_\star} &= -\frac{u_\star}{f}\frac{\partial}{\partial z}\left(\frac{\langle vw\rangle}{u_\star^2}\right) = -\frac{\partial}{\partial(z/z_i)}\left(\frac{\langle vw\rangle}{u_\star^2}\right) \equiv F(\xi) \\
\frac{V-V_g}{u_\star} &= \frac{u_\star}{f}\frac{\partial}{\partial z}\left(\frac{\langle uw\rangle}{u_\star^2}\right) = \frac{\partial}{\partial(z/z_i)}\left(\frac{\langle uw\rangle}{u_\star^2}\right) \equiv G(\xi),
\end{aligned} \tag{4.3.6}$$

with the two non-dimensional functions, F and G.

In the surface layer we have the logarithmic wind profile. For completeness we here write both components:

$$\begin{aligned}
\frac{U}{u_\star} &= \frac{1}{\kappa}\log\left(\frac{z}{z_0}\right) \\
\frac{V}{u_\star} &= 0.
\end{aligned} \tag{4.3.7}$$

Again we introduce a non-dimensional number $\delta = z/z_0$ and rewrite the above equations

$$\begin{aligned}
\frac{U}{u_\star} &\equiv f(\delta) \\
\frac{V}{u_\star} &= 0,
\end{aligned} \tag{4.3.8}$$

with the non-dimensional function, f.

We now assume that there exists a layer in the ABL, in which both profiles are valid. Using the chain rule of differentiation we compute $\partial U/\partial z$ through eq. 4.3.6 (only the U-component for now):

$$\frac{\partial U}{\partial z} = u_\star \frac{\partial F}{\partial \xi}\frac{\partial \xi}{\partial z} = \frac{u_\star}{z_i}\frac{\partial F}{\partial \xi}, \tag{4.3.9}$$

and through eq. 4.3.8:

$$\frac{\partial U}{\partial z} = u_\star \frac{\partial f}{\partial \delta}\frac{\partial \delta}{\partial z} = \frac{u_\star}{z_0}\frac{\partial f}{\partial \delta}. \tag{4.3.10}$$

Equating the two equations and multiply both sides by $z/u_\star$ we arrive at the relation

$$\xi\frac{\partial F}{\partial \xi} = \delta\frac{\partial f}{\partial \delta}. \tag{4.3.11}$$

This means that both sides must be equal to a constant. If we take this to be $1/\kappa$ we have

$$f(\delta) = \frac{1}{\kappa}(\log\delta + b) = \frac{U}{u_\star} \tag{4.3.12}$$

$$F(\xi) = \frac{1}{\kappa}(\log\xi + A) = \frac{U - U_g}{u_\star}, \tag{4.3.13}$$

where b and A are two integration constants. Since $f(\delta)$ is given by the log-law we have $b = 0$. Subtracting the two equations from each other and rearranging, we arrive at

$$\frac{U_g}{u_\star} = \frac{1}{\kappa}\left(\log\left(\frac{z_i}{z_0}\right) - A\right). \tag{4.3.14}$$

We now turn towards the V-component, which turns out to be quite easy since $V = 0$, and hence $G(z/z_i)$ must be a constant, which we take to be B/κ. That is

$$\frac{V_g}{u_\star} = -\frac{B}{\kappa}. \tag{4.3.15}$$

Combining eq. 4.3.14 and 4.3.15 through the vector relation $G^2 = U_g^2 + v_g^2$, where G is the geostrophic wind speed, we finally arrive at the geostrophic drag law,

$$\boxed{G = \frac{u_\star}{\kappa}\sqrt{\left(\log\left(\frac{u_\star}{fz_0}\right) - A\right)^2 + B^2}.} \tag{4.3.16}$$

A and B are determined from experiments. In neutral stratification good estimates are, $A = 1.8$ and $B = 4.5$. In non-neutral conditions they become functions of the non-dimensional parameter, $u_\star/(fz_0)$, also known as the friction Rossby number.

A quantity often of interest is the angle, α, between the surface wind and the geostrophic wind. It is given by

$$\tan\alpha = \frac{V_g}{U_g}. \tag{4.3.17}$$

The geostrophic drag law thus relates surface parameters, $u_\star$ and z_0 with the geostrophic wind aloft. It does, however, not give any information regarding what goes on between the surface layer and the top of the ABL. The geostrophic wind is given, but the height of the top of the ABL is not.

In WAsP [4.3.1] the Wind Atlas method is utilized; the geostrophic wind is used to relate measurements of wind in one position with siting of turbines at another position nearby, that is within tens of kilometers or so. From wind measurements, the surface characteristic, z_0 and $u_\star$ are obtained by the log-law. Based upon these, the geostrophic wind is calculated through the GDL given by eq. 4.3.16. Assuming that the free atmosphere is in geostrophic balance over the area of

[4.3.1] WAsP is a software package developed at Risø DTU for calculating the power production, when siting turbines at specific geographical locations with a given wind climate (`www.WAsP.dk`).

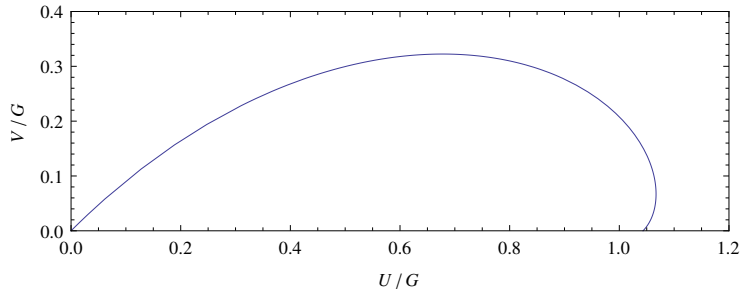

Figure 4.3.2: Ekman spiral derived with constant valued ν_T.

interest, i.e. the effect of the centrifugal force is negligible over a distance equal to the distance between the position of wind measurements and turbine position, we can use the GDL again, but this time as an implicit equation of the surface characteristic at the turbine site. These can then be used together with the log-law in order to get the mean wind at the turbine hub height. In the real world the terrain is rarely completely flat and covered by uniform roughness. These effects are also included in WAsP, and will be covered in Chapter 8.

Exercise 4.3.2 (Ekman spiral) *Eq. 4.3.5 is the starting point for deriving the Ekman solution / spiral. Use the eddy viscosity hypothesis given by eq. 4.3.3 and assume constant ν_T.*

*Solve the equations for U and V (*Hint: *Introduce a complex velocity, $W = U + iV$), with appropriate boundary conditions and show that the solution is given by*

$$\begin{aligned} U &= U_g(1 - \exp(-\gamma z)\cos(\gamma z)) \\ V &= U_g \exp(-\gamma z)\sin(\gamma z)), \end{aligned} \tag{4.3.18}$$

where $\gamma = \sqrt{f/(2\nu_T)}$, and the coordinate system is oriented with x pointing in the direction of the geostrophic wind, i.e. $U_g \equiv G$. The solution, the Ekman spiral, is presented in Figure 4.3.2.

Is it realistic with constant ν_T in the ABL?

Exercise 4.3.3 (Angle between surface- and geostrophic wind) *Calculate the angle, α, between the mean wind and the geostrophic wind for typical surface parameters, $u_\star$ and z_0. Compare the result with the angle given by the Ekman spiral in Exercise 4.3.2 (*Hint: *Make a Taylor series expansion to first order in z of U and V).*

Exercise 4.3.4 (Geostrophic drag law - hands-on examples)

1. *Find the geostrophic wind, when the pressure gradient is given as $\nabla p = (2.5, 4)10^{-4}\,Pa\,m^{-1}$. Setup a coordinate system with x in east-west direction, and y in the north-south direction. Find the direction of the geostrophic relative to the abscissa. What is the magnitude of the geostrophic wind G? Assume that the pressure gradient is measured at 50°N.*

2. *Find u_* if the roughness length $z_0 = 0.01\,m$ and find the wind speed 10 m above the flat, homogeneous terrain.*

3. *Suppose a meteorological mast measures a long term average wind speed of* $6\,m\,s^{-1}$ *at* $z = 10$ *m over a flat homogeneous terrain with a surface roughness length of* $z_0 = 0.5$ *m. Calculate from the logarithmic wind profile an average* u_* *and the average geostrophic wind speed.*

4. *Based on the measured mean wind speed above calculate the average wind speed at* $z = 10$ *and 60 m over homogeneous, flat landscapes with the following roughnesses: 0.001, 0.01, 0.05, and 0.3 m.*

CHAPTER 5

INSTRUMENTS

In this chapter we will discuss in brief two anemometers which are widely used for atmospheric boundary layer measurements namely the cup and the sonic anemometers. These instruments are called *in situ* sensors because the wind is measured at the position of the instrument, opposed to remote sensing, where the wind is measured in a location remote to the anemometer. The wind lidar is a prime example of a remote sensing instrument growing quite popular in the wind energy community. By the end of this chapter we will have a look at why that might be.

5.1 The cup anemometer

The cup anemometer is probably the most widely used instrument for wind measurements in the atmosphere. You always see them at weather stations, in airports, on top of wind turbines, etc.

Invented by the Irish astronomer T. R. Robinson in 1846, the basic design of the cup anemometer has not changed significantly in the last 160 years. The cup anemometer shown in Figure 5.1.1 has been used by Risø National Laboratory in almost unaltered design since 1970.

A cup rotates because the drag with the concave side of the cup facing the wind is larger than for the convex. A simple mathematical model for a cup would be to assume that the drag on the concave side of the anemometer can be described in terms of a drag coefficient C_D^+ which is independent of wind speed U and the density of air, ρ. Then

$$F^+ = \frac{1}{2}\rho(U - rS)^2 A C_D^+, \tag{5.1.1}$$

where S is the angular speed, r the distance from the axis of rotation to the center of the cup, and A the area of the cup. Similarly, for the 'convex side' of the anemometer:

$$F^- = \frac{1}{2}\rho(U + rS)^2 A C_D^-. \tag{5.1.2}$$

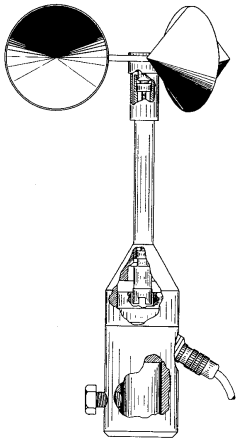

Figure 5.1.1: The cup anemometer model Risø-70. The height is 27 cm and the rotor, made of carbon fiber reinforced plastic, weighs 40 g.

Assuming internal friction in the cup anemometer to be negligible the two forces should be equal in a steady wind. Equating eq. 5.1.1 and eq. 5.1.2 leads to

$$\frac{rS}{U} = \frac{1-\sqrt{C_D^-/C_D^+}}{1+\sqrt{C_D^-/C_D^+}}, \tag{5.1.3}$$

which shows the purely geometric linear relation between the speed of rotation S and the wind speed. Wind tunnel tests with speeds between 0 and 80 $\mathrm{m\,s^{-1}}$ indeed show that the linear relationship is valid within 10 cm/s above a few meters per second, where internal friction can be ignored.

When placed in the turbulent wind the cup anemometer may overestimate the mean wind speed. This phenomenon is referred to as overspeeding. This is mainly due to the fact, that an ideal cup measures the horizontal projection of the total length of air passing through the cup. The implication is that the average measured wind speed will be

$$\boxed{\left\langle \sqrt{(U+u)^2+v^2} \right\rangle \approx U + \frac{\langle v^2 \rangle}{2U},} \tag{5.1.4}$$

If the cup is combined with a vane (which measured wind direction and hence effectively measures v), this error can be eliminated, and one can get a better estimate of U. Other overspeeding errors are generally very small (Kristensen, 1998).

A cup anemometer does not respond instantaneously to changes in the wind. For normal cup anemometers the wind filtered by the inertia and size of the cup roughly corresponds to a first order filter width a length scale-of 1 to 2 meters. Expressed differently the cup responds to eddies down to the size of 1 to 2 meters.

Figure 5.2.1: The sonic anemometer Solent R3 from Gill. The three acoustic paths has a length of 149 mm.

Cups are extraordinarily robust. They routinely measure wind speeds unattended for years in the atmosphere without changing their calibration.

Exercise 5.1.1 (Cup anemometer) *Verify eqn. 5.1.4 by making a Taylor expansion in the fluctuations, u and v.*

5.2 The sonic anemometer

In contrast to the cup, the sonic anemometer can measure all three components of the turbulent wind velocity. The basic principle is as follows. Consider two acoustic transducers capable of emitting and receiving sound pulses. One is placed in a distance l downstream of the other in a steady flow with velocity U.

The time it takes for a sound pulse to travel from the transducer upstream to the one downstream is

$$t_1 = \frac{l}{c+U}, \tag{5.2.1}$$

where c is the speed of sound. The time it takes for a pulse to travel upstream is

$$t_2 = \frac{l}{c-U}, \tag{5.2.2}$$

and solving these two equations for U we get

$$U = \frac{l}{2}\left(\frac{1}{t_1} - \frac{1}{t_2}\right). \tag{5.2.3}$$

It can be shown that this result is insensitive to any flow component perpendicular to the acoustic path. I.e. by measuring the two travel times you measure the velocity component of the flow parallel to the acoustic path. By combining *three* transducer pairs such that the acoustic paths span all three dimensions, the velocity vector can be calculated by a simple linear transformation. A sonic anemometer is shown in Figure 5.2.1.

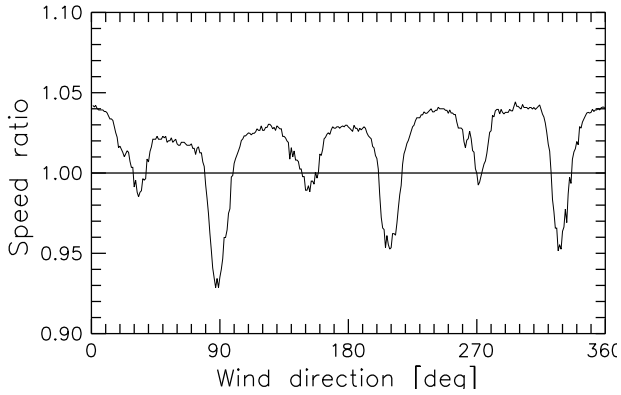

Figure 5.2.2: Flow distortion by the sonic from Gill in Figure 5.2.1. The ratio of measured speed to wind tunnel speed is plotted as a function of angle. (Courtesy by N. G. Mortensen.)

Instead of eq. 5.2.3 we could also have formed the equation

$$t_2 - t_1 = \frac{2l}{c^2 - U^2} U. \tag{5.2.4}$$

In for typical atmospheric conditions, the speed of sound, c, is ≈ 340 m s^{-1}, and hence $U^2 \ll c^2$, and we have

$$t_2 - t_1 = \frac{2l}{c^2} U. \tag{5.2.5}$$

Since c is a function of temperature and water vapor, we can actually get an estimate of the virtual temperature (the temperature of an dry air parcel having the same pressure and density as a moist air parcel with temperature, T - consult for example Wyngaard (2010) for a derivation) from a sonic measurement. And even more important, we can estimate the heat flux, $Q = \langle w' T_v' \rangle$, used when estimating the Obukhov length scale given by eq. 4.2.11. This makes the sonic very useful for quantification of the stratification of the atmosphere. For precise absolute temperature estimation the sonic is, however, not as precise as conventional temperature sensors.

Although the measurement by a sonic is theoretically almost point-like in time there is some spatial averaging. This is determined by the length of the acoustical paths which are typically of the order of 10 to 20 cm. The spatial resolution is a factor of ten better than that of the cup anemometer and good enough for almost any stochastic load problem in the atmosphere. In practice the sonic also performs some temporal averaging. Typical velocity vector rates from a sonics range from 10 to 20 Hz. The instrument is not quite as robust as the cup. It can typically operate unattended for months collecting atmospheric data.

The calibration, however, is not as simple as one might think, i.e. just measuring l accurately, and it is much more complicated than for the cup. As one might imagine looking at Figure 5.2.1 the instrument itself distorts the flow. Figure 5.2.2 was obtained by placing a sonic in a wind tunnel at a known speed and continuously record the sonic speed as it was slowly turned around its vertical axis. The figure shows the deviation of the measured speed to the true. The dips in the curve at various angles are caused by the wakes of the transducers. Probably because the sonic contracts the flow a bit there is a general speed-up at the angles outside the wakes.

For calibration of all three velocity components the sonic also have to be turned around the other axes. This makes the calibration quite cumbersome.

In order to reduce flow distortion the support frame and the transducers could be made more slender. However, this introduces another problem, namely that the sonic may not be stiff enough at high wind speeds.

5.3 Wind lidars

A slide show by Rozenn Wagner, DTU, will be presented on this subject.

CHAPTER 6

TURBULENCE SPECTRA AND STOCHASTIC WIND LOADS

We now turn the focus towards turbulence in the surface layer once again, but this time in a little bit more systematic way with emphasis on the spectral spatial properties of turbulence and the associated loads on structures, such as for example wind turbines. In Section 3.6 we introduced the spectrum of a time series. Hence in a temporal domain. In this chapter we will introduce the spectrum in a spatial domain.

6.1 Spatial representation of turbulence

The atmospheric turbulent velocity field is described by $\boldsymbol{u}(\boldsymbol{x})$, where $\boldsymbol{x} = (x_1, x_2, x_3) = (x, y, z)$. The fluctuations around the mean wind, $\boldsymbol{u} = (u_1, u_2, u_3) = (u, v, w)$, are assumed to be homogeneous in space, which is often the case in the horizontal directions but is only a crude approximation in the vertical. The mean wind field is allowed to vary as a function of z. Because of homogeneity, the covariance tensor

$$R_{ij}(\boldsymbol{r}) = \langle u_i(\boldsymbol{x}) u_j(\boldsymbol{x}+\boldsymbol{r}) \rangle \tag{6.1.1}$$

is a function of the separation vector $\boldsymbol{r}$ only. Recall Section 3.4 where we due to stationarity could define the covariance tensor in the temporal domain, as a function of time lag, τ, only. Eq. 6.1.1 expresses the same thing, just in the spatial domain. In general everything we learned in that section can be applied here for spatial domain settings.

We shall use a concept called Taylor's 'frozen' turbulence hypothesis (Panofsky and Dutton, 1984) to interpret time series as 'space series'. The idea is, that if turbulent structures are advected past an anemometer faster than the eddies have time to alter (decay), then the time series we are measuring can be interpretet as a spatial signal. This limit corresponds to $\sigma \ll U$, meaning that $I_u \ll 1$. So for most applications in flat terrain, where the turbulence intensity, I_u, rarely exceeds

10%, Taylor's hypothesis can be justified. We hence have

$$\boldsymbol{u}(x,y,z,t) = \boldsymbol{u}(x-Ut,y,z,0). \tag{6.1.2}$$

This is also the reason why we can suppress the time argument in $\boldsymbol{u}$.

For stochastic load calculations mainly the statistics of the wind fluctuations of second order are of interest. It is still not clear how much influence the statistic of higher orders, such as skewness and kurtosis, have on stochastic loads.

All second order statistics can be derived from the covariance tensor or its Fourier transform, the spectral tensor:

$$\boxed{\Phi_{ij}(\boldsymbol{k}) = \frac{1}{(2\pi)^3}\int R_{ij}(\boldsymbol{r})\exp(-\mathrm{i}\boldsymbol{k}\cdot\boldsymbol{r})\mathrm{d}\boldsymbol{r},} \tag{6.1.3}$$

where $\int \mathrm{d}\boldsymbol{r} \equiv \int_{-\infty}^{\infty}\int_{-\infty}^{\infty}\int_{-\infty}^{\infty}\mathrm{d}r_1\mathrm{d}r_2\mathrm{d}r_3$.

Is it very difficult to measure the spectral tensor directly. Instead cross-spectra, defined as

$$\chi_{ij}(k_1,\Delta y,\Delta z) = \frac{1}{2\pi}\int_{-\infty}^{\infty} R_{ij}(x,\Delta y,\Delta z)\mathrm{e}^{-\mathrm{i}k_1 x}\mathrm{d}x \tag{6.1.4}$$

are often measured, say by two instruments separated by Δy in the horizontal direction perpendicular to the wind and Δz in the vertical, and are used in practical applications. The connection between the components of the spectral tensor and the cross-spectra is

$$\chi_{ij}(k_1,\Delta y,\Delta z) = \int_{-\infty}^{\infty}\int_{-\infty}^{\infty}\Phi_{ij}(\boldsymbol{k})\mathrm{e}^{\mathrm{i}(k_2\Delta y+k_3\Delta z)}\mathrm{d}k_2\mathrm{d}k_3. \tag{6.1.5}$$

When the two indices i and j are the same and $\Delta y = \Delta z = 0$, eq. 6.1.5 becomes the one-point spectrum $F_i(k_1) = \chi_{ii}(k_1,0,0)$.

In the inertial subrange we have, following Kolmogorov's results in eq. 4.1.5, the much celebrated $-5/3$ law

$$\boxed{F_i(k_1) = \alpha_i \varepsilon^{2/3} k_1^{-5/3}.} \tag{6.1.6}$$

for $i = 1$, F_1 is the streamwise velocity spectrum, F_u for which the Kolmogorov constant is around 0.5. A related law, the 4/3 law (see Pope (2000) for a derivation), says that the ratio between the constants, α_i, is: $(4/3)\alpha_1 = \alpha_2 = \alpha_3$.

The variance, σ_i^2, is given by

$$\sigma_i^2 = \int_{-\infty}^{\infty} F_i(k_1)dk_1 = \int_{-\infty}^{\infty} k_i F_i(k_1) d\log k_1. \tag{6.1.7}$$

To distinguish between spectra as functions of wave number, k_1, which by the aid of Taylor's hypothesis can be written as $k_1 = 2\pi f/U$, and frequency, f, we use F for the former and S for the latter, i.e. $S_i(f)\mathrm{d}f = F_i(k_1)\mathrm{d}k_1$. This implies that

$$\boxed{F_i(k_1) = \frac{U}{2\pi}S_i(f).} \tag{6.1.8}$$

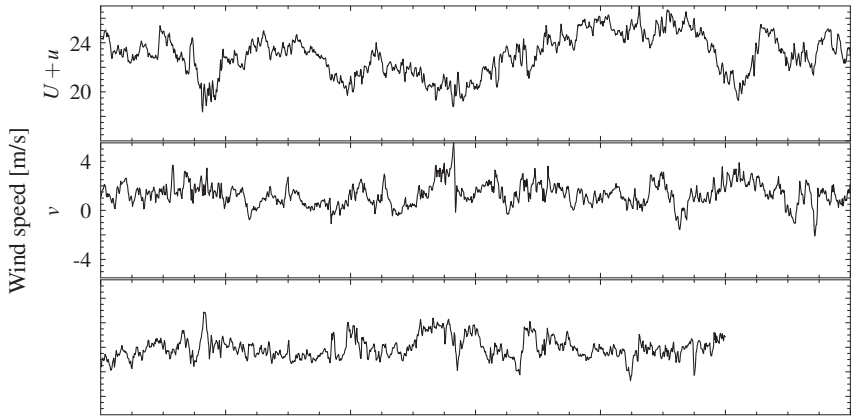

Figure 6.1.1: Two minutes time series of the three components of velocity measured in the same point 70 m over the Great Belt.

6.1.1 Spatial coherence

In the temporal domain coherence were defined in eq. 3.6.20. The spatial coherence is defined as

$$\mathrm{coh}_{ij}(k_1,\Delta y,\Delta z)=\frac{|\chi_{ij}(k_1,\Delta y,\Delta z)|^2}{F_i(k_1)F_j(k_1)}. \tag{6.1.9}$$

Davenport (1961) found that the coherence of the u components vertically separated by a distance Δz could be well approximated by

$$\mathrm{coh}_{uu}(f,\Delta z)=\exp\left(-a\frac{f\Delta z}{U}\right), \tag{6.1.10}$$

where U is the mean wind speed at an average height and a a constant of the order of 8. It can be shown both experimentally and theoretically, that the coherence does not go to zero for $f\to 0$ for $\Delta z>0$ and that the coherence is smaller for large distances than indicated by the Davenport model (Kristensen and Jensen, 1979; Mann, 1994). In spite of these shortcomings eq. 6.1.10 is widely used and has been extended to coherences of the other wind components (with other values of a) and to horizontal separations (Panofsky and Dutton, 1984; Simiu and Scanlan, 1996; Dyrbye and Hansen, 1997).

At a fixed separation Δz (or Δy) the coherence decreases as a function of frequency. This has the following crude interpretation: Eddies contributing to the spectrum at higher frequencies are smaller, they can therefore not cover both of the two points of measurements simultaneously and consequently the coherence gets smaller. On the other hand, when we look at the very lowest frequencies we are describing larger eddies which has a large probability of 'hitting' the two instruments simultaneously, and thus the coherence is large.

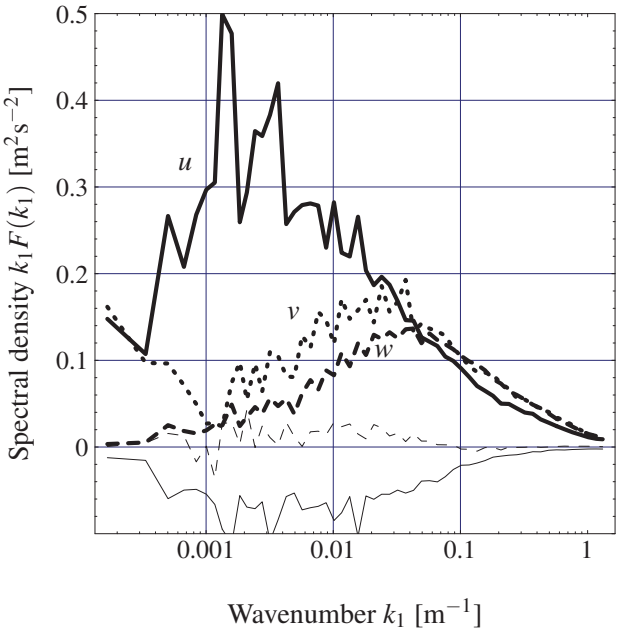

Figure 6.1.2: Spectra from Great Belt. The thick curves are are spectra of the components u (full line), v (dotted), and w (dashed). The thin, solid curve is the real value of the one-point cross-spectrum of u and w, and the dashed the imaginary value.

6.1.2 Example: the Great Belt bridge

To get acquainted with the concepts of spectra and coherences of atmospheric turbulence we shall look at some data from an experiment which was designed (with Dr. Davenport involved in the first phase of design) to know more about the stochastic loads on the Great Belt Bridge. Three sonic anemometers (see Section 5.2) were mounted at the tops of two 70 m high mast corresponding to the height of the bridge deck. The horizontal separations were $\Delta y = 15$, 32.5, and 47.5 m.

The experiment acquired data for one year Mann et al. (1991) but for the purpose here we shall only look at two hours of data taken during a Christmas storm in 1990 with a mean speed of 23 m s^{-1} and direction perpendicular to the array of anemometers. Two minutes of data from one the sonics are shown in Figure 6.1.1. It may be seen that the variances of the velocity components obey $\sigma_u^2 > \sigma_v^2 > \sigma_w^2$ implying that the turbulence is certainly not isotropic. Note also that the wavelength containing the most variance (or more or less equivalently, the integral scale) is largest for u and smallest for w. The u- and the w-signals are anti-correlated, which can be difficult to judge from Figure 6.1.1.

The spectra shown in Figure 6.1.2 calculated from the entire two hour record also reflect these properties. The component spectra also obey Kolmogorov's -5/3-law for high frequencies or wave numbers and the associated 4/3-law law for the ratio between the w- or v-spectrum to the u-spectrum. Integrating the real part of the cross-spectrum (the thin solid line in figure 6.1.2)

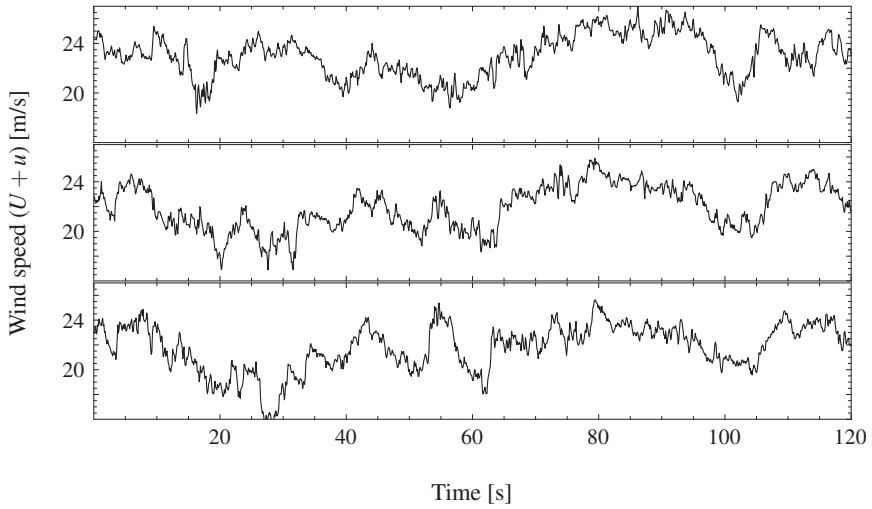

Figure 6.1.3: A two minute fraction of u measured at positions separated in the horizontal direction perpendicular to the wind. The instruments used for the two lowest plots are separated by $\Delta y = 15$ m, the upper and the middle by 32.5 m, and the upper and the lower by 47.5 m.

from $-\infty$ to ∞ we get by definition $-u_*^2$.

The often used model spectra of Simiu and Scanlan (1996) have the same functional shapes as in Kaimal et al. (1972) but the numerical constants are different:

$$\frac{fS_u(f)}{u_*^2} = \frac{100n}{(1+50n)^{5/3}}, \tag{6.1.11}$$

$$\frac{fS_v(f)}{u_*^2} = \frac{7.5n}{(1+9.5n)^{5/3}}, \tag{6.1.12}$$

and

$$\frac{fS_w(f)}{u_*^2} = \frac{1.68n}{1+10n^{5/3}}, \tag{6.1.13}$$

where $n = fz/U$. These spectra obey closely the $\frac{5}{3}$- and $\frac{4}{3}$-laws mentioned above and also fit the observations at the Great Belt quite well. Note, that these spectra are two-sided, i.e. we get the variance by integrating from $-\infty$ to ∞.

Figure 6.1.3 shows simultaneously recorded wind histories separated in the horizontal direction by various distances. The coherences calculated from these time series are shown in figure 6.1.4. At $\Delta y = 47.5$ m is less than implied by the Davenport model.

6.2 Loads

We now go through an analysis of stochastic forces on point- and line-like structures in some detail. These examples are both treated with and without the inclusion of the movements of the structure itself.

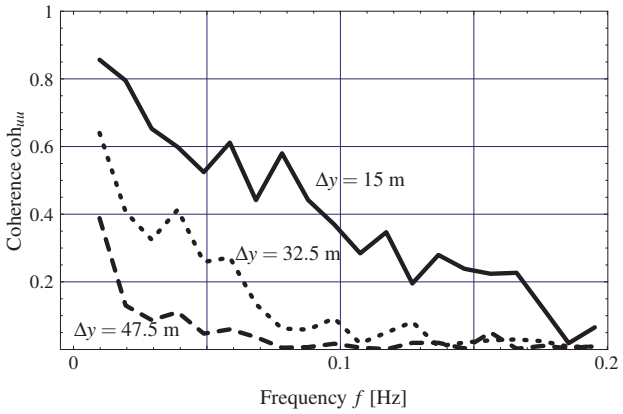

Figure 6.1.4: Coherences from two hours of data. Parts of the time series are shown in figure 6.1.3.

6.2.1 Loads on a point-like structure

Consider a small body subjected to atmospheric turbulence. Suppose that the instantaneous drag force in the mean wind direction can be written as

$$F_D(t) = \frac{1}{2}\rho A C_D (U + u(t))^2, \tag{6.2.1}$$

where C_D is the drag coefficient and A its area. Usually, the mean wind is much larger than the fluctuations ($U \gg u$) so we might write the fluctuating force F'_D as

$$F'_D(t) \approx \rho A C_D U u(t). \tag{6.2.2}$$

The auto-correlation of the force is

$$R_F(\tau) = \left\langle F'_D(t) F'_D(\tau + t) \right\rangle = \rho^2 U^2 A^2 C_D^2 R_u(\tau). \tag{6.2.3}$$

Fourier transforming both sides of this relation leads to

$$S_F(\omega) = \rho^2 U^2 A^2 C_D^2 S_u(\omega). \tag{6.2.4}$$

Suppose now that the body can move in the wind direction as a damped harmonic oscillator. If x denotes the displacement from the mean position (determined by the mean force) the equation of motion is

$$\ddot{x} + 2\eta\dot{x} + \omega_0^2 x = \frac{F'_D}{m}, \tag{6.2.5}$$

where ω_0 is the natural (angular) frequency of the oscillator, η the damping and m the mass. It is well known (Dyrbye and Hansen, 1997) that if x obeys eq. 6.2.5 then the spectrum of x is given by

$$\boxed{S_x(\omega) = |H(\omega)|^2 S_F(\omega)} \tag{6.2.6}$$

where the frequency transfer (or response) function is given by

$$|H(\omega)|^2 = \frac{1}{m^2}\frac{1}{(\omega_0^2-\omega^2)^2+4\eta^2\omega^2}. \tag{6.2.7}$$

However, in the case of stochastic wind loads of flexible structures, where $\dot{x}$ may be as large as u, the drag force is not given by eq. 6.2.2 but by

$$F_D'(t) = \rho A C_D U(u(t)-\dot{x}). \tag{6.2.8}$$

Defining the aerodynamic damping as

$$\eta_a = \frac{1}{2}AC_DU \tag{6.2.9}$$

the equation of motion, eq- 6.2.5, can be written as

$$\ddot{x}+2(\eta+\eta_a)\dot{x}+\omega_0^2 x = \frac{F_D'}{m}, \tag{6.2.10}$$

where F' still is given by eq. 6.2.2. Now the response spectrum is given by (6.2.6) with the response function

$$|H(\omega)|^2 = \frac{1}{m^2}\frac{1}{(\omega_0^2-\omega^2)^2+4(\eta+\eta_a)^2\omega^2}. \tag{6.2.11}$$

instead of eq. 6.2.7. For structures with very low structural damping such as slender steel bridges and some masts the aerodynamic damping can be much larger than the structural.

For mainly two reasons the assumptions leading to eq. 6.2.4 does not hold. Firstly, no structures are point-like and the gusts at different points of the structure are not completely correlated. Secondly, sudden variations in wind speed (even fully correlated over the structure) do not give instantaneous changes in the drag and especially lift forces. It takes some time to build up a lift (Fung, 1969). Both effects lead to a reduction of the force at high frequencies and is sometimes taken into account by multiplying the right hand side of eq. 6.2.4 by an empirically or theoretically determined function, $\chi^2(\omega)$, the aerodynamic admittance. To include these effects we will now take a look at line-like structures.

6.2.2 Loads on a line-like structure

The fluctuating part of the force on a horizontal line-like non-moving structure standing perpendicular to the wind is approximately

$$F'(t) = \rho B C_D U \int_{-L/2}^{L/2} u(t,y)\mathrm{d}y, \tag{6.2.12}$$

where B is the with and L is the length. The auto-correlation of the force is consequently

$$\begin{aligned}\frac{\langle F'(t)F'(t+\tau)\rangle}{(\rho BC_DU)^2} &= \left\langle \int_{-L/2}^{L/2} u(t,y)\mathrm{d}y \int_{-L/2}^{L/2} u(t+\tau,y')\mathrm{d}y' \right\rangle \\ &= \int_{-L/2}^{L/2}\int_{-L/2}^{L/2} R_{uu}(\tau,y-y')\mathrm{d}y\mathrm{d}y', \end{aligned} \tag{6.2.13}$$

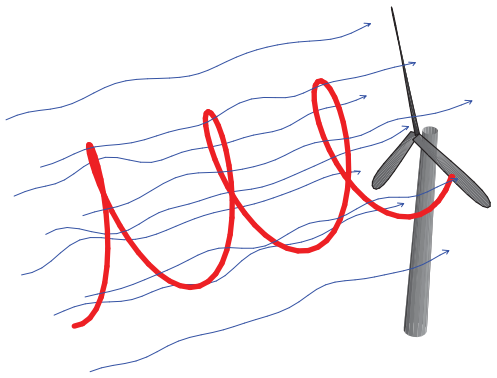

Figure 6.2.1: Sketch of the measurements of wind from the rotating blade of a wind turbine

which according to eq. 6.1.4 can be Fourier transformed to give

$$S_F(\omega) = (\rho B C_D U)^2 \int_{-L/2}^{L/2} \int_{-L/2}^{L/2} \chi_{uu}(\omega, y - y') \mathrm{d}y \mathrm{d}y'. \tag{6.2.14}$$

We now assume that the cross-spectrum can be modelled according to Davenport's model, eq. 6.1.10, i.e.

$$\chi_{uu}(\omega, \Delta y) = S_u(\omega) \exp(-\Delta y / \lambda) \tag{6.2.15}$$

where $\lambda^{-1} = \frac{a\omega}{4\pi U}$, in which case eq. 6.2.14 after some manipulations reduces to

$$S_F(\omega) = (\rho A C_D U)^2 S_u(\omega) 2 \frac{\lambda^2}{L^2} \left((\mathrm{e}^{-L/\lambda} - 1) + \frac{L}{\lambda} \right), \tag{6.2.16}$$

where $A = BL$. This equation is identical to eq. 6.2.4 except from the terms after $S_u(\omega)$. These are the aerodynamic admittance and goes to 1 as ω approaches zero and to zero as the frequency approaches infinity.

In exact parallel to the derivation made for a point-like structure it can be shown that if the line-like structure moves in the along wind direction as a harmonic oscillator, then the response spectrum is

$$\boxed{S_x(\omega) = (\rho A C_D U)^2 |H(\omega)|^2 S_u(\omega) \chi^2(\omega),} \tag{6.2.17}$$

where H is given by eq. 6.2.11 and

$$\chi^2(\omega) = 2 \frac{\lambda^2}{L^2} \left((\mathrm{e}^{-L/\lambda} - 1) + \frac{L}{\lambda} \right) \tag{6.2.18}$$

from eq. 6.2.16.

This is an example where it is easy to derive an expression for the aerodynamic admittance.

6.2.3 Gusts on a wind turbine

The interaction of wind turbines with atmospheric turbulence is complicated. Each blade samples the turbulence along a spiral (see figure 6.2.1), so the fluctuation in wind velocity seen from the blade have drastically different characteristics compared to measurements in a stationary point.

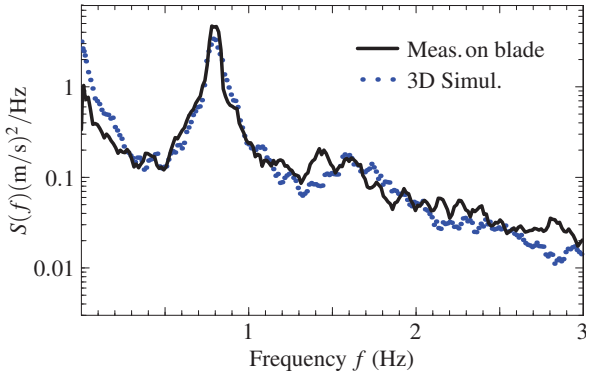

Figure 6.2.2: Measured and simulated spectra of wind speed as seen from a point on a rotating wing. See Petersen et al. (1995)

To illustrate this point a Pitot tube capable of measuring all three velocity components was mounted on a blade of a wind turbine to sample the velocity along the approximate helix spanned by a fixed point on a rotating wing. The measured spectrum of speed fluctuations seen in figure 6.2.2 does not at all resemble the spectra shown in Figure 6.1.2.

To model these spectra we first used a program to simulate three-dimensional fields of all three velocity components. The program is based on a theoretical modelling of the entire second order structure of surface layer turbulence as described f.ex. by the covariance tensor, eq. 6.1.1, or the spectral tensor, eq. 6.1.3 (Mann, 1994, 1998). Then the relative speed was calculated along the helix and Fourier transformed to give the spectrum. The resulting modelled spectrum is very close to the measured (see Figure 6.2.2) and it turned out that the inclusion of all three velocity components in the simulation was necessary to get this good agreement.

To summarize: For wind turbines it is important to model all three components of the wind and their coherences for various separations in order to get the dynamic loads right.

CHAPTER 7

EXTREME WIND ESTIMATION

This far in the course we have spent a lot of time discussing atmospheric turbulence. For a turbine the day to day loads and hence the fatigue of the turbine is a funcion of turbulence spectrum. The quantification of turbulence is hence important in the context of the life time of a turbine. Fatigue is, however only one way, from which the turbine is damaged. Another important factor damaging turbines is extreme winds. These are rarely occurring winds, which has the potential to completely destroy the turbine - just with a single wind blow - so to speak. Today, wind turbines are built to last at least 20-30 years. If we can predict the highest wind, the extreme wind, at some specific geographical location within this time frame, we have the possibility of choosing a turbine for the site specifically designed to withstand even the most extreme wind known to occur. The only problem is, however, that we cannot!

Due to chaos, a weather forecast in our latitudes is limited to a few days. The statistical mean of the general atmospheric circulation, the climate, is, however, as we have discussed in Section 2, to a large extent the same from year to year. To be more precise, the time series of the different meteorological parameters, such as mean wind speed, are stationary, i.e. we can determine well defined averages over time, without carrying for local fluctuations on smaller time scales. This is the reason why, we to some degree, can predict the climate evolution even though the predictability of weather is limited. Global warming, anthropogenically forced or not, is something which affects the climate. Global warming means that the mean temperature of the globe, defined in some suitable way, is increasing. This means that the assumption of stationarity is violated since the mean, at least of the temperature, is now a function of time. A likely outcome of global warming is the possible change of preferred storm pattens and large scale ocean currents: it does not say anything about at which time and day a storm of a given size will hit Denmark, e.g. instead it changes the likelihood, the probability, of when a storm will hit Denmark. For example, many people attribute the current observed extreme weather as a consequence of global warming. The statistics of extreme wind might therefore be affected.

In this section we will discuss extreme winds and present a robust method which gives a more or less reliable estimate of the extreme wind. We will define the extreme wind in the following

way: by the extreme wind, U_{50}, we consider the mean wind speed, which on average is exceeded once time during a period of 50 years by the 10 minutes average wind speed, U. The extreme wind, U_{50}, is thus the larges wind one will, on average, experience within a 50 years time span. The 50 years is denoted the return period while the 10 minutes is denoted the averaging time. We choose the values of 50 and 10 in accordance with the IEC 61400-1 standard.

The method is based on a statistical analysis of a number of maximum wind speeds recorded over a large number of years. In order to do so we will assume the maximum wind speed to be a stationary time series within fifty years. We thus rule out the potential effect of global warming.

The most naive estimate of U_{50} is given by

$$U_{50} = 5U, \tag{7.0.1}$$

where the U is the mean wind speed. Despite its simplicity the relation is included in many standards today, like IEC (see Chapter 9), and it often comes surprisingly close to the Gumbel methods we will discuss later in this chapter.

7.0.4 A simple approach

Before moving on we will present a simple interpretation of the fifty-year extreme wind, U_{50}, in terms of yearly maximum wind speeds. If we collect many yearly maximum wind speeds, U_{1y} we can construct the probability density function of yearly maxima. The probability that a yearly maximum, U_{1y}, exceeds the desired U_{50} is then given by (assuming stationarity)

$$P\{U_{1y} > U_{50}\} = 1 - F(U_{50}) = 1/50 = 0.02, \tag{7.0.2}$$

where $F(U_{50})$ is the cumulative distribution function of yearly maxima, which is given by

$$F(U_{50}) = 1 - 1/50 = 0.98. \tag{7.0.3}$$

In other words: every year there is a 98% probability that the fifty year extreme wind, U_{50}, is NOT exceeded. This is illustrated in Figure 7.0.1. Using instead monthly maximum, U_{1m}, the probability can be written

$$P\{U_{1m} > U_{50}\} = 1 - F(U_{50}) = 1/(12 * 50) = 0.001667. \tag{7.0.4}$$

I.e. every month there is a 0.17% probability that the monthly maximum is exceeded. Due to the seasonal cycle and its impact on storms and hence the maximum wind speed, it is not a very good strategy to use monthly maxima. In Denmark, for example, the maximum wind speed is most likely associated with mid-latitude cyclones moving in over the country from west to east. These storms are much more likely to occur during winter than during summer. This means that assigning a constant monthly probability of exceeding the fifty year extreme wind, U_{50} is a very bad assumption.

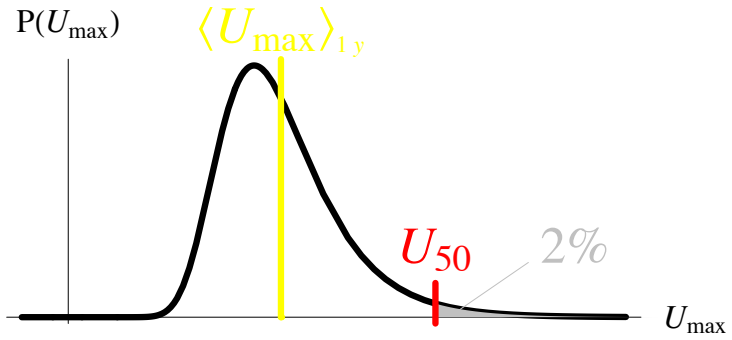

Figure 7.0.1: A definition of the extreme wind, U_{50}, based on the pdf of yearly maxima.

7.1 Threshold crossing and the Poisson process

Before presenting a robust method for obtaining the extreme wind, U_{50} from a time series of wind measurements we introduce a necessary and important concept, namely the concept of threshold crossing and the associated Poisson process and distribution.

7.1.1 *Derivation of the Poisson process

A stochastic variable, X, and an associated threshold value, ξ, is presented in Figure 7.1.1. Lets

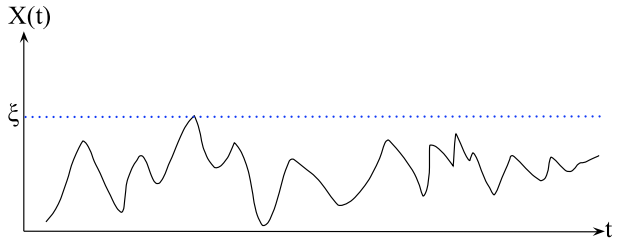

Figure 7.1.1: Time series of the stochastic variable, X and threshold value, ξ.

consider values of X which exceed ξ. We will denote these by up-crossings. Properly defined an up-crossing satisfy $x(t_i) > \xi$ conditioned on $x(t_{i-1}) < \xi$. In Figure 7.1.1, a snapshot of a much longer series, there is one up-crossing - in principle there could be many more. In order to derive the Poisson process we will make the following three assumptions:

- Any given two up-crossings are mutually independent.
- The probability of having an up-crossing within the infinitesimal time between Δt and $t + \Delta t$ is proportional to Δt an independent of t (stationarity).
- More than one up-crossing between Δt and $t + \Delta t$ is unlikely, i.e. up-crossings cannot happen simultaneous (I guess that is obvious!).

We now let, $P_n(t) \equiv P\{n,t\}$ denote the probability that within the time interval, t, we have n up-crossings. From the above assumptions we arrive at,

$$P_1(\Delta t) = \lambda \Delta t \tag{7.1.1}$$
$$P_0(\Delta t) = 1 - \lambda \Delta t, \tag{7.1.2}$$

where λ is the rate of up-crossings. We see that the probabilities are normed correctly so that the sum of the probabilities equals one. In general we have, using independence of up-crossings,

$$P_n(t+\Delta t) = P_n(t)P_0(\Delta t) + P_{n-1}(t)P_1(\Delta t). \tag{7.1.3}$$

A little explanation might help to understand the above equation. Since there might be either zero or one up-crossing during the time interval, dt, we split the left hand side in two terms. If there is zero, the n up-crossings must all occur within t (the first term). In the case that there is one up-crossing during dt, $n-1$ up-crossings must occur within t (the second term).

We can now turn eq. 7.1.3 into a differential equation by letting $\Delta t \to 0$, hence

$$\frac{dP_n(t)}{dt} = \lambda P_{n-1}(t) - \lambda P_n(t). \tag{7.1.4}$$

The recurrence character of the equation means that we can calculate $P_1(t)$ from $P_0(t)$, and then $P_2(t)$ from $P_1(t)$, and so on... We thus start by solving for $n = 0$ ($P_{-1} = 0$ by definition):

$$\frac{dP_0(t)}{dt} = -\lambda P_0(t). \tag{7.1.5}$$

The solution is given by

$$P_0(t) = \exp(-\lambda t), \tag{7.1.6}$$

since the integration constant, $P_0(0)$ must equal unity due to normalization. We now solve for $n = 1$:

$$\frac{dP_1(t)}{dt} = \lambda \exp(-\lambda t) - \lambda P_1(t), \tag{7.1.7}$$

which is a first order inhomogeneous equation with solution

$$P_1(t) = \lambda t \exp(-\lambda t). \tag{7.1.8}$$

Continuing this process we end up with the final expression for the Poisson distribution

$$\boxed{f_{\lambda t}(n) \equiv P_n(t) = \frac{(\lambda t)^n}{n!} \exp(-\lambda t).} \tag{7.1.9}$$

There exist a huge number of well known examples of processes being Poisson distributed: radioactive decay from nucleus measured by a Geiger counter, the number of mutations in biological DNA, the number of calls received at a telephone central, stock market fluctuations and even the number of goals in a football match, to name just a few.

Exercise 7.1.1 *The Poisson process, $f_{\lambda t}(n)$, given by eq. 7.1.9 is a discrete process in contrast to the distributions we have used so far, the Gaussian and Weibull distributions, which are continuous. This mean that instead of defining normalization and moments trough integrals like in Section 3.1, we use sums.*

The non-central moments of $f(n)$ are thus given by

$$E[X^m] \equiv \mu_m = \sum_{n=0}^{\infty} n^m f(n).. \tag{7.1.10}$$

Show that the mean, $\mu \equiv \mu_1$, and the variance, $\sigma^2 = \mu_2 - \mu_1^2$, of the Poison process equals λt by writing up the sum and manipulate the limits.

7.1.2 Waiting times and independence of storms

Lets again consider the wind speed, here denoted by the stochastic process, X. We consider the cumulative distribution function, $F_X(\xi,t)$, which express the probability that $X < \xi$ during the time interval, t. In terms of wind speed it means that the wind speed stay below some given threshold corresponding to a some local maximum. We just learned that this probability is given by the Poisson distribution with $n = 0$, hence

$$F_X(\xi,t) = \exp(-\lambda t), \tag{7.1.11}$$

where we have actually implicitly assumed that the wind speed is below the given threshold, ξ, at $t = 0$. We already discussed the fact that there often is a strong seasonal dependence on the occurrence of large storms and hence the maximum wind speed. We therefore consider time intervals of one year. In this way we are also sure that two up-crossings are independent of each other. For example the maximum wind speed in two consecutive years.

More formally (turning again away from yearly maximum wind speeds) we now, define $\lambda_1(\xi)$ as the mean number of up-crossings of the threshold value, ξ, in one year. The associated probability is

$$F_1(\xi) = \exp(-\lambda_1(\xi)). \tag{7.1.12}$$

Due to independence of up-crossings in the different years, the probability that the wind speed stays below, ξ, during, T number of years is given by

$$F_T(\xi) = [F_1(\xi)]^T = \exp(-\lambda_1(\xi)T). \tag{7.1.13}$$

Finally we define the mean waiting time between up-crossings also called the recurrence period, $T(\xi)$, as the time for which the mean equals one. From exercise 7.1.1 the mean, μ of a Possion process equals λt. Hence we have

$$T(\xi) = 1/\lambda_1(\xi). \tag{7.1.14}$$

That is, the probability that there is no up-crossings within the time interval, T, equals e^{-1}. In other words, $T(\xi)$ is the average time you have to wait before you will encounter an up-crossing. The analogy to extreme wind speeds should be clear: When do we on average expect the next extreme wind speed to happen? In $T(\xi)$ years. In the next section we will see how we can use this result given a series of yearly maximum wind speeds.

7.2 The Gumbel distribution

We have already moved far ahead towards a formal expression for the extreme wind, U_{50}. The introduction of the Gumbel distribution contribute to the last step. If we assume that the rate of up-crossings, $\lambda_1(\xi)$, is exponential

$$\lambda_1(\xi) = \exp\left(-\frac{\xi-\beta}{\alpha}\right), \tag{7.2.1}$$

where α and β are two free parameters, the cumulative distribution given by eq. 7.1.12 is the - in wind energy extreme wind analysis - famous Gumbel distribution:

$$F_1(\xi) = \exp\left[-\exp\left(-\frac{\xi-\beta}{\alpha}\right)\right]. \tag{7.2.2}$$

In the same way, eq. 7.1.13 is also given by a Gumbel distribution

$$F_T(\xi) = \exp\left[-\exp\left(-\frac{\xi-\beta-\alpha\log T}{\alpha}\right)\right]. \tag{7.2.3}$$

This mean that whatever the value of T is, the functional form of F_T is the same. The only difference is that β is replaced by $\beta+\alpha\log T$, in other words, it becomes a functions of T. More generally, we can define a function, $G(x)$, through the following property

$$[G_X(x)]^T = G_X(a(T)x-b(T)). \tag{7.2.4}$$

Distributions, $G_X(x)$, with this property are called Fisher-Tippet extreme value distributions of type I, II or III. The most common and the one in wind energy associated with extreme wind is the type I distribution also called the Gumbel distribution (Gumbel, 1958) for which $a(T)=1$. The cumulative Gumbel distribution is plotted in Figure 7.2.1, and it is given by

$$\boxed{F_X(x) = \exp\left(-\exp\left(-\frac{x-\beta}{\alpha}\right)\right).} \tag{7.2.5}$$

Exercise 7.2.1 *Show that the pdf, $f_X(x)$, of the Gumbel distribution is given by*

$$f_X(x) = \frac{1}{\alpha}\exp\left(-\exp\left(-\frac{x-\beta}{\alpha}\right)\right)\exp\left(-\frac{x-\beta}{\alpha}\right), \tag{7.2.6}$$

and that the mean and variance is given by $\mu=\alpha\gamma+\beta$ and $\sigma^2=\alpha^2\pi^2/6$, with the Euler constant,

$$\gamma = -\int_0^\infty e^{-x}\log x dx = 0.57721.... \tag{7.2.7}$$

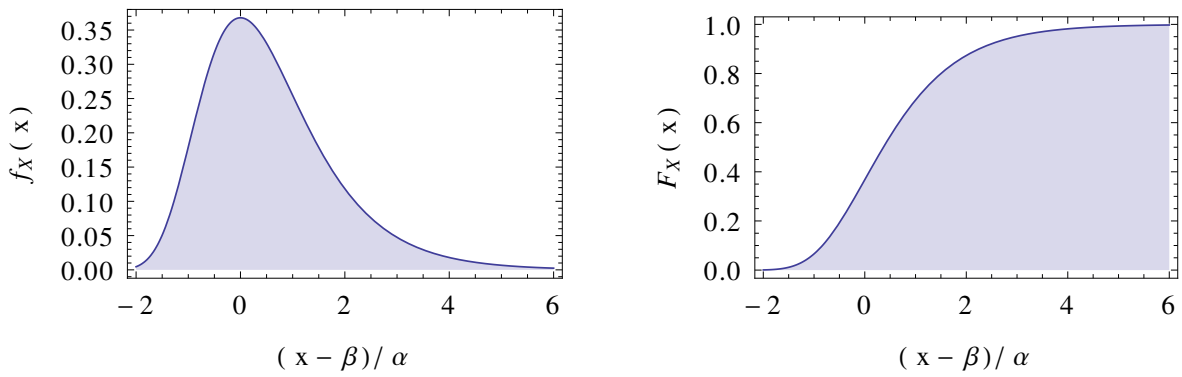

Figure 7.2.1: Gumbel distribution - pdf (*left*) and cdf (*right*.)

The Gumbel distribution and its two free parameters, α and β, are the foundation on which we will determine the extreme wind, U_T, here given for an arbitrary number of years, T, instead of of the usual choice of 50 years. Given α and β, U_T can be determined through the definition of the mean waiting time, i.e. the time for which $F(U_T) = e^{-1}$. We have

$$e^{-1} = \exp\left(-T\exp\left(-\frac{U_T-\beta}{\alpha}\right)\right) \tag{7.2.8}$$

Rearranging we arrive at the formula for the extreme wind, U_T,

$$\boxed{U_T = \alpha\log T + \beta.} \tag{7.2.9}$$

U_T, the extreme wind, is thus the largest wind we expect on average during T years. As said the most common value for T is 50 years. Since the mean waiting time is the average time between events, i.e. local extreme wind speeds, it is also the average time for which no extreme wind speeds occur. For wind turbines and other structures this makes perfect sense, since only the first event (think in terms of the Poisson process) is important: If the a storm tears down everything we don't really care about whether or not a second storm hits: the damage has already been done!

Peak-over-threshold is several very popular methods for obtaining U_{50}. They are closely related to the Poisson process. For exponential event rate, λ, the method becomes similar to those based on the Gumbel distribution and soon to be derived. One could, however, determine, λ, differently, for example by identifying individual storms. We will, however, not go further into the method in this course.

7.2.1 *Derivation of the Gumbel distribution

We now make a more formal proof of eqn. 7.2.4. In other words, we want to show that the distribution of extreme events of a series of stochastic variables, $X_1, X_2, ..., X_n$ with common cdf denoted by $F_{X_i}(x) = F_X(x)$, like for example the rare up-crossings just discussed, are given by the Gumbel distribution.

The extreme value, here taken as the maximum, is

$$X_{max,n} = \max(X_1, X_2, ..., X_n). \tag{7.2.10}$$

By independence of the events we have

$$F_{X_{max},n}(x) = P\{X_{max} \leq x\} = \Pi_{i=1}^{n} P\{X_i \leq x\} = [F_X(x)]^n. \tag{7.2.11}$$

For N going to infinity we see that $F_{max,X}(x)$ equals zero if $F_X(x) < 1$ and one if $F_X(x) = 1$. This is called a degenerate distribution, and as such of no use to us. In order to come around this result, we can reduce the maximum value by applying a linear transformation, $(a(n)X_{max,n} + b(n))$. If there is a limiting distribution of interest it must be the limiting distribution of some sequence of the transformed variables. If we take N number of such variables, we arrive at

$$[G_X(x)]^N = G_X(a(N)x + b(N)), \tag{7.2.12}$$

where we have denoted the limiting distribution of the N maxima by $G_X(x)$. As you can see, this is the same relationship as given in eqn. 7.2.4. It is often denoted the stability postulate in the literature. We will only focus on the case when $a(N) = 1$, which is the Gumbel distribution case.

Now lets take the M'th power of eq. 7.2.12

$$[G_X(x)]^{NM} = G_X(x + b(N))^M = G_X(x + b(N) + b(M)). \tag{7.2.13}$$

We can, however, also express it as

$$[G_X(x)]^{NM} = G_X(x + b(NM)). \tag{7.2.14}$$

This means that $b(N) + b(M) = b(NM)$. The only function which satisfy this relationship is the logarithm. I.e. $b(N) = \alpha \log N$, where α is a positive number.

We now take the logarithm twice on both sides of eq. 7.2.12 and remember that $G_X(x) \leq 1$ (it is a cdf), i.e. introducing a minus sign since we are interested in real valued numbers:

$$\log N + \log(-\log G_X(x)) = \log(-\log(G_X(x + \alpha \log N)). \tag{7.2.15}$$

If we define $h(x) = \log(-\log G_X(x))$ and $N = \exp(x/\alpha)$ we can rewrite eq. 7.2.15

$$h(x) = h(0) - \frac{x}{\alpha}. \tag{7.2.16}$$

Using the definition of $h(x)$ and setting $\beta = \alpha \log(-\log G_X(0))$ we end up with the Gumbel distribution

$$G_X(x) = \exp\left(-\exp\left(-\frac{x-\beta}{\alpha}\right)\right). \tag{7.2.17}$$

As a last result in this section we present a sufficient condition for the existence of a limiting distribution, i.e. that the extremes are Gumbel distributed. If the cumulative distribution is denoted $F(x)$ with derivative $f(x)$ (pdf) then the following criterion must be fulfilled (Conradsen, 1976):

$$\lim_{x \to \infty} \frac{d}{dx}\left(\frac{1 - F(x)}{f(x)}\right) = 0. \tag{7.2.18}$$

With x going to infinity is understood that we are only interested in the tail of the distribution, i.e. high values of x, hence the extreme values. It turns out that all exponential functions, $F(x)$, satisfies this criterion, i.e. both Gaussian distributions and Weibull distributions.

Exercise 7.2.2 *Show that the Weibull distribution satisfy eq. 7.2.18, which mean that the extreme winds of averaged wind speeds are Gumbel distributed.*

7.3 Application of the Gumbel distribution

By assuming a Gumbel distribution, the extreme wind, U_{50} is given by eq. 7.2.9. Our only job is thus to determine the parameters, α and β. There are many methods from which these can be found. The two most promising are given here.

They both use the statistical concept of *order statistics*. The idea is to arrange all our data in ascending order. Lets say that we have N number of yearly maximum, $U_{max,1}, U_{max,2}, ..., U_{max,N}$. After the arrangement we have $X_1, X_2, ..., X_N$ where $X_1 < X_2 < ... < X_N$, i.e. $U_{max,1}, U_{max,2}, ..., U_{max,N}$ in ascending order.

7.3.1 The Gumbels fitting method

The most simple and straight forward method is due to Gumbel (1958), who showed that one can assign a cumulative probability F_i to each X_i according to

$$F_i = \frac{i}{N+1}. \tag{7.3.1}$$

Plotting X_i versus $-\log(-\log(F_i))$, we can fit a straight line and obtain the parameters, α and β. Ott (2006) discuss this method and show that the it systematically overestimate the value of α and β and hence the extreme wind, U_{50}, through eqn. 7.2.9.

7.3.2 Method by Annual maximum - Probability weighted moments

A much better method is based on probability weighted moments (PWM), b_m. These are defined as

$$b_m = \int_0^\infty x[F(x)]^m f(x)dx, \tag{7.3.2}$$

in contrast to the more usual defined moments of eq. 3.1.11. For the Gumbel distribution the two first PWM, are given by

$$\begin{aligned} b_0 &= \alpha\gamma + \beta \\ b_1 &= \frac{1}{2}((\gamma + \log 2)\alpha + \beta), \end{aligned} \tag{7.3.3}$$

leading to

$$\begin{aligned} \alpha &= \frac{2b_1 - b_0}{\log 2} \\ \beta &= b_0 - \gamma\alpha. \end{aligned} \tag{7.3.4}$$

If we know b_0 and b_1 we can thus calculate α and β and hence U_{50} from eq. 7.2.9. The reason that we choose to work with PWM, is the existence of an unbiased estimate for the PWM moments of ordered series:

$$b_m = \frac{1}{N}\sum_{r=1}^{N} \frac{(r-1)(r-2)\cdots(r-m)}{(N-1)(N-2)\cdots(N-m)} X_r, \tag{7.3.5}$$

where r is the rank in the series of extreme values, $X_1, ..., X_N$.

The two first two moments are given by

$$\begin{aligned} b_0 &= \frac{1}{N}\sum_{i=1}^{N} X_i \\ b_1 &= \frac{1}{N(N-1)}\sum_{i=1}^{N} (i-1)X_i, \end{aligned} \tag{7.3.6}$$

both which can easily be estimated from our data. Some details have been skipped in the above discussion so interested readers might consult Abild (1994).

We can also calculate the uncertainty on U_{50}: since we are trying to construct a Gumbel distribution from only a finite number of data, a not negligible error is introduced.

The standard deviation of U_{50} for Gumbel distributions with various values of α is presented in Figure 7.3.1. The curves in the plot are produced by sampling of Gumbel distributed random numbers. For each value of n, a ensemble size of 100.000 has been used. Using the law of transformation of probabilities given in eqn. 3.2.10, a Gumbel distributed (with given α and β) random number, X, is obtained through

$$X = \beta - \alpha \log(-\log(U)), \tag{7.3.7}$$

where U is uniformly distributed between 0 and 1. Looking at the plot, the most striking is the fast increase in $\sigma(U_{50})$ with decreasing n. In many situations you often do not have more than a couple of years of measurements, which hence leads to a large uncertainty. It is also notably that extreme wind climates associated with high α values will always have a high uncertainty. On the other hand these climates will also have a large value of U_{50}, so the relative error $\sigma(U_{50})/U_{50}$ stays more or less the same. The annual maximum PWM method presented in this section is believed to be the best available method providing an unbiased estimate of U_{50}. Its only drawback seems to be the relatively many years of data needed.

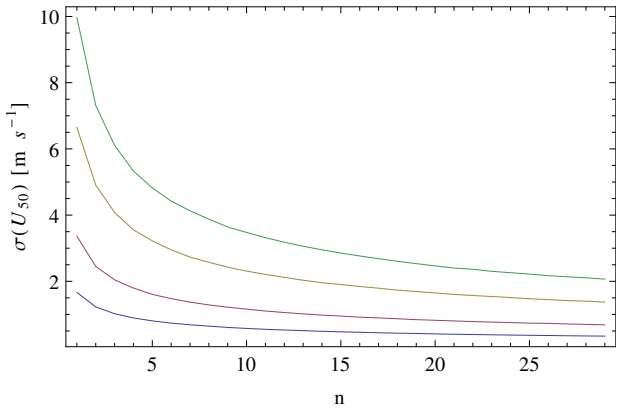

Figure 7.3.1: Uncertainty, $\sigma(U_{50})$, of the Gumbel distribution for different values of α. α is increasing upwards given values, 0.5,1,2 and 3. The smallest uncertainties in the plot is thus for $\alpha = 0.5$.

7.3.3 The Weibull parameter method

The last method we want to discuss is the Weibull parameter method, in which α and β, are directly determined from the Weibull parameters A and k given in eq. 3.2.3. Here

$$\begin{aligned} \beta &= A(\log n)^{1/k} \\ \alpha &= \frac{A}{k}(\log n)^{1/k-1}, \end{aligned} \tag{7.3.8}$$

with n being the number of independent events, i.e. maximum wind speeds. Determining n is the real problem. Dekker and Pierik (1999) recommend to set $n = 0.438N_U$, where N_U is the number of 10 minutes averages measured. This is not very realistic: events separated by only around 20 minutes are definitely not independent in the sense of large scale storms. Another critical thing about this method is the fact that we often estimate the Weibull parameters, A and k, from fits to the bulk of the Weibull distribution, whereas the maximums are located in the tail. The method is therefore rarely recommended unless all other methods fail. The latter could be due to very limited amount of data - for example only one year.

7.4 Final remarks

In calculating the extreme wind we have to be really careful since we are using only a finite number of measurements. For the annual maximum PWM method we learned that the uncertainty increases dramatically with decreasing number of years. Whether the data ARE Gumbel distributed at all is another issue. For measurements in mixed climates, as for example areas which are hit by storms of both tropical cyclones and mid-latitudes character, the extreme wind will not follow one but two distributions. This means that obtaining a set of parameters, α and β, to only one Gumbel distribution will fail. Instead we will have to divide the storm events into the two families and hence get two set of Gumbel parameters. We might also run into trouble with

the Gumbel methods in situations where the role of global climate phenomena like El-Niño and the North Atlantic Oscillation (NAO) is significant.

Data quality and especially sampling technique also plays a crucial role for estimating U_{50}. Data must be of good quality with spikes removed. In addition, whether data are sampled contiguously, disjoint or block is important. In the first case data are sampled at a very high frequency and averages, like U, is performed on all the raw data. In comparison, in disjoint sampling, the instrument only records every, lets say, 30 minute. This means that the peak in wind speed is most likely not captured. When making block average, only averages over a long time, like one hour, are stored. Again this gives a smaller value of U_{50} since the peaks are smoothed. A study by Larsén and Mann (2006) investigate the different ways of sampling and its consequences for wind energy extreme wind estimates.

If no measurements exist or if they for some reasons are not trusted, the reanalysis data by NCEP / NCAR [7.4.1] is a very good alternative. It is data from a global meteorological model, which has been run in hindcast for the last 40 years: the globe is divided into a large number of boxes and in each box all the relevant meteorological parameters, such as wind speed, temperature, surface pressure etc. are calculated. Its drawback is that data are disjointly sampled at three hours, which underestimates the extreme wind. Since a given wind speed represents a large geographical area it is recommended to use a surrogate for the geostrophic wind and use the geostrophic drag law to estimate the surface wind.

As a conclusion on this section it is recommended to use an ensemble of methods when estimating U_{50}.

[7.4.1] `http://www.esrl.noaa.gov/psd/data/reanalysis/reanalysis.shtml`

CHAPTER 8

HETEROGENEOUS TERRAIN

So far we have only considered homogeneous terrain, i.e. flat terrain in which the roughness length is constant over a large surface area. Mathematically, this means that the terms including the partial derivatives, $\partial/\partial x$ and $\partial/\partial y$ in eq. 4.3.1 vanish (except for the pressure gradient). In the general case of heterogeneous terrain this is not true. An direct implication is, that the flow is not described by the logarithmic wind profile close to heterogeneous features. As we will see, the concept of a logarithmic layer is, however, still very useful.

In this Chapter we will relax the assumption of homogeneity by introducing roughness change and orography (surface elevation) and discuss the possible implications this might have on the flow in the surface layer. Besides changes in roughness and surface elevation, changes in heat flux also creates inhomogeneity. This effect is, however, of minor importance in wind energy applications due to the often high wind speeds.

8.1 Roughness change

The terrain is characterized by a surface roughness, determining the wind profile. In case of uniform roughness we encounter the logarithmic wind profile. In most cases, however, uniform roughness only holds for a smaller surface area. In rural areas, in Denmark for example, the landscape is covered by various types of bushes, trees, fields, grass, villages, lakes and so on. Every time the wind flow encounter a change in surface roughness a new wind profile in equilibrium with the new surface characteristics downstream of the transition, is building up. This new transition layer is called an internal boundary layer (IBL). An internal boundary layer develops in both the case of a smooth-to-rough transition with $z_{01} < z_{02}$, and in the case of a rough-to-smooth transition with $z_{01} > z_{02}$, although with different strength. In the latter z_{01} refers the upstream roughness length, while z_{02} refers the downstream roughness length (see Figure 8.1.1).

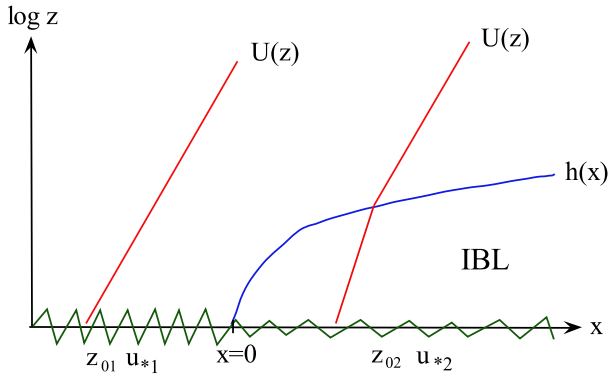

Figure 8.1.1: Simple view of a rough-to-smooth roughness change at $x = 0$. In the depicted case $z_{01} > z_{02}$ and $u_{\star,1} > u_{\star,2}$.

The strength of the transition is normally characterized by the number

$$\boxed{M = \log\left(\frac{z_{01}}{z_{02}}\right),} \tag{8.1.1}$$

so that a smooth-to-rough and rough-to-smooth transitions is characterized by negative and positive values of M, respectively. In the first case, for example moving from grass to bushes, the flow is slowed down. Moving in the opposite direction the flow accelerates. We will for simplicity consider the problem two-dimensional, so that roughness changes occur perpendicular to the mean flow determined by $U(z)$. In this case the position of the roughness change is given by $x = 0$, with x increasing downstream. For $x < 0$ the flow follows a logarithmic profile given by the upstream surface characteristic, z_{01} and $u_{\star,1}$, and far downstream of the roughness change, $x \gg 0$, a new logarithmic profile based on the new roughness length, z_{02}, and surface friction, $u_{\star,2}$, will be established. At $x = 0$ an IBL develops. The height, $h(x)$ of the IBL is a monotonic increasing function of its argument x. Above the IBL, $z > h(x)$, the wind profile is determined by the upstream surface characteristic, z_{01} and $u_{\star,1}$, while the wind profile inside the IBL, $z < h(x)$, is determined by downstream surface characteristic, z_{02} and $u_{\star,2}$. This is a somehow simplified picture of roughness changes (Kaimal and Finnigan, 1994; Garratt, 1990), but seems to match experimental data quite well.

Let us consider a simple picture (Kaimal and Finnigan, 1994). At $x = 0$ there is a change in vertical momentum flux, $u_\star$. We now assume that this change in flux is diffusing vertically upward, i.e. described by the vertical velocity fluctuations, σ_w. The governing equation is

$$\frac{\partial h}{\partial t} + U(h)\frac{\partial h}{\partial x} = A\sigma_w, \tag{8.1.2}$$

where we have included the time dependence of h, and A is some non-dimensional constant. Assuming stationarity and using the relation in eq. 4.2.6 we have

$$\frac{u_{\star,2}}{\kappa}\log\left(\frac{h}{z_{02}}\right)\frac{\partial h}{\partial x} = Bu_{\star,2}. \tag{8.1.3}$$

where the numeric value of B is different from A. Isolating $h(x)$ and integrating from $h(x=0) = z0_2$ to $h(x)$ yields

$$h\left[\log\left(\frac{h}{z_{02}}\right) - 1\right] + z_{02} = B\kappa. \tag{8.1.4}$$

This final expression is implicit in $h(x)$ and therefore not very useful for most practical applications. We can see that $h(x)$ increases slower than x. Therefore explicit formulas for $h(x) \sim x^n$ where $n < 1$ are popular choices. The most popular is due to Elliot (1958) who suggested $n = 0.8$ and furthermore introduces a weak dependence on M, i.e. so that $h(x)$ depends both on the upstream and downstream surface characteristics in contrast to eq. 8.1.4, where only the downstream surface characteristics matters:

$$\boxed{h(x) = z_{02}(0.75 + 0.03M)\left(\frac{x}{z_{02}}\right)^{0.8}.} \tag{8.1.5}$$

This formula is also currently incorporated in the software WAsP.

From matching the wind profiles above and inside the IBL, i.e. studying the discontinuity at $U(z = h(x))$ we get

$$\frac{u_{\star,2}}{u_{\star,1}} = 1 + \frac{\log\left(\frac{z_{02}}{z_{01}}\right)}{\log\left(\frac{h}{z_{02}}\right)}. \tag{8.1.6}$$

At some point far downstream $h(x)$ becomes of the same size as the height of the surface layer. The exact point of course depends on M, but for most practical application it happens at between 500m and 2km. In a more complete picture of roughness change the IBL is bounded from below by an equilibrium layer, in which the wind profile is given by the downstream surface characteristics, while the wind profile in the IBL is asymptotically approaching the two limits above and below. The growth of the equilibrium layer is much slower than the IBL, and a general rule of thumb is 1/100 of the downstream distance from the roughness change compared to approximately 1/10 for the height of IBL.

8.2 Orography

A slideshow will be presented on this subject.

8.3 Model hierarchy

Due to the difficulties in writing up analytical expressions for the flow in heterogeneous terrain, numerical models are often used in order to gain insight into the flow properties. These range from simple models like the one presented in eq. 8.1.4 for the growth of the IBL to Direct Numerical Simulation (DNS) in which the full Navier-Stokes equation presented in eq. 4.1.3. Whereas the last model is impossible to solve for flows with Reynolds numbers as encountered in the surface layer and complex boundaries as hills and roughness changes, a variety of numerical

models exists which somehow gives decent results. For completeness we list the most popular choices of model types. The models are ranged after complexity with the most simple in the top and the most complex in the end, the DNS just mentioned. Increasing downward is also the computational demand of running the models. Choosing a model is therefore always a tradeoff between accuracy and CPU time.

- **Engineering / Simple models**
  These models are often over simplified but, still, however, give a somehow valuable insight into a given problem. They are primarily analytically meaning that results can be obtained on the fly. These notes are full of them...

- **Linearized models**
  These models are based on linearization of the RANS equation, eq. 4.3.1. Solutions of the mean wind speed is obtained in a given coordinate system, and often includes the effects of both hills and roughness change as well as nearby obstacles. Being a linear model, many complex flow phenomena cannot be captured, for example are flow around steep hills in complex terrain very poorly represented, if at all! The BZ model (Troen and de Baas, 1986) working inside WAsP and the LinCom model (Astrup and Larsen, 1999) working inside WEng [8.3.1] are well known candidates of linear flow models. The first models were developed by J. Hunt and co-workers (Jackson and Hunt, 1975; Hunt et al., 1988).

- **Reynolds average Navier-Stokes (RANS)** The full set of RANS equations, eq. 4.3.1, are solved in a computational grid. The eddy viscosity is modeled; often by 1.5 order closures like the $K-\varepsilon$ model Pope (2000), in which two equations, one for the kinetic energy and one for the dissipation are added to the equations given in eq. 4.3.1. Although non-stationary (transient) version exists most models are stationary in time. There exists a number of commercial models as well as research models mainly working within universities. Of these the Risø DTU model EllipSys3D (Sørensen, 1995) have provided excellent results. Also worth mentioning is the Open Source C++ toolbox OpenFoam [8.3.2].

- **Large Eddy Simulation (LES)**
  Like RANS the governing equations are averaged Navier-Stokes equations. Instead of time averages, like in RANS, spatial averaging is used when performing LES. Details are given in Pope (2000). Turbulence is resolved in LES simulations down to a size in the order of the grid size. Below that, modeling is used. Being the first model in the complexity ranking that resolves turbulence and hence are capable of producing turbulence spectra used for load calculations, LES is a major step towards true physical modeling of the ABL. However, the computational costs, are huge and one of the main principles of modeling becomes clear: the model only calculate what you have told it to. By this is understood the fact, that in order to get decent turbulence spectra, for example, a good representation of turbulence

[8.3.1] Like WAsP, WAsP Engineering (WEng) is a software tool developed at Risø DTU. Where WAsP focus on wind climate and power production of wind turbines, WEng are mainly for site assessment, where estimates of turbulence and extreme wind calculations are needed (`www.WAsP.dk`).

[8.3.2] `www.openfoam.com`

must be present in the model setup /code. This also mean that LES models, so far, have not shown too promising results when it comes to flow in really complex terrain. Bechmann and Sørensen (2010) have shown promising results with the EllipSys3D code running in a LES mode. In homogeneous terrain with non-neutral stratification LES has proven very successful with good representation of the turbulence during non-steady situations, like the daily cycle (Wyngaard, 2010).

- **Direct Numerical Simulation (DNS)**
  A direct numerical simulation of the Navier Stokes equation, i.e. turbulence on all scales from the scale of forcing to the Kolmogorov scale where dissipation kicks in. The equations, eq. 4.1.3 are often solved in spectral space by the use of Fourier transforms. Due to the extremely high computational costs, applications in the ABL is very far from being realizable, and as such of probably very little interest as well. See Pope (2000) for a mathematical description.

CHAPTER 9

IEC AND SITE ASSESSEMENT

The science of micro scale meteorology for wind energy have now been introduced at a level suited for most basic tasks. Working as a wind engineer within siting and or wind resource estimation there is, however, one more thing you need to know, and that little thing is non negligible. We are talking about standards and especially the IEC standard. This chapter is devoted to this.

9.1 Introduction

Engineering standards codify a widely-accepted 'best practise' . This is an advantage in business contracts and legal disputes, where it is more practical to work with concepts like 'a certified IEC Class II_B turbine' than lengthy design reports, which might not be read or fully understood by the decision makers. Rules in standards reflect reality, but they are deliberately simplified and often slightly conservative.

9.1.1 Wind-engineering standards

There are several engineering standards for wind loads on structures like buildings, bridges, and masts. Extreme wind is the key parameter and it is defined as the level, which a sustained wind is expected to exceed only once during a very long period, called the *return period*. Extreme winds are averaged over a suitable period called the *averaging period* in order to exclude turbulent effects. The return period could be the planned life time of the structure or another period reflecting the acceptable risk.

Most wind engineering standards operate with a *reference wind* defined as the extreme wind at a reference height over idealized flat terrain with uniform surface roughness. The Eurocode 1 standard, used all over Europe for the design of buildings, applies a reference wind defined as an extreme wind with an averaging period of 10 minutes, a return period of 50 years, a reference height of 10 m, and a standard surface roughness of 0.05 m. Regional reference wind are prescribed, e.g. 24 m/s in all of Denmark except in a 50 km wide zone at the west coast where it

gradually increase towards the coast at 27 m/s. For a given project, the effects of terrain topography, surface roughness, and height above terrain are estimated by coefficients on the reference wind. This leads to a local extreme wind.

A *gust* is a peak velocity including turbulent velocity fluctuations. Gust statistics will depend on turbulence characteristics and sampling method, which usually is a moving averaging with a *filter time* corresponding to the dynamics of the building, e.g. 3 sec. The gust is sometimes estimated by the mean wind plus the standard deviation of the turbulent velocity fluctuations multiplied by a *peak factor*. The sample period, e.g. 10 min, will both affect mean statistics and the peak factor.

Loads and material strength have natural variations and even the strongest design may fail under rare conditions. In practice, the acceptable safety margin becomes a compromise between material costs and consequences of failures. Engineering standards address this problem by a system of *partial safety factors*, which nominally increases design loads and decreases material strengths relative to their expectation values. Partial safety factors are calibrated by probability theory.

9.1.2 The IEC 61400-1 wind turbine safety standard

The *International Electrotechnical Commission (IEC)* provides standards for all kinds of electrical equipment. Among these is the IEC 61400-1 standard for wind turbine safety (International Electrotechnical Commission, 1999, 2005, 2010). This standard covers topics like structural integrity, turbine control, electrical safety, and environmental conditions. Here, however, we only discuss the wind-related aspects.

The standardization work is organized in expert groups representing manufactures, universities, and certification agencies. These groups study new research results and turbine failure reports. Occasionally and based on consensus they decide to revise the standard.

As mentioned in section 9.1.1, most wind-engineering standards specify a reference wind for a particular part of the world and algorithms for load predictions. Wind-energy applications are slightly different, as here the objective is to select a commercial turbine and verify that it is safe for a particular project. The IEC 61400-1 approach is first to classify turbines and then to verify that site-specific conditions are within the design limits of the turbine class of the selected turbine. Turbine classification is the responsibility of the manufacturer, and site assessment is the responsibility of the project developer.

9.2 Turbine Classification

Edition 3 of IEC 61400-1 declares turbine classes I, II & III with a reference wind V_{ref} set to 50 m/s, 47.5 m/s and 37.5 m/s, respectively. I.e. a U_{50} extreme wind This reference wind is defined as the 10-min average wind speed at hub height. In addition, three turbulence categories A, B & C are defined by the *reference turbulence intensities* I_{ref} set to 16%, 14% and 12%, respectively. The reference turbulence intensity is the mean turbulence intensity of the longitudinal velocity fluctuations measured over a random 10-min period with mean wind speed of 15 m/s. The turbine

Wind turbine class		I	II	III	S
V_{ref}	(m/s)	50	42,5	37,5	Values
A	I_{ref} (-)	0,16			specified
B	I_{ref} (-)	0,14			by the
C	I_{ref} (-)	0,12			designer

Figure 9.1.1: The IEC 61400-1 Ed. 3 classification system

is characterized by its wind class and turbulence category, e.g. a turbine for medium extreme wind and medium turbulence is certified as a class II_B turbine, see table 9.1.1. There is an additional class S for which the manufacturer specifies reference wind and reference turbulence intensity. Class S is typically used for offshore turbines.

Manufactures often hire an independent certification agency - such as *Det Norske Veritas (DNV)* or *Germanisher Lloyd (GL)* - to verify the turbine classification. This is done by checking that the turbine is able to survive a range of pre-defined load cases specified by combinations of turbine mode of operation, load type, and wind condition. Typically, the manufacture produce a multitude of load simulations and reports which the certification agency review and accept.

9.2.1 Turbine operation modes

The modes of operation include normal power production, turbine start up and shut down, sudden failure of turbine control or electrical-network, operation under sever yaw error, and turbine in parked or idling states. These states are identified by the cut-in velocity V_{in}, rated velocity V_r, and cut-out velocity V_{out} of the turbine power curve, where rated wind is the lowest wind speed with full production.

9.2.2 Load types

The load types are either ultimate load or fatigue-damage load over a turbine life time set to 20 years for class I-III or determined by the manufacturer for class S. The wind conditions are defined by simple models scaled by V_{ref}, I_{ref}, and turbine hub height z_{hub}. Fatigue loads are calculated as the accumulated effect of turbine operation under a specified wind speed distribution plus a representative number of start-up and shut-down situations. Ultimate loads are both calculated for the extreme wind speeds (turbines in parked or idling mode) and for a range of operating wind speeds. The loads are simulated by aeroelastic models like FLEX, HAWC2 [9.2.1], or BLADED [9.2.2].

[9.2.1] HAWC2 is a load simulation program by DTU Wind Energy (`www.risoe.dtu.dk/sitecore/content/risoe_dk/home/hawc2.aspx`)

[9.2.2] Bladed is a load simulation program by GL Gerrrad Hassan (`www.gl-gerradhassan.com/en/GHBladed.php`)

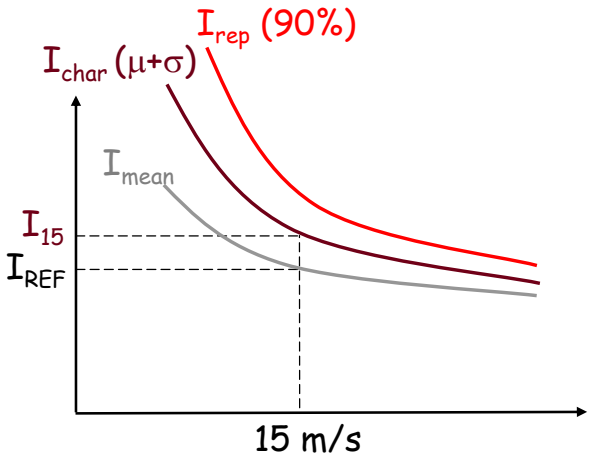

Figure 9.2.1: Sketch of IEC 61400-1 turbulence-intensity definitions. Edition 2 is based on the characteristic turbulence intensity I_{char} and edition 3 is based on the representative turbulence I_{rep} intensity.

The load-simulation programs need input from turbulence-simulation programs. Various turbulence models can be used for this purpose, including the one of WAsP Engineering Mann (1998, 2000) and a simpler one based on a Kaimal power spectrum and Davenport coherence (see Section 6.1.1). The only requirement is that the high-frequency end of the spectrum, called the inertial subrange, is within certain boundaries.

9.2.3 Wind conditions for load simulation

The wind-speed distribution needed to calculate accumulated fatigue loads is modelled by a Weibull distribution with shape factor $k = 2$ and averaged velocity set to 20% of the reference wind, $V_{\text{ave}} = 0.2V_{\text{ref}}$.

Wind profiles are modelled by the normal wind profile model (NWP) which is a power law

$$V(z) = V_{\text{hub}} \left(z/z_{\text{hub}}\right)^{\alpha} \tag{9.2.1}$$

where the shear coefficient α is set to 0.2 for fatigue loads and 0.11 for ultimate loads. Furthermore, the effects of flow inclination up to 8° from horizontal, independent of height, must be evaluated.

Typically, a few very strong gusts are responsible for most of the fatigue damage. Therefore, the normal turbulence model (NTM) applies the 90% percentile of the standard deviation of turbulent fluctuations in random 10-min average turbulence intensity. This is modelled by:

$$\sigma_{1,90\%} = I_{\text{ref}} \left(\tfrac{3}{4} V_{\text{hub}} + 5.6\right) \tag{9.2.2}$$

The variability is most significant at low wind speeds, so the *representative turbulence intensity* $I_{\text{rep}} = \sigma_1 / V_{\text{hub}}$ is a decreasing function of wind speed.

The extreme-wind condition includes both average and gust velocity and, according to the extreme wind model (EWM), the turbine must survive a steady wind set to 1.4 V_{ref} for the fifty-year return period and 1.12 V_{ref} for the one-year return period, where the latter is used in combination with a yaw misalignment of 15°. Turbulence is not included in these cases and the wind shear coefficient is moderate, $\alpha = 0.11$. In addition, turbines are tested by somewhat lower extreme winds $V_{\text{e50}} = V_{\text{ref}}$ and $V_{\text{e1}} = 0.8\,V_{\text{ref}}$, however, this time *including* turbulence scaled by $\sigma_1 = 0.11 V_{\text{hub}}$.

Finally, IEC 61400-1 specifies the following extreme wind events also sketched in figure 9.2.2:

- Extreme operating gust (EOG) - the wind is specified first to decrease, then dramatically increase and finally to decrease again. This event may fool the control system of a pitch-regulated turbine to take an unnecessary high wind load. The time scale of the event is 10.5 sec, and the amplitude is parameterized by reference wind speed V_{ref}, actual wind speed V_{hub}, turbulence fluctuations $\sigma_1(V_{\text{hub}})$, and the ratio between rotor diameter D and turbulence length scale $\Lambda_1 = \min(0.7 z_{\text{hub}}, 42\text{m})$;

- Extreme directional change (EDC) - a change of wind direction over 6 sec is specified. The magnitude of this change depends on wind speed V_{hub}, turbulence $\sigma_1(V_{\text{hub}})$, and the ratio of the rotor diameter and turbulence length scale $D/\Lambda_1(z_{\text{hub}})$;

- Extreme coherent gust with directional change (ECD) - the wind speeds up by 15 m/s during a period of 10 sec while the direction changes $\Delta\theta = \max(180^\circ, 720^\circ \text{m/s}\,/V_{\text{hub}})$;

- Extreme wind shear (EWS) - a transient vertical or horizontal wind shear over the turbine rotor is superimposed on a wind profile with strong shear, $\alpha = 0.2$. One positive or negative excursion with a duration of 12 sec and an amplitude depending on turbulence $\sigma_1(V_{\text{hub}})$ and the ratio between rotor diameter and turbulence length scale $D/\Lambda_1(z_{\text{hub}})$.

The shape and amplitudes of these excursions are specified in the standard. In general, velocity jumps increase with the mean wind speed while directional changes decrease.

9.2.4 Differences between IEC 61400-1 editions 2 and 3

Some turbines are still certified according to the previous edition 2 of the standard International Electrotechnical Commission (1999). The most significant differences are that edition 2 had an additional wind class IV, with reference wind set to 30 m/s, but only two turbulence categories, A and B. Furthermore, edition 2 operated with a turbulence measure called the *characteristic turbulence intensity* I_{15} referring to the *mean plus standard deviation* of random 10-min turbulence intensity at 15 m/s. The characteristic turbulence intensity is 18% and 16% for class A and B, respectively. Instead of the 90% percentile used in the current edition, edition 2 operated with mean plus standard deviation of the turbulence intensity and this was modeled by:

$$\sigma_{1,\mu+\sigma} = I_{15} \frac{15\text{m/s} + a V_{\text{hub}}}{1 + a} \tag{9.2.3}$$

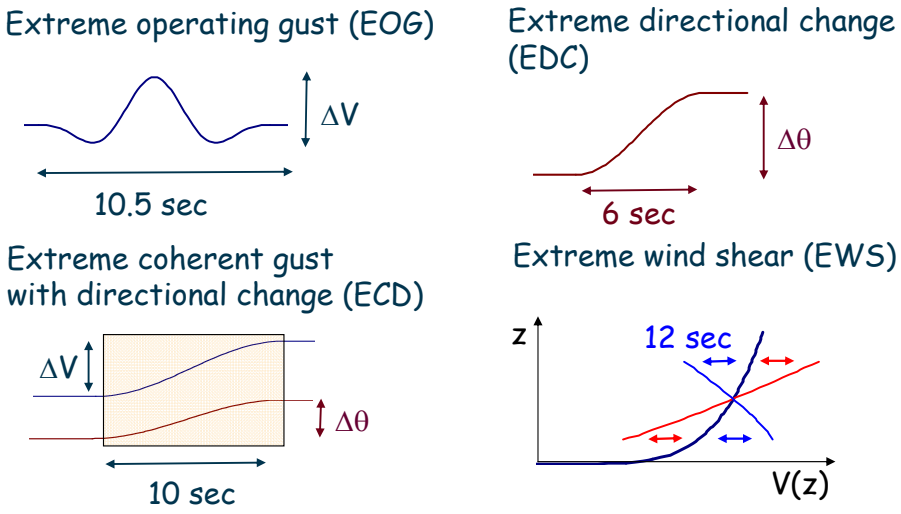

Figure 9.2.2: Sketch of IEC extreme wind events.

Here, the constant a is set to 2 and 3 for turbulence categories A and B, respectively. The design turbulence intensity of edition 2 (I_{15}) appears higher than that of edition 3 (I_{ref}), but this is mainly because it includes standard deviation among random 10-min averaging periods, see figure 9.2.1.

9.2.5 Offshore conditions

Offshore wind turbines must follow all the design criteria of the IEC 61400-1 safety standard plus some extra criteria specific for offshore conditions defined in the IEC 61400-3 offshore standard (International Electrotechnical Commission, 2009). The extra aeroelastic simulations must model the turbine and its foundation as a combined system. The extra load cases involves sea waves, currents and ice working in combination with wind loads.

Offshore surface roughness excursions and can be found by an implicit equation

$$z_0 = \frac{A_z}{g}\left[\frac{\kappa V_{\text{hub}}}{\ln\left(z_{\text{hub}}/z_0\right)}\right]^2 \tag{9.2.4}$$

where A_c is Charnock's constant. This is used for assessment of the standard deviation of the longitudinal velocity fluctuations

$$\sigma_{1,90\%} = \frac{V_{\text{hub}}}{\ln\left(z_{\text{hub}}/z_0\right)} + 1.28 \times 1.44 \times I_{15} \tag{9.2.5}$$

This offshore turbulence intensity initially decays with wind speed, as for the onshore case, but increases at higher wind speeds.

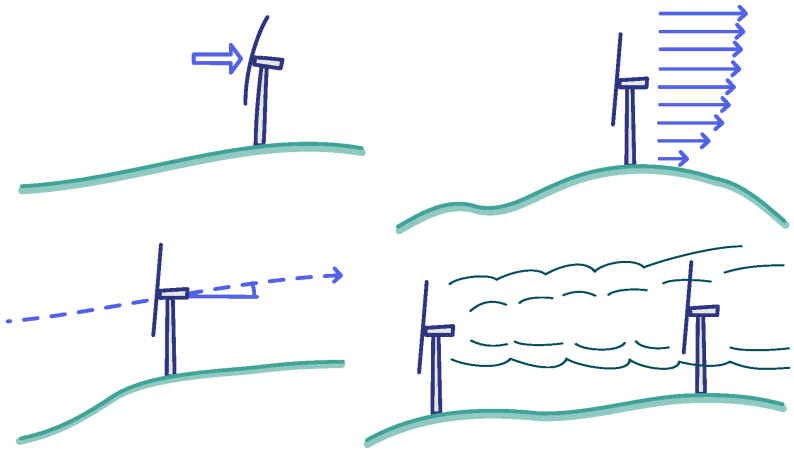

Figure 9.2.3: Extreme wind, shear, flow inclination and turbulence

9.3 Site Assessment

The project developer must check that site conditions are less severe than assumed in the turbine certificate. The rules are:

- The 50-year extreme wind must be lower than the reference wind of the turbine class;
- Flow inclination at hub height must be within $\pm 8^\circ$ for all wind directions;
- The wind-shear exponent at hub height α, averaged for all direction, must be positive but less than 0.2. The reason to avoid negative shear is risk of blade-tower interaction and the reason to avoid excessive shear is enhanced fatigue damage;
- The wind-speed probability density distribution must be lower than that of the certificate in a range of 0.2 to 0.4 times the reference wind. More exposure in this wind range would enhance fatigue damage;
- For turbines with edition 3 certificates, the effective turbulence intensity, see below, must be lower than the representative turbulence intensity in a range from 0.6 times the rated velocity to cut-out velocity. For turbines with edition 2 certificates, the effective turbulence intensity is compared to the characteristic turbulence intensity. The effective turbulence intensity must include contributions from wakes of neighbor turbines.

These criteria apply to every turbine site in the wind farm. An additional rule states that turbulence must be scaled by a safety factor if the terrain is complex and turbulence intensity has not been measured. The reason is that in complex terrain the turbulent energy is redistributed among the three velocity components. Terrain complexity is evaluated by criteria based on terrain slopes in the area around each turbine site. The final version of these rules were defined in an

amendment to the IEC 61400-1 Ed.3 International Electrotechnical Commission (2010). Unlike the original version the terrain slopes are now evaluated in sectors and the overall conclusion on terrain complexity also depends on wind distribution.

Sometimes the site-assessment criteria are only slightly exceeded. E.g. the turbulence level could be acceptable except for a small part of the range of wind speeds where the turbine is operating. Formally the site has not passed the test, but there might be an unused safety margin in the accumulated fatigue load. A possibility is to repeat the calculations with site-specific conditions. A full set of new aeroelastic simulations might not be necessary, it might suffice to evaluate the fatigue-load calculation with a realistic mean wind distribution.

9.3.1 *Effective turbulence intensity

Fatigue damage is the accumulated effect of multiple load cycles. The damage of similar cycles is considered proportional to their number and their load range raised to a power called the Wöhler exponent m. The Wöhler exponent is a material constant, which is low for a ductile material (steel) and high for a brittle material likely to break after a few extreme-load cases (glass fibre). To verify the safety of the entire turbine, one must apply the Wöhler exponent of the most sensitive material, usually that of the blades. Turbulence intensity depends on upwind conditions, which typically has a directional variation. Effective turbulence intensity is defined as the constant turbulence intensity causing the same material damage as variable turbulence from all directions. It is estimated in analogy to the equivalent load range.

$$I_{\mathrm{eff}}(u) = \left[\int_0^{2\pi} p(\theta\,|u)\, I^m(u,\theta)\, d\theta \right]^{1/m} \tag{9.3.1}$$

The implicit assumption behind this concept is that load ranges for a fixed wind speed are proportional to turbulence intensity and that possible variations of the shape of the load spectrum are of minor importance. The IEC61400-1 standard allows a uniform wind distribution for this integral, but ideally a wind rose should be used.

9.3.2 *Wake turbulence

IEC61400-1 states that turbulence from wakes of neighbour turbines must be included. Edition 2 did not specify exactly how, but edition 3 suggests a simplified version of Frandsen's wake model (Frandsen, 2005). Here, wake turbulence is modelled as a combination of background turbulence and added turbulence.

$$I_{\mathrm{wake}} = \sqrt{I_{\mathrm{added}}^2 + I_{\mathrm{ambient}}^2} \tag{9.3.2}$$

Both a uniform and directional distribution of the ambient turbulence intensity is allowed. Frandsen modelled added turbulence intensity by

$$I_{\mathrm{added}}^2 = \frac{1}{\left(1.5 + 0.8d/\sqrt{C_{\mathrm{T}}(u)}\right)^2} \tag{9.3.3}$$

where d is the distance to a neighbor turbine normalized by the rotor diameter and C_T is the thrust coefficient depending on wind velocity u. At close distance the rotor appears larger on the horizon, but there is a counteracting effect of wake expansion in the downwind direction. Frandsen studied these effects and concluded that it is sufficient to consider a simplified wake with uniform top-hat turbulence distribution and a fixed exposure angle of 21.6^o at the downwind site. Another important conclusion was that, for a given direction, only the nearest turbine affects the turbulence level. IEC61400-1 includes simple I_{eff} expressions for regular turbine arrays and uniform directional wind and turbulence distributions.

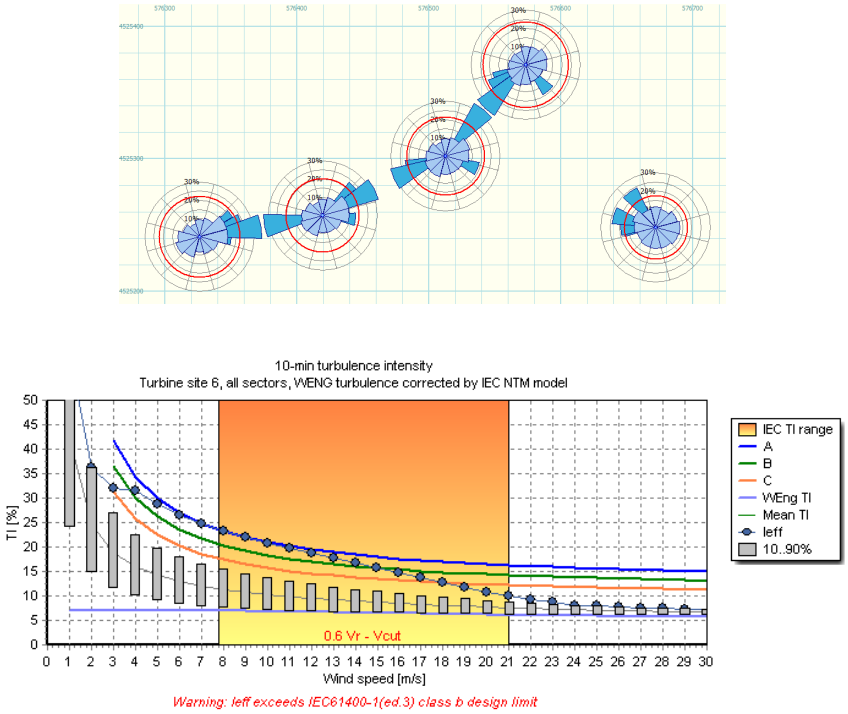

Figure 9.3.1: Plots from the WAT program. *Top:* Turbulence intensity roses, including backround turbulence (light blue), added wake turbulence (darker blue) and effective turbulence intensity I_{eff} (red curve). *Bottom:* Comparison between I_{eff} and representative turbulence intensity and I_{rep} for a range of wind speeds.

9.3.3 *Modelling by Risø programs

Predictions for site assessment may be modelled by a WAsP Engineering script [9.3.1] which also invokes the wind-resource program WAsP. In this way site-specific WAsP Engineering predictions of extreme winds, flow-line inclination, wind-shear exponent, and turbulence are combined

[9.3.1] WEng can be invoked by scripts - see `www.WAsP.dk/products/weng.aspx`.

with WAsP predictions of the statistical wind distribution. The results are then used as input to a third program called the Windfarm Assessment Tool [9.3.2]. which calculates wake- and effective turbulence intensities by the Frandsen model. For this purpose the directional frequency of occurrence at a fixed wind speed is modelled by

$$p(\theta|u) = \frac{p(u|\theta)\,p(\theta)}{p(u)} = \frac{p\left(u\middle|A_j,k_j\right)f_j}{\sum_{i=0}^{N-1} p(u|A_i,k_i)\,f_i} \tag{9.3.4}$$

Here, f_j is the sector-wise frequency of occurrence and A_j and k_j are Weibull parameters and index j refers to the wind direction sector corresponding to wind direction θ. The wind-speed distribution is modeled by

$$p\left(u\middle|A_j,k_j\right) = k_j/A_j\left(u/A_j\right)^{k_j-1}\exp\left[-\left(u/A_j\right)^{k_j}\right] \tag{9.3.5}$$

The effective turbulence intensity can be calculated for irregular turbine arrays and directional variation of ambient turbulence and wind-speed distribution, see figure 9.3.1a. Note how the wake of the nearest turbine hides the wakes of more distant turbines. The effective turbulence intensity is calculated for a range of wind speeds and compared to the representative turbulence intensity of the relevant wind turbine class.

9.4 Summary

Unlike most wind-engineering standards, IEC 61400-1 does not attempt to predict local wind conditions. Instead, in the IEC standard, turbine types are classified by a range of design load cases and wind farms are evaluated by a set of site-assessment rules. This chapter is merely an introduction and the standard should be consulted for accurate site assessment. Please note that rules may change in future editions.

[9.3.2] WAT belongs to the WAsP family but as such is a stand alone program - see `www.wasp.dk/products/wat.aspx`.

Assignment 5 (Site assessment) *The purpose of this exercise is to do close to a full site assessment, i.e. use most of the concepts you have learned in the course. Like in the previous assignments we use wind measurements from the Sprogø mast. The assignment is divided in three parts each covering a important aspect of the course core elements. First we estimate the Annual Energy Production (AEP) at two hypothetically turbine sites. Hereafter the extreme winds are estimated at those sites. Finally, the turbulence is reviewed (assignment 3), and everything is put into context of the IEC standard.*

We consider two locations for wind turbine siting

A) In the western Great Belt close to Nyborg.

B) In the eastern Great Belt close to Korsør.

Look on a map and make yourself comfortable with the geography. Also inspect the Danish Wind Atlas. We use constant roughness length of $z_0 = 0.0002$ m over water and $z_0 = 0.1$ m over land. We set the wind turbine hub height to 50 m.

The AEP in one sector is

$$E_i = T f_i \int_0^\infty p_i(U) P(U) \mathrm{d}U \tag{9.4.1}$$

where T is the time length of one year, f_i the frequency of the sector in question, $p_i(U)$ the pdf of wind in sector i, and $P(U)$ is the power curve, here given by the simple expression:

$$P(U) = 1MW \times \begin{cases} \left(\frac{U}{12\mathrm{m/s}}\right)^3 & \text{for } U < 12 \text{ m/s} \\ 1 & \text{for } 12 < U < 25 \text{ m/s} \\ 0 & \text{for } U > 25 \text{ m/s} \end{cases} \tag{9.4.2}$$

1. *Calculate the AEP in units of MWh of the turbine in the two sites from the Sprogø data (file: sprog.tsv). You may use the A and k shape parameters from the Weibull distributions obtained in assignment 1, and assume that k does not change when going from Sprogø to the two sites. You probably wanna disregard the effect of wind veer.*

2. *Get yourself familiar with the concepts of extreme wind and estimate the U_{50} by different methods.*

3. *Discuss the assumptions behind your choices and the strengths and limitations of the used methods.*

4. *Discuss the siting of turbines in the Great Belt in terms of the IEC standard. Remember to also consider the turbulence level (assignment 3).*

BIBLIOGRAPHY

Abild, J. (1994). Application of the Wind Atlas Method to Extremes of Wind Climatology. *Risø DTU report*, Risø-R-722(EN):1–174.

Astrup, P. and Larsen, S. E. (1999). WAsP Engineering – Flow Model for Wind over Land and Sea. Technical Report RISØ-R–1107(EN), Risø National Lab.

Bechmann, A. and Sørensen, N. N. (2010). Hybrid RANS/LES method for wind flow over complex terrain. *Wind Energy*, 13(1):36–50.

Bechmann, A., Sørensen, N. N., Berg, J., Mann, J., and Rethore, P.-E. (2011). The Bolund Experiment, Part II: Blind Comparison of Microscale Flow Models. *Boundary-Layer Meteorol.*, 141:245.

Berg, J., Mann, J., Bechmann, A., Courtney, M. S., and Jørgensen, H. E. (2011). The Bolund Experiment, Part I: Flow Over a Steep, Three-Dimensional Hill. *Boundary-Layer Meteorol.*, 141:219.

Charnock, H. (1955). Wind stress on a water surface. *Q. J. R. Meteorol. Soc.*, 81:639–640.

Conradsen, K. (1976). *En Introduktion til Statistik*. iMSOr.

Courtney, M. and Troen, I. (1990). Wind speed spectrum from one year of continuous 8 Hz meassurements. In Jensen, N. O., Kristensen, L., and Larsen, S. E., editors, *Ninth Symposium on Turbulence and Diffusion*, pages 305–308. American Meteorological Society.

Davenport, A. G. (1961). The spectrum of horizontal gustiness near the ground in high winds. *Q. J. R. Meteorol. Soc.*, 87:194–211.

Dekker, J. W. M. and Pierik, J. T. G. (1999). European Wind Turbine Standard II, ECN-C-99-073. Technical report, ECN.

Dyrbye, C. and Hansen, S. O. (1997). *Wind Loads on Structures*. John Wiley & Sons.

Elliot, W. P. (1958). The growth of the atmospheric internal boundary layer. *Trans. Amer. Geophys. Union*, 39:1048.

ESDU International (1982). *Characteristics of wind speed in the lower layers of the atmosphere near the ground: strong winds (neutral atmosphere)*. ESDU International, London.

Frandsen, S. (2005). Turbulence and turbulence-generated fatigue loading in wind turbine clusters. Report risø-r-1188(en), Risø National Laboratory.

Frisch, U. (1995). *Turbulence – the legacy of A. N. Kolmogorov*. Cambridge.

Fung, Y. C. (1969). *An introduction to the Theory of Aeroelasticity*. Dover, 2 edition.

Garratt, J. (1990). The internal boundary layer - a review. *Boundary-Layer Meteorol.*, 50:171.

Garratt, J. R. (1977). Review of Drag Coefficients over Oceans and Continents. *Monthly Weather Review*, 105:915–929.

Geernaert, G. L. (1987). On the importance of the Drag Coefficient in Air-Sea Interactions. *Dynamics of Atmospheres and Oceans*, 11:19–38.

Grotjahn, R. (1993). *Global Atmospheric Circulations*. Oxford university press.

Gumbel, E. J. (1958). *Statistics of Extremes*. Columbia University Press.

Hahmann, A., Rostkier-Edelstein, D. A., Wagner, T. T., Vandenberghe, F., Liu, Y., Babarsky, R., and Swerdlin, S. P. (2010). A Reanalysis System for the Generation of Mesoscale Climatologies. *J. Appl. Meteor. Climate*, 49:954.

Högström, U. (1988). Non-dimenisional wind and temperature profiles in the atmosperic surface layer. *Boundary-Layer Meteorol.*, 42:263–270.

Holton, J. R. (1992). *An introduction to dynamic meteorology*. Academic press.

Hunt, J. C. R., Leibovich, S., and Richards, K. J. (1988). Turbulent shear flows over low hills. *Q. J. R. Meteorol. Soc.*, 114:1435.

International Electrotechnical Commission (1999). *IEC 61400-1 Ed.2 Wind turbine generator systems - Part 1: Safety requirements*. International Electrotechnical Commission.

International Electrotechnical Commission (2005). *IEC 61400-1 Ed.3 Wind turbines - Part 1: Design requirements*. International Electrotechnical Commission.

International Electrotechnical Commission (2009). *IEC 61400-3 Wind turbines - Part 3: Design requirements for offshore eind turbines*. International Electrotechnical Commission.

International Electrotechnical Commission (2010). *IEC 61400-1 A1 Ed.3 Ammendment to IEC 61400-1 Ed.3: Wind turbines - Part 1: Design requirements*. International Electrotechnical Commission.

Jackson, P. S. and Hunt, J. C. R. (1975). Turbulent wind flow over a low hill. *Q. J. R. Meteorol. Soc.*, 101:929.

Kaimal, J. C. and Finnigan, J. J. (1994). *Atmospheric Boundary Layer Flows*. Oxford University Press, 304 pp.

Kaimal, J. C., Wyngaard, J. C., Izumi, Y., and Coté, O. R. (1972). Spectral charcteristics of surface-layer turbulence. *Q. J. R. Meteorol. Soc.*, 98:563–589.

Kristensen, L. (1998). Cup Anemometer Behavior in Turbulent Environments. *J. Atmos. Ocean. Technol.*, 15:5–17.

Kristensen, L. and Jensen, N. O. (1979). Lateral Coherence in Isotropic Turbulence and in the Natural Wind. *Boundary-Layer Meteorol.*, 17:353–373.

Larsén, X. G. and Mann, J. (2006). Effects of stride and averaging times on annual extreme wind data. *J. Wind Eng. Ind. Aerodyn.*, 94(8):519–539.

Lenschow, D. H., Mann, J., and Kristensen, L. (1994). How Long Is Long Enough When Measuring Fluxes and Other Turbulence Statistics? *J. Atmos. Ocean. Technol.*, 11(3):661–673.

Mann, J. (1994). The spatial structure of neutral atmospheric surface-layer turbulence. *J. Fluid Mech.*, 273:141–168.

Mann, J. (1998). Wind Field Simulation. *Prob. Engng. Mech.*, 13(4):269–282.

Mann, J. (2000). The spectral velocity tensor in moderately complex terrain. *J. Wind Eng. Ind. Aerodyn.*, 88:153 – 169.

Mann, J., Kristensen, L., and Courtney, M. S. (1991). The Great Belt Coherence Experiment – A study of atmospheric turbulence over water. Technical Report R–596, Risø National Laboratory.

Ott, S. (2006). Extreme Winds in the Western North Pacific. *Risø DTU report*, Risø-R-1544(EN):1–36.

Panofsky, H. A. and Dutton, J. A. (1984). *Atmospheric Turbulence*. John Wiley & Sons, New York.

Peña, A. (2009). *Sensing the wind profile*. PhD thesis, University of Copenhagen (Risø-PhD-45(EN), www.risoe.dtu.dk).

Petersen, J. T., Kretz, A., and Mann, J. (1995). Importance of transversal turbulence on lifetime predictions for a HAWT. In Tsipouridis, J., editor, *5th European Wind Energy Association conference and exhibition. EWEC '94*, volume 1, pages 667–673. The European Wind Energy Association.

Pope, S. B. (2000). *Turbulent Flows*. Cambridge University Press, 770 pp.

Press, W. H., Teukolsky, S. A., Vatterling, W. T., and Flannery, B. P. (2002). *Numerical Recipes in C++*. Cambridge University Press.

Simiu, E. and Scanlan, R. H. (1996). *Wind Effects on Structures, 3. ed.* John Wiley & Sons.

Sørensen, N. N. (1995). General Purpose Flow Solver Applied to Flow over Hills. PhD thesis Risø–R–864(EN), Risø National Laboratory.

Tennekes, H. and Lumley, J. L. (1972). *A First Course in Turbulence*. MIT Press.

Troen, I. and de Baas, A. (1986). A spectral diagnostic model for wind flow simulation in complex terrain. In *Proceedings of the European Wind Energy Association Conference & Exhibition*, pages 37–41, Rome.

Troen, I. and Petersen, E. L. (1989). *European Wind Atlas*. Risø National Laboratory, Roskilde, Denmark, 656 pp.

Wyngaard, J. C. (2010). *Turbulene in the Atmosphere*. Cambridge University Press.

DTU Wind Energy is a department of the Technical University of Denmark with a unique integration of research, education, innovation and public/private sector consulting in the field of wind energy. Our activities develop new opportunities and technology for the global and Danish exploitation of wind energy. Research focuses on key technical-scientific fields, which are central for the development, innovation and use of wind energy and provides the basis for advanced education at the education.

We have more than 230 staff members of which approximately 60 are PhD students. Research is conducted within 9 research programmes organized into three main topics: Wind energy systems, Wind turbine technology and Basics for wind energy.

Technical University of Denmark
DTU Vindenergi
Frederiksborgvej 399
Building 125
4000 Roskilde
Denmark
Telefon 45 25 25 25
info@vindenergi.dtu.dk
www.vindenergi.dtu.dk